Natural Resources Canada | Ressources naturelles Canada

GEOLOGICAL SURVEY OF CANADA
OPEN FILE 8909

Georgian Bay bedrock erosion: evidence for regional floods, Ontario

D.R. Sharpe, G. Leduc, C.S. Smart, and J. Shaw

2023

Canada

GEOLOGICAL SURVEY OF CANADA
OPEN FILE 8909

Georgian Bay bedrock erosion: evidence for regional floods, Ontario

D.R. Sharpe[1], G. Leduc[2], C.S. Smart[3], and J. Shaw[4]

[1]Geological Survey of Canada, 601 Booth Street, Ottawa, Ontario
[2]Independent Researcher, 11 bis rue de la Poste, Auby, France
[3]Department of Geography and Environment, University of Western Ontario, 1151 Richmond Street, London, Ontario, retired
[4]Faculty of Science, University of Alberta, 116 Street and 85 Avenue, Edmonton, Alberta, deceased

2023

© His Majesty the King in Right of Canada, as represented by the Minister of Natural Resources, 2023

Information contained in this publication or product may be reproduced, in part or in whole, and by any means, for personal or public non-commercial purposes, without charge or further permission, unless otherwise specified.
You are asked to:
- exercise due diligence in ensuring the accuracy of the materials reproduced;
- indicate the complete title of the materials reproduced, and the name of the author organization; and
- indicate that the reproduction is a copy of an official work that is published by Natural Resources Canada (NRCan) and that the reproduction has not been produced in affiliation with, or with the endorsement of, NRCan.

Commercial reproduction and distribution is prohibited except with written permission from NRCan. For more information, contact NRCan at copyright-droitdauteur@nrcan-rncan.gc.ca.

Permanent link: https://doi.org/10.4095/331409

This publication is available for free download through GEOSCAN (https://geoscan.nrcan.gc.ca/).

Recommended citation
Sharpe, D.R., Leduc, G., Smart, C.S., and Shaw, J., 2023. Georgian Bay bedrock erosion: evidence for regional floods, Ontario; Geological Survey of Canada, Open File 8909, 77 p. https://doi.org/10.4095/331409

Publications in this series have not been edited; they are released as submitted by the author.

ISSN 2816-7155
ISBN 978-0-660-47527-1
Catalogue No. M183-2/8909E-PDF

Table of Contents

ABSTRACT

We provide an updated presentation of the spectacular erosion forms at French River Ontario based on new methods of data collection and wider observations. This work includes ~10 detailed study sites, documentation of the range of forms over a large area, the use of extensive drone image capture, ground surveys, and a detailed inventory of forms. Key sites are illustrated using video images.

This update extends the previous conclusions regarding the significance and scale of subglacial meltwater erosion. We document the importance of plucking (including hydraulic plucking) and the control of structure on s-forms, Apparent cavitation erosion forms are prominent across the study area and provide support for inferred high-velocity meltwater flow. A growing interpretative framework includes discussion of evidence to test a theorized hydraulic sequence of sheet-channel-distributed flow, followed by re-grounding of glacial ice as meltwater flow waned. This hydraulic sequence is complementary to observations in thick sediment terrain down flow.

INTRODUCTION

Background and rationale

The Georgian Bay area was the site of potentially the first recorded sculpted erosion form (Andrews 1883). Andrews' sketch of unstriated 'scoop-marks' curving around a Key River rock boss (**Fig. 1**), captured the quintessential transverse-to-flow sickle-shaped, erosion form (sichelwannen) of the northern Georgian Bay terrain, a form missed by a number of later researchers. There is, however, notable literature on sculpted bedrock features including benchmark papers by Ljungner (1930), Dahl (1965) and Gjessing 1965, and, a thorough update by Shaw et al. (2020).

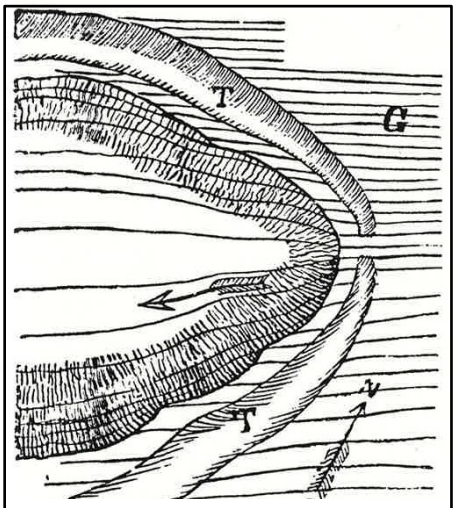

Figure 1: Andrews' sketch of unstriated 'scoop-marks' curving around a Key River rock boss. Note that erosional troughs (T) form a crescentic pattern around the rock while main flow lines trend across the rock rise.

Detailed work by Kor et al. (1991) put Andrews' 'scoop-marks' into a framework of erosional forms. They also mapped a series of sculpted erosional forms that highlight the significance of meltwater processes across a 70 km wide zone of scoured bedrock along the shores of northeastern Georgian Bay. Forms include the classic transverse, longitudinal, and non-directional classes (Kor et al. 1991): i) transverse forms (troughs, muschelbruche, sichelwannen, and commas) are preferentially located on stoss slopes; ii) longitudinal forms (spindle flutes, cavettos, furrows and remnant ridges) on lee slopes, and, iii) non-directional forms (undulating surfaces and potholes) on distal slopes; whereas, potholes occur at major breaks in slope. Kor et al. (1991) also showed that bed topography exerted control on both form shape and location. Form geometry thus relates to coherent structures in the formative flow and to interaction with the bed. For example, (Allen 1984) shows that s-forms are related to coherent flow structures such as vortices, or to assemblages of turbulent flow structures across multiple scales.

According to Kor et al. (1991, figure 4) sequences of forms can be linked to process. For example, muschelbruche, trend down flow toward sichelwannen due to the very shallow polished depressions being too small to cause flow separation (Allen 1984, p. 113). Muschelbruche likely result from low-angle, vortex impingement on the bed within turbulent flow (Kor et al. 1991, figure 5). As the muschelbruch deepened, its proximal slope steepened to the point where flow separation occurred, resulting in classical sichelwanne (Allen 1984; figure 5c). Hence, secondary flow created by bed forms appears to be an important part of the glaciofluvial erosion process, and forms self-perpetuate. In all, flow scale, vorticity, separation, bifurcation, strength, and direction were all inferred attributes of the mapped erosional marks in French River (Kor et al. 1991).

A further significant finding was the observation of sculpted forms at different scales, and inferred flow structures that likely operated over the same multiple range of scales. The combination of form attributes, boulder lags, and inferred flow structures reflect erosion by powerful, turbulent, subglacial meltwater flows. Coherent SW paleoflow direction, observed across the ~70 km flow width, indicates regional-scale flow, comparable in discharge (~1 x 10^6 m^3/s) with floods from glacial Lake Missoula (Baker 2009; Carling et al. 2009) and elsewhere (Carling et al. 2010).

Study area

Location and physiography

The area comprises the low-relief Georgian Bay, sediment poor, physiographic region of Grenville Province Canadian Shield (Chapman and Putnam 1984) terrain, with prominent rock outcrops and structural joints and banding. Elevation models, down flow of the French River study sites (**Fig. 2**), show a network of channels eroded in bedrock on the floor of Georgian Bay (Blasco 2001; Sharpe et al. 2018). The channel network extends across Georgian Bay to Manitoulin Island, ranging south into northern portions of Lake Huron (Todd and McNamara 2018). The network includes channel segments that rise down flow to the south and breaches low scarps of Niagara Escarpment around Tobermory. The channels also extend on land south of Georgian Bay as eroded sediment sequences (Sharpe et al. 2018; Pugin et al. 2018). All channel segments that trend towards Niagara Escarpment become part of a deep depression at the foot of the escarpment, or merge into escarpment gaps or re-entrant valleys (Kor and Cowell 1998).

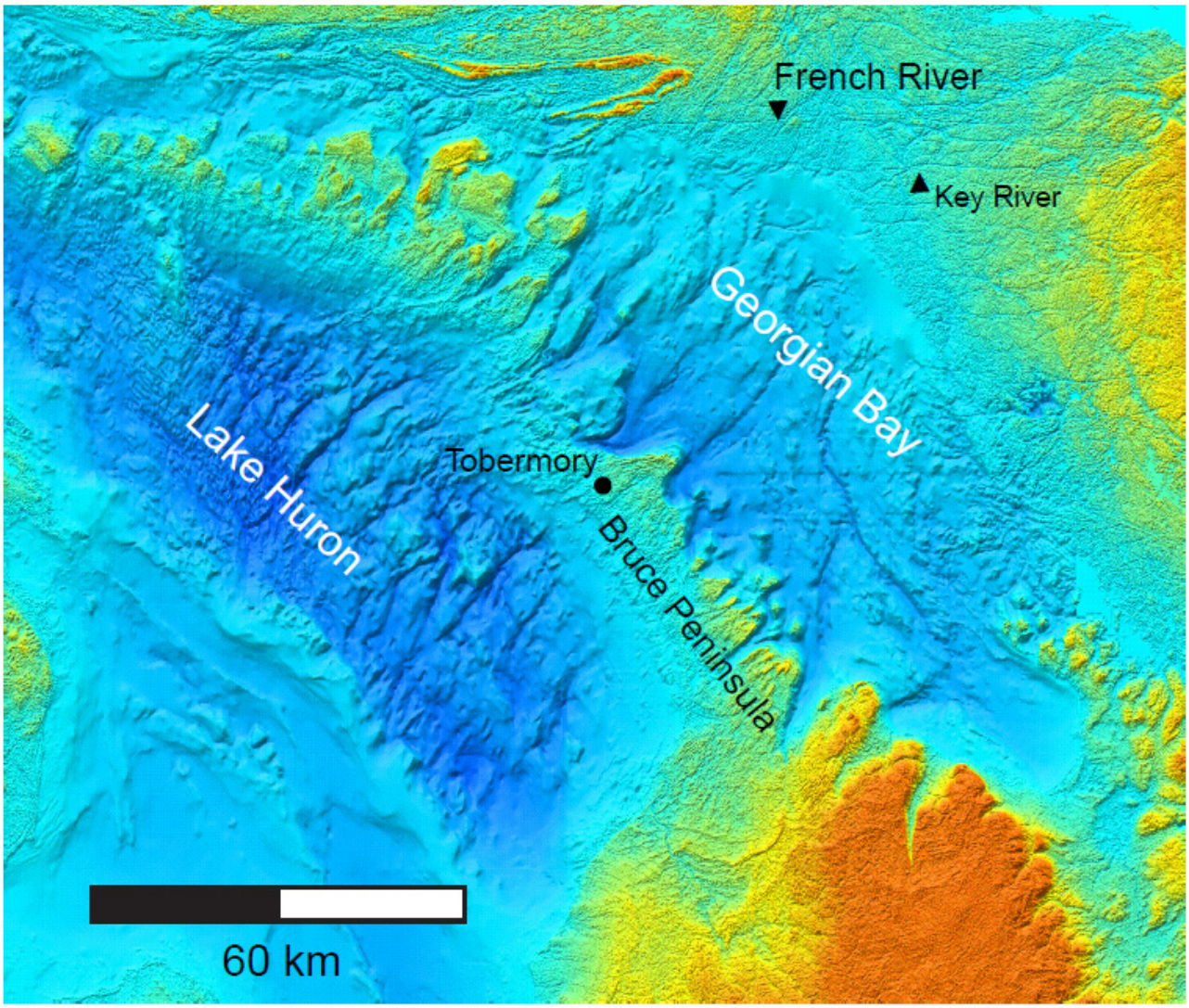

Figure 2: DEM of study area shows a network of channels on the floor of Georgian Bay and northern Lake Huron (e.g., Blasco 2001; Sharpe et al. 2018; Todd and McNamara 2018) down flow of detailed study sites from Key River to French River. Note that channels on the floor of Georgian Bay rise up and over Niagara Escarpment along the Bruce Peninsula, into gaps often termed re-entrant valleys. The Georgian Bay channels continue southwest into Lake Huron.

Bedrock geology

Many large-scale, structural depressions in the bedrock, including joints and faults, now form waterways (e.g., Henvey inlet, Key, French rivers) in the study area (**Fig. 3**). Bedrock lithology consists of metamorphic and granitic rocks of Grenville Province Neoproterozoic to Late Paleoproterozoic age (Culshaw et al. 1987-1990; 2004). Subglacial processes most likely differentially eroded each rock unit according to structure and lithology. Differing morphologies of the 16 studied sites (**Fig. 3**) responded to three key erosion factors. These include i) metamorphic grade and heterogeneity of different rock layers; ii) strike and dip of the rocks associated with compositional layering and/or parallel tectonic foliation; and, iii) direction of the erosive flow relative to the strike and dip of the rocks (suspected subglacial ice and water flow). For example, N-S-oriented inlets occur on the west side of a significant synform in the area (and linked to geological units), whereas, none occur on the east side of the synform (**Fig. 3**). Key River and Henvey Inlet are orientated E-W and correspond to a graben-type normal fault system.

Previous studies

The practical significance of inferred subglacial meltwater erosion in the study region was reported by (Hallet 2011) from research related to a nearby low-level reactive waste disposal site at the Bruce Nuclear (**Fig. 2**, ~ 100 km south of Tobermory). Hallet (2011) reports that some of the clearest and most convincing evidence for subglacial floods, recognized worldwide, is in this southern Ontario region, particularly around French River (e.g., Kor et al. 1991). Directly down flow, Kor and Cowell (1998) found "spectacular suites of erosional marks across Bruce Peninsula, indicating a continuous flow from French River, a regional event on the scale of 1000s km^2. Catastrophic glacial floods can be very erosive such as the floods from former Lake Missoula (e.g., Baker 1973; Monro-Stasiuk 2009) and similar flood events documented in southern Ontario (e.g., Kor et al. 1991; Tinkler and Stenson 1992; Brennand and Shaw 1994; Gilbert and Shaw 1994; Kor and Cowell 1998; Shaw 2002) that covered vast, low-relief areas. Bedrock channels (> 50 m depth) present on the floor of Georgian Bay (**Fig. 2**) may indicate the total depth of erosion related to catastrophic outburst floods, with a regional erosion estimate of 1 to 30 m (Hallet 2011).

Despite the above studies, some (Eyles 2012; Krabbendam et al. 2015) consider the French River sculpted rocks to be mainly eroded by ice. On the north shores of Georgian Bay, they report tracts of well exposed, well-developed glacial streamlining (their Fig. 3). Large-scale elongate rock forms are considered to be eroded preferentially by focused ice abrasion, or by lateral ice plucking. They report the presence of meltwater bed forms (s-forms; e.g., Kor et al. 1991), curvilinear 'gutters', cut by subglacial meltwaters (Krabbendam et al. 2015; their figure 3) They also report curvilinear or sinuous forms, metre-scale or less, commonly asymmetric in cross-section with locally steep, or undercut margins associated with straight mega-grooves. These meltwater forms are easily distinguished from the much larger, linear and symmetric, abrasional mega-grooves according to Krabbendam et al. (2015). Further, Krabbendam et al. (2017) incorrectly quotes Kor et al. (1991) that: 'abundant bed forms such as sinuous grooves formed by subglacial erosion as sediment-laden meltwaters moved through interlinked ice cavities'. In fact, (Kor et al. 1991) explains the 70 km wide scale Georgian Bay s-forms to result from regional sheet flow consistent southwest glaciofluvial paleo-flow indicators. To the west (Manitoulin Island), Eyles (2012) shows ~20 cm long hairpin scours with no striations in the lateral furrows (his figure 16), and similar larger forms, both of which he attributes to abrasion by debris-rich streaming ice.

Gray (1981) summed up the contrast in interpretations in such rock forms. 'Although many authors favour cavitation and/or corrasion by debris in meltwater streams to explain sculpted forms (e.g., Ljunger 1930; Hjulstrom 1935; Dahl 1965; Bernard 1971; Sharpe and Shaw 1989), others have named similar forms "glacial grooves" without any substantive discussion of their origin (see Sugden and John 1976; Boulton, 1974)'.

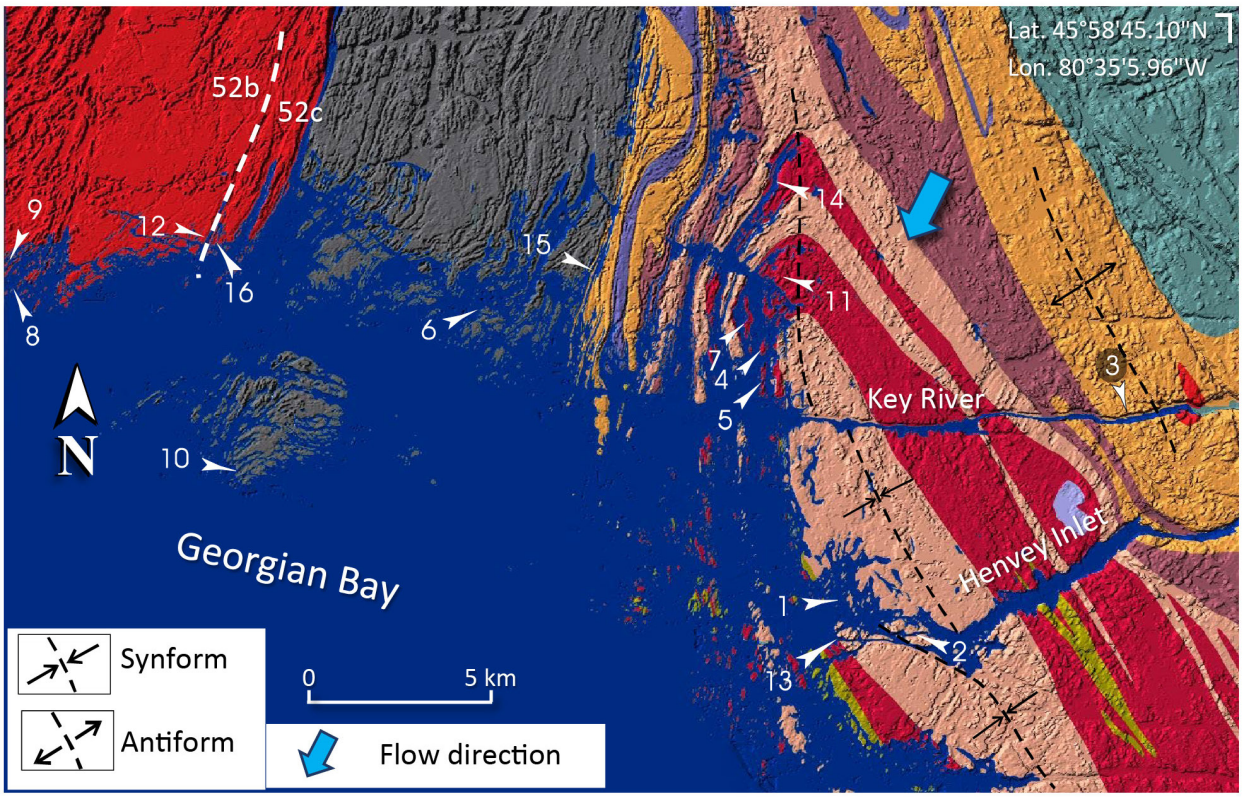

MESOPROTEROZOIC	
47	Mafic Intrusive Rocks: Anorthosite suite
50	Intermediate to Felsic Intrusive Rocks; Weakly foliated to gneissic: Site 1, 2 & 13.
51	Felsic to Intermediate Intrusive Rocks; Weakly foliated to gneissic: Sites 3 & 15.
52	Unit 52b Felsic Intrusive Rocks: Sites 8, 9 & 12. Unit 52c is strongly foliated to protomylonitic: Site 16.
EARLY MESOPROTEROZOIC to LATE PALEOPROTEROZOIC	
1	Intermediate migmatitic rocks with amphibolite dikes: Sites 6 & 10.
4	Intermediate to felsic rocks: Sites 4, 5, 7, 11 & 14.
5	Intermediate to Mafic Migmatitic Rocks.

Figure 3: Geological map adapted from Culshaw et al. 2004 with shaded digital elevation map. Numbered arrows indicate study sites.

Objectives

1. We update a benchmark paper on remarkable erosion forms in northern Georgian Bay (Kor et al. 1991).
2. We re-assess and extend the Kor et al. (1991) conclusions relative to the role of subglacial meltwater and ice abrasion /plucking to explain a vast sculpted landscape.
3. We focus on new observations that include ~16 study sites, detailing the range of forms over a larger area, through extensive use of captured drone imagery.
4. Our new observations document the importance of plucking (including likely hydraulic mechanisms), which we incorporate into an updated erosional framework

5. This study also highlights the importance of cavitation erosion forms and understanding of erosional processes from experimental hydraulic engineering studies.
6. We use short videos with animations to present key observations and interpretations.
7. We test the ice stream 'hard bed' abrasion model recently proposed to re-interpret the erosion forms of the study area.

Methods

We inspected ~10 new study sites in addition to those sites studied by Kor et al. (1991). We mapped, captured drone video imagery, and photographed a range of erosion forms at each new site. We recorded rock type and relevant structure and feature orientation. Field measurements of paleo-flow direction were supplemented with GPS- measurements using the collected field imagery as well as using Google Earth tools. We updated the s-from classification scheme of Kor et al. (1991).

We surveyed the sites using drones (DJI Phantom pro 3 and 4) to produce videos, images, and photogrammetric 3d models (Agisoft Photoscan Standard v. 1.3.2). The 3D models are available for viewing online at https://sketchfab.com/geodoxa/collections/french-river-2017 with flyby videos at https://www.youtube.com/playlist?list=PLxGPyXgrP6G7wIdT8zGIw-ZZ1tlP78f31, and on https://youtu.be/8pGhIdQobA4 (This paper seven videos) at https://www.youtube.com/c/Geodoxa/playlists

OBSERVATIONS

Forms

We observed all of the sculpted forms and features previously documented by Kor et al. (1991) and adopted their main classification scheme of s-forms (**App. 1**): longitudinal, transverse and non-directional classes. We also identified additional forms, distinguished as asymmetric and pitted, which we have added to the classification scheme (**Table 1**, see pages 35-37).

In addition, we identified a number of plucked forms (new in this study), and striations, which have been traditionally found in glaciated terrain (e.g., Hallet, 1996). Plucked forms, streaks, striations, bedding, joints and boulders add to the inventory of terrain elements in the study area (**Table 2**).

Table 2: S-form Classification (expanded from Kor et al. 1991)

Georgian Bay Terrain Elements		
1	**Longitudinal forms (low relief):** 1989 main site, Bottle, Hanvey flat, Germain south	1.1. cavettos
		1.2 furrows
		1.3 stoss-side furrows
		1.4 spindle flutes
		1.5 remnant ridges: i) rat-tails; ii) rock drumlin; iii) rock fluting (mega-lineation)
2	**Transverse forms (low relief):** Fox, Bottle, Hanvey flat, Germain south	2.1 commas
		2.2 sichelwannen
		2.3 muschelbruche (sg. muschelbruch)
		2.4 transverse trough
3	**Non-directional s-forms**	3.1 Vertical forms (potholes): Key River; Hanvey Inlet
		3.1.1 steep lee side
		3.1.2 flat uplands
		3.1.3 flat
		3.2 Undulating
4	**Asymmetric forms (low relief)**	4.1 stoss side ramp
		4.2 stoss side oblique
		4.3 lee side oblique
		4.4 lee side ramp
5	**Pitted forms**	5.1 pitted surfaces
		5.2 –streaks-tapered depressions
		5.3 –streaks in fields-tapered depressions
6	**Striation**	6.1 on s-forms
		6.2 striation or cavitation?
		6.3 striated clasts
7	**Plucked forms**	7.1 lee side
		7.1.1 small block
		7.1.2 steep blocks
		7.1.3 sheet
		7.1.4 oblique
		7.1.5 modified
		7.1.6 crescentic blocks
		7.2 stoss side (crescentic)
8	**Boulders**	8.1 rounded
		8.2 angular
		8.3 stoss
		8.4 lee side
		8.5 textured (percussion, elephant, faceted, multi-faceted)

The mapped s-form classes emphasize negative erosional features that represent zones of high relative rates of erosion. We also observed distinctive positive forms that result from this differential erosion. The median ridges of sichelwannen and residual ridges between diverging furrows are "streamlined;" they have broad, rounded upstream rises and tapered tails (Shaw et al., 2020). Thus, we add remnant ridges as an additional longitudinal class (**Table 2**). Remnant ridges described as 'rock drumlins," may be considered a class of erosional drumlins (e.g., Shaw and Sharpe 1987).

Assemblages of forms

Form assemblages appear to trace flow paths onto, across, and around rock uplands as noted by Kor et al. (1991, figure 4). Transverse s-forms are prevalent in upstream and flanking faces on rock rises greater than ~5 m in relief. Longitudinal forms are more common on local topographic uplands and on the gently sloping distal portions of rock drumlins and fluting. Cavettos, being partially curvilinear, are observed on some steep flanks. The down flow portions of some transverse forms (arms of commas and sichelwannen) are also elongate ("streamlined") due to the fact that the longitudinal

arms extend along the flanks of rise rises. Small-scale s-forms also occur on the surfaces of longitudinal forms like rock drumlins (**App. 2,** Kor et al. 1991).

FRENCH RIVER TERRAIN ELEMENTS

The significant terrain elements for the study area are shown in **Table 2**. Below is a summary of each study site, including geographic name, description, and location (**Fig. 3**) linked to illustrations of the terrain features.

Site Descriptions

1. **Henvey Flats** (45°50'57"N, 80°43'08"W; 176 m a.s.l.)

Henvey Flats is part of a low relief (< 2 m) coastal island complex (**Site 1, Fig. 3**) of massive granitic gneiss. The low site topography likely relates to the massive lithology and low angle layers in mid-synform setting (**Fig. 3**). We observed and recorded all s-from types recognized and shown in **Table 2**, except pitted forms. Henvey Flats erosion forms are oriented NE-SW, slightly oblique to normal to the structural trend, NNW-SSE (**Fig. 4a**). This setting resulted in a predominant erosion form: a network of rock drumlins formed at NE-facing structural breaks that separate many island groups. Each rock drumlin (**Fig. 4b**; **Plate 1.5a)** is outlined by up flow crescentic furrows with lateral furrows adjacent to streamlined rock ridges (**Figs. 4b, 5**). Multiple scales (~metre scale, 10-100 m, 1km) of rock drumlins with crescentic scours overlain by sparse boulders and boulder clusters were observed (**Fig. 5;** see also Kor et al. 1991, figures 11 and 12).

Up flow from Henvey Flats, rock drumlin forms up to 5 m high become lower relief residual forms (< 1m, residual ridges, rr), down flow to the southwest (**Plate 1.5a, b**). Sichelwannen are common with rock drumlin medial ridges and prominent furrows running alongside the ridge **(Plate 2.2)**; these forms are transitional to commas, spindles, fluting and undulating surfaces down flow (e.g., **Plate 2.1; 1.5a, b)**. Small steps in the bedrock show rounded plucking features and potholes. Most prominent are sichelwannen troughs filled with rounded and sub-angular boulders (**Plate 8.1)**. Boulders commonly display concoidal fractures, rounding, and occasional faceting (**Plate 8.5b**).

2. **Henvey Inlet** (45°50'32"N, 80°41'40"W; 176 m a.s.l.)

This site is at an EW structural break containing a prominent waterway (**Fig. 3**). The site has potholes on the down flow, steep, south-facing step (~5 m), north side of Henvey Inlet (**Plate 3.1a**). The area has a NE-SW rock-drumlin flow pattern, which is prominent in aerial views (**Figs. 5, 6**). The up-flow (north)-facing, gentle slope of the Inlet has stoss-side ramps with stoss-side furrows (**Plate 1.3**). In places, where the up flow-facing slope becomes more gentle, rock drumlins with crescentic furrows, sichelwannen, streaks and comma forms are observed. The lee side of the inlet displays plucking (**Fig. 6**) on the steep step at the fractured fault zone.

Most significant at this site are potholes in the lee of the bedrock step (**Fig. 6**). Potholes are ~5 m high and ~1 m across at the step and smaller (<0.5 m across) on level, upland rock surfaces. The 1 m deep furrows lead into potholes at the step face (**Plate 3.1a**). Also see **video 2** (**App. 3**).

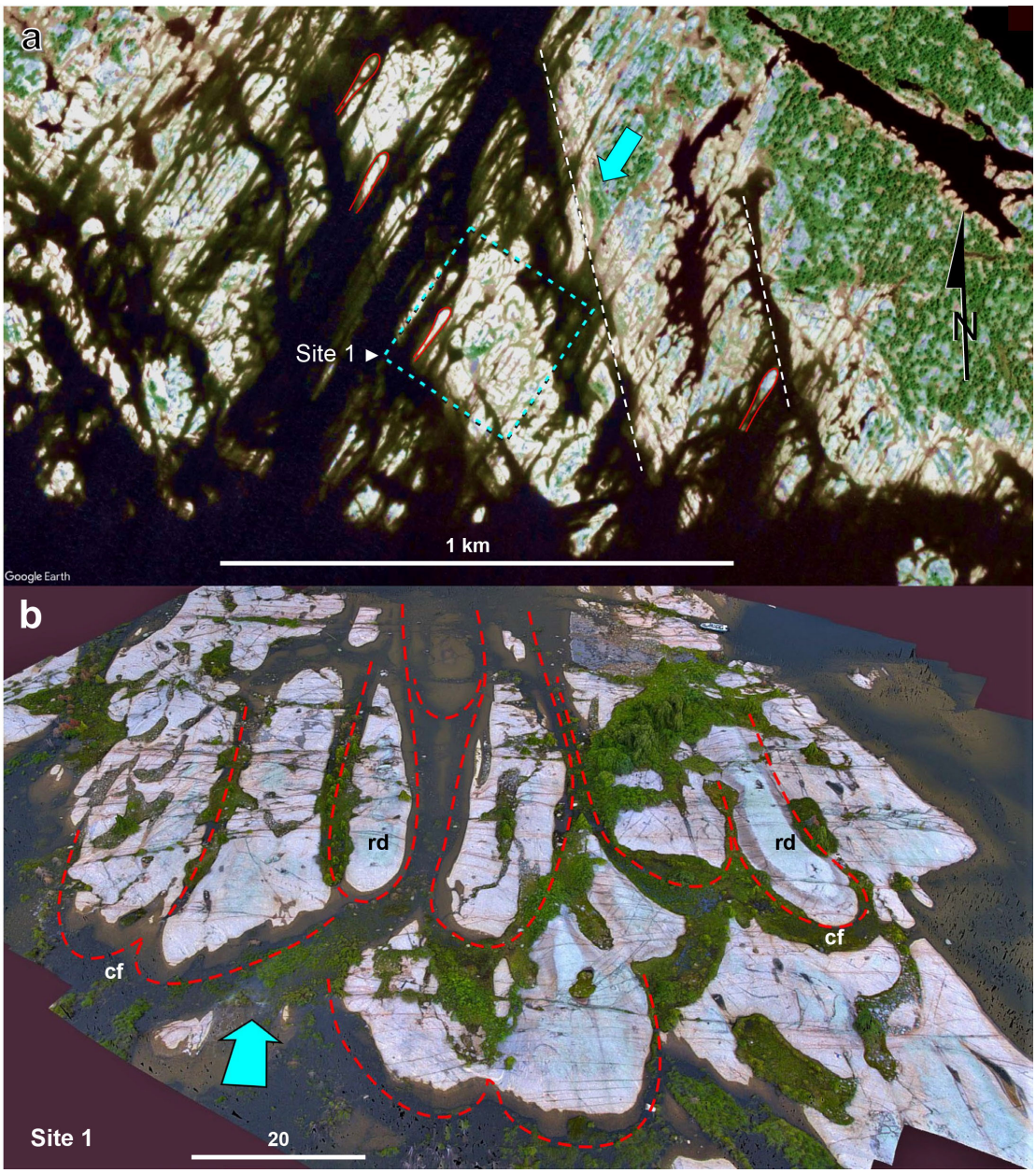

Figure 4: a) Aerial view of Henvey Flat study site with streamlined bedrock landforms, Site 1. a) rock drumlins (examples in red outline) occur in clusters down flow of structural breaks (dashed white lines) that create rock rises. Google Earth image, north-east corner is 45°51'18 44"N, 80°42'10.03"W; b) 3D photogrammetry of site 1; rock drumlins (rd) sculpted by crescentic furrows (cf) and straight furrows, highlighted by dashed red lines, to form the streamlined bedrock. Blue arrows indicate NE-SW flow direction. Photo courtesy of Guy Leduc.

Figure 5: Aerial view of Henvey Inlet (near study site 1) shows crescentic furrows (cf) around rock drumlins (rd). Note boulders (b) present in erosional furrows. Blue arrow indicates flow direction. Photo courtesy of Guy Leduc.

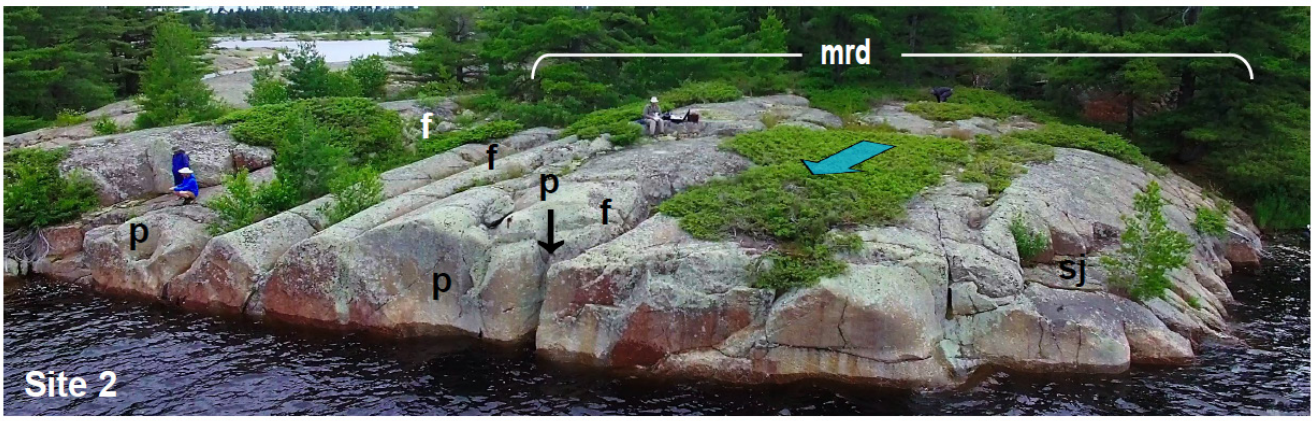

Figure 6: Aerial view of Henvey Inlet (site 2), with potholes (p) at break in slope. Note longitudinal furrows (f) that indicate paleo flow orientation of vortex flow from the northeast. The bracketed rock upland defines a mega rock drumlin (mrd). Break in slope is controlled by systematic joints (sj) of the fault zone. Photo courtesy of Guy Leduc.

3. **Key River** (45°53'18"N, 80°37'48"W; 180 m a.s.l.)

The Key River site is an ~EW structural break containing a waterway. It has potholes on the down flow, south-facing, ~15 m step (**Fig. 7**) on the north side of Key River (**Fig. 3**). The area has a NE-SW rock-drumlin, flow pattern that is perpendicular to the prominent structural grain, NNW-SSE (**Plate 10.3**). The up-flow (north-facing), modest slope of the river has a stoss-side ramp with stoss-side furrows (**Fig. 7,** similar to **Plate 9.4**). Towards the mouth of Key River (west), the upflow-facing slope is gentle, and exhibits rock drumlins with crescentic furrows, sichelwannen, comma forms and low-relief scour and undulations (**Fig. 8**).

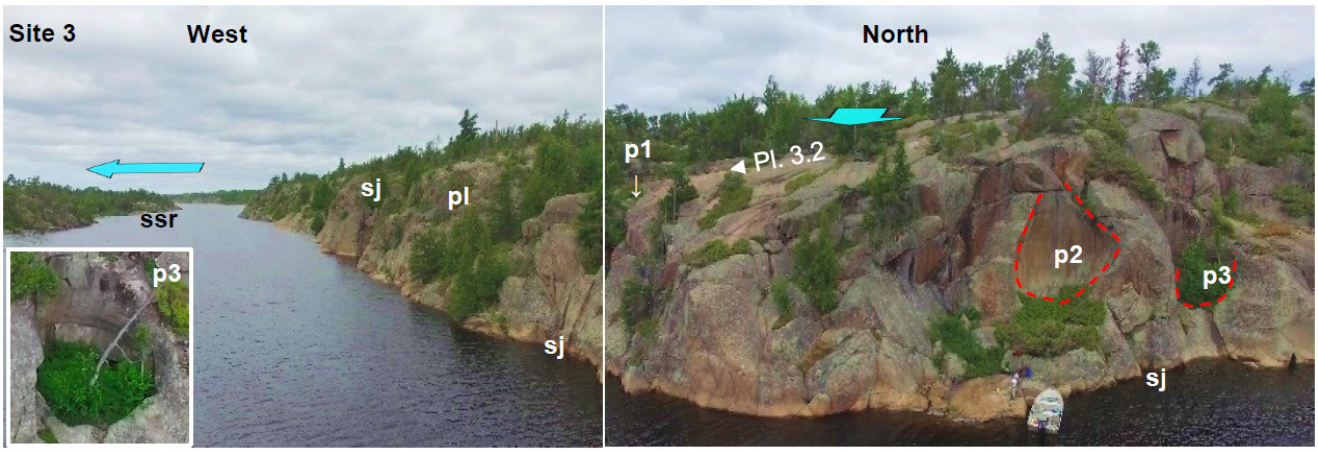

Figure 7: Panoramic mosaic of two drone photos of Key River inlet (study site 3), a break in slope with potholes (p) on the north side of river. Blue arrows indicate flow from the northeast. The up-flow (north-facing) moderate to gentle slopes have stoss-side ramps (ssr). The lee side (south-facing) steep cliff shows systematic joints (sj) of the inlet fault lines and plucking (pl), modified by giant potholes (p2, ~8 m in diameter; "The Giant's Chair" and ~5 m wide p3 (see inset view detail). A pothole, p1 (located), is 0.8 m wide and 3m high; Pl. 3.2 ► indicates view direction of the small pothole of Plate 3.2. For context, refer to plate 10.3, an aerial view showing lineated landscape oriented NE-SW. Photo courtesy of Guy Leduc.

Figure 8: South slope of Key River shows gentle stoss side ramp (ssr) pointing into flow (blue arrow); rock drumlins (rd) eroded by crescentic furrow (cf), cavetto (ca), and sichelwanne (sc); plucking (pl) occurs on the lee side of the rock drumlin. Boat is ~ 8m long. Photograph by D.R. Sharpe. NRCan photo 2022-506.

A giant pothole (~8 m in diameter, "The Giant's Chair") is observed at the Key River structural step (**Fig. 7**; **Plate 3.1b)**. Several ~1-2 m diameter potholes were also observed on the undulating upland above the Key River rock step. The upland is marked by rock drumlins and adjacent furrows, some, where flow likely spiralled over the structural step towards vertical potholes (**Plate 3.2**). The stepped wall has smoothed surfaces between pothole forms. The setting and erosion forms at Key River are similar to those at Henvey Inlet, except that the Key River step is 2-3 times higher, at ~15 m. Also see **video 5** (**App. 3**).

4. **Plucking Island** (45°54'17"N, 80°44'43"W; 176 m a.s.l.)

The Plucking Island site is essentially a large ~NNE-SSW rock drumlin (**App. 7**), where we observed all the documented Key River erosion forms shown in **Table 1**. The rock drumlin flow pattern is slightly oblique to the structural grain of the island, ~N-S (**Fig. 3**). The up flow (NNE-facing) end of the island has a well-formed stoss-side ramp with stoss-side furrows that lead into commas, furrows and sichelwannen forms, similar to those at other sites (**Plates 2.2, 2.5, 4.1**); their medial remnant ridges form low-relief rock drumlins (**Plate 2.2**).

Most significant is the number of observed plucking sites and a range of s-forms **(Plate 5.1.1; App. 7**). We surveyed the central part of the island in detail using drone photogrammetry (**App. 7**). Plucking is common on the down flow end of rock drumlins (e.g., **Plate 5.1.1**); some show as lateral plucking on the sides of rock drumlins (**Plate 5.1.4**). With flow from the NE across the island, asymmetric erosion occurs such as 'stoss' side ramps on one side with lateral plucking on the other (**Plate 5.1.4; App. 7.5**). Down flow, plucking appears to be controlled by joints perpendicular to flow orientation; on closer inspection however, the common presence of crescentic plucking (**Plates 5.1.4; App. 7.5)**, which is independent of joint control, likely requires a different mechanism. Further down flow, and rising up the large island rock drumlin, thin, stoss-side plucking is observed (**Plate 5.2; App. 7.3).** As the island rock drumlin becomes lower and tapers down-flow,

large, plucked blocks were removed and nearby down-flow steps trapped angular blocks and rounded transported boulders (**Plate 8.2**), including boulders with percussion marks (**Plate 8.5b**).

To understand the relationship between crescentic fractures and crescentic plucking (**Plate 5.5; App. 7.5**), we use detailed photogrammetric surveys to cover critical areas of interest. We speculate that these features may have a hydraulic influence as vortices flowed rapidly over a steep step down (**Video 6**; **App. 3**).

We also observed a field of potholes with shallow furrows and small rock drumlins (**Plate 3.3a, b**) on the NW island flank (slightly protected from NE flow). Most surprisingly, we observed a series of pitted forms (**Plate 6.1-**Germain Island**)**, linear streaks on the stoss-side ramp on the NE end of the island. These forms occur as single pits (**Plate 6.2a**) with tapered-down-flow depressions (~1-2 mm), carrot shaped, formed in fields with streaks parallel to former flow (as observed elsewhere, **Plate 6.2b)**; carrots are observed in association with spindle flutes, commas and shallow furrows (e.g., **Plate 6.3,** Fox Island).

5. **Germain Island** (45°53'48"N, 80°44'50"W; 176 m a.s.l.)

Germain Island comprises a series of rock drumlins within a wider surrounding landscape of rock drumlins and furrows (**Fig. 9; Plates 1.6, 12.1, 12.2**). The NE-SW-oriented forms on the island were eroded on the west limb of a large fold with NNE trending structure (**Fig. 3**). Rock drumlins with crescentic lateral furrows occur at multiple scales: island scale (km), 100-200 m, 10's of metres and metre scale (**Plate 12.2**).

Figure 9: Aerial view of Germain Island study site with prominent rock drumlins (rd) at multiple scales. - Details of rock drumlin clusters are provided in Plate 12. Photo courtesy of Guy Leduc.

On the up flow, northeast flank of the island, sichelwannen, commas, furrows, flutes and streaks were observed on low relief outcrops on the rising island slope, to 100 m scale rock drumlins and furrows (**Plate 12**). On the northwest flank of the island, cavettos (**Plate 1.1**) and lateral plucking features were observed along steeper, obliquely down flow rock walls. The down flow (SSW) low relief end of the island has a well-developed sequence of longitudinal and transverse forms. These include <10 m scale, sichelwannen, commas, furrows, spindles, cavettos, rock drumlins, potholes, pitted streaks and patches, and boulder clusters, some with percussion marks.

Of note, pitted streaks occur on the down flow side of rock drumlins with sculpted lee surfaces (**Fig. 10a**), as well as within and outside of s-form surfaces such as sichelwannen (**Fig. 10b**).

A 3D photogrammetric survey (**Plates 12a, 12b**) reveals an overlapping sequence of large to smaller rock drumlins (1, **Plate 12.6**). Large crescentic furrows (**Plate 12.5**) are eroded by medium size rock drumlins (2, **Plate 12.6**), then smaller

rock drumlins (3, **Plate 12.6**). The photogrammetric survey also reveals structural influence (gneiss layers) on sculpting and plucking (**Plates 12.5, 12.7, 12.8**).

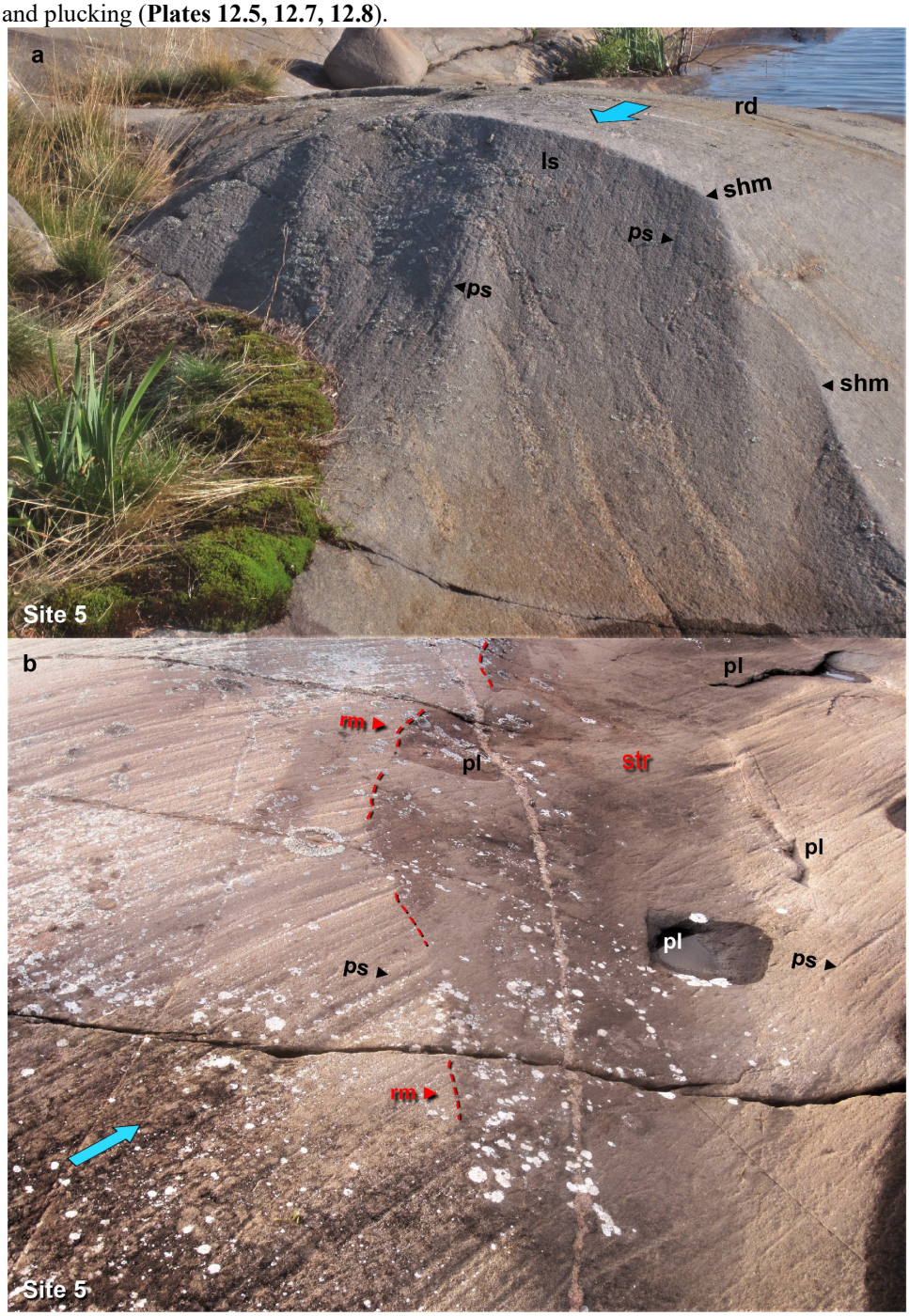

Figure 10: a) pitted streaks (ps) on the down flow, steep lee surfaces of rock drumlins (rd); note sharp margin (shm) on sculpted surface; such downflow crescentic scours are found in high flow rivers (Wilson et al. 2018); b) pitted streaks (ps) of variable thickness within and outside of a sichelwannen trough (str); minor plucked (pl) areas are present within the trough. Note indistinct up flow trough rim (rm) (red dashed line). Blue arrow indicates flow direction. Photographs by D.R. Sharpe. NRCan photos 2022-507 and 2022-508.

5a. Small Island (~75m east of Germain Island) (45°54'2.81"N, 80°44'36.71"W; 176 m a.s.l.)

This small island has a gentle stoss-side ramp and a steep lee side (**Plate 9.5**) modified by cavetto and plucking. The island is oriented NNE with main geological structure (**Fig. 3**) similar to Germain Island. Rock drumlins are less developed, and topography is controlled by bedding joints parallel to the gneissosity, with orthogonal stress joints. Of note, a 3m high overhang fracture is modified by a cavetto.

6. **Outer Fox Island** (45°54'33"N, 80°50'03"W; 176 m a.s.l.)

This site is on low relief islands where bedrock structure is trending ~NW-SE and eroded forms are oriented NE-SW (**Figs. 3, 11**). Furrows are prominent s-from and are associated with shallow sichelwannen, commas, musclebruche, small rock drumlins and cavettos. Furrows have elongate arms that extend from sichelwannen and commas. The arms extend into sichelwannen and commas down flow (**Fig. 11)**. Furrow straight segments are up to 50-75 m in length along the length of the level outcrop. It should be noted that furrows carry few if any striations (**Plate 1.4**). Pitted forms were observed on the low-relief portion of this site.

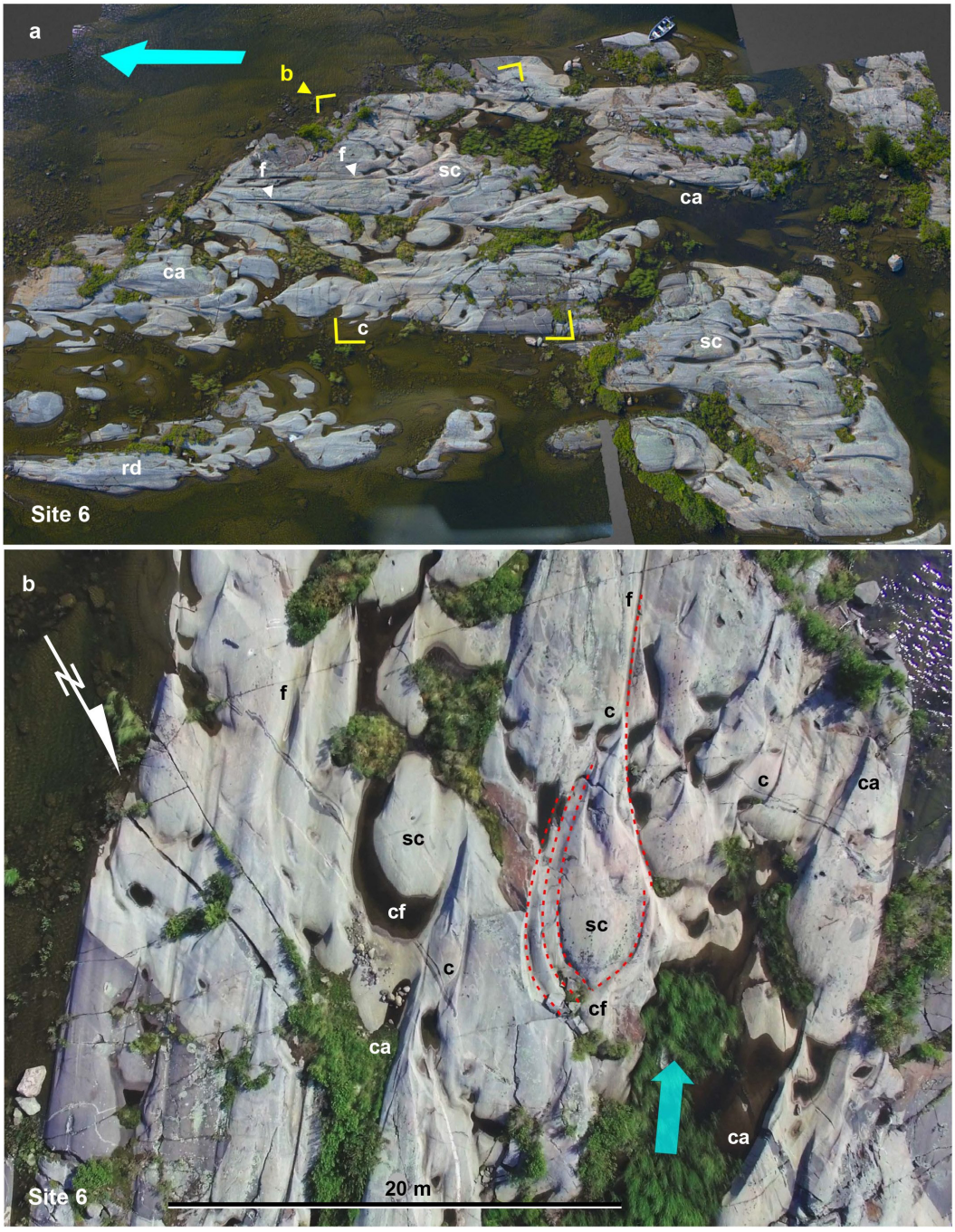

Figure 11: Outer Fox Island study site (6): a) 3D Photogrammetry survey; prominent furrows (f), commas (c), sichelwannen (sc), and rock drumlins (rd); b) aerial photo of a detailed area (site 6); red lines indicate multi-crescentic furrows (cf) that are similar to sichelwanne (sc); crescentic furrows (cf), commas (c) become furrows (f) down flow; cavetto (ca). Blue arrows indicate flow direction. Photos courtesy of Guy Leduc.

7. Cavitation Island (east of Puddick) (45°54'40"N, 80°45'02"W; 176 m a.s.l.)

This is a low relief island where the structural trend is ~NW with erosion forms eroded by flow from the NE. Forms were observed around the less vegetated shoreline areas. Spindle flutes, muchelbruche, transverse troughs, commas and vertical forms are common (**Plate 5.1.2**). Plucking observed at structural and lithological breaks is interspersed with commas, spindles and sichelwannen. This thin, sheet-like erosion has both rounded and ragged edges and pitted forms (**Plate 11**). There appears to be a close relationship between s-forms and plucking that warrants a discussion on possible contemporaneous formation (**Plates 5.1.2, 11.1, 11.2, 11.5**). Sichelwannen occur on rock rises along with crescentic chatter marks (**Plate 11.4)**.

An aerial photogrammetric survey reveals a "fish scale" terrain pattern (**Plate 11.1**), with sculpted forms on the stoss side and plucked forms on the lee side. Slabs of rock were slightly displaced from crescentic breaks/ steps particularly where gneissic bedding-joints occur. Long crescentic steps are linked to smaller crescentic steps, modified by s-forms (**Plates 11.1, 11.5, 11.6**). A second type of crescentic step involves fractures in gneiss that are independent of gneissosity (**Plates 11.1, 5.1.2**).

Pitted surfaces and elongate pitted forms are common at site 7 and cover wide areas of low-relief bedrock **(Plates 6.3; 11**). These small-scale linear erosion forms are non-traditional due to their pitted nature (**Table 2**). Most common are carrot (tadpole)-shaped pitted forms arranged as oriented streaks; they occur with a primary pit, or a series of pits, with a tapered, down-flow depression **(Fig. 11; Plate 11.8**). These pitted forms occur in fields (**Plate 11.6)** in intimate association with spindle flutes, commas, shallow furrows, musclebruche and at sculpted bedrock steps (**Fig. 11**; **Plate 6.3**). They may also be present within sculpted forms, or stepped depressions (**Plate 11b**) yet they are more prevalent on slight rises adjacent to s-forms (**Fig. 12**) and with plucking. Fine, delicate, s-forms and pitted forms remained preserved in pristine state down flow of plucked crescentic steps (**Plates 11.6, 11.7**). This includes mineral lamination observed in furrows linked to a 40 cm high stoss-side ramp.

Sets of overlapping sichelwannen clearly lead down flow to commas forms and then aligned with comma cavitation marks and crescentic chatter marks (**Plate 11.4**). Some of these streaks are slightly comma-shaped in the same field as the comma-shaped arm of sichelwannen, apparently providing a direct link between similarly-shaped forms with smooth (comma arm) and rough (pitted streak) surfaces (**Fig. 12 b, c**). Such pitted forms are unlike classic striations found on classic abraded rock surfaces (Iverson 1991a).

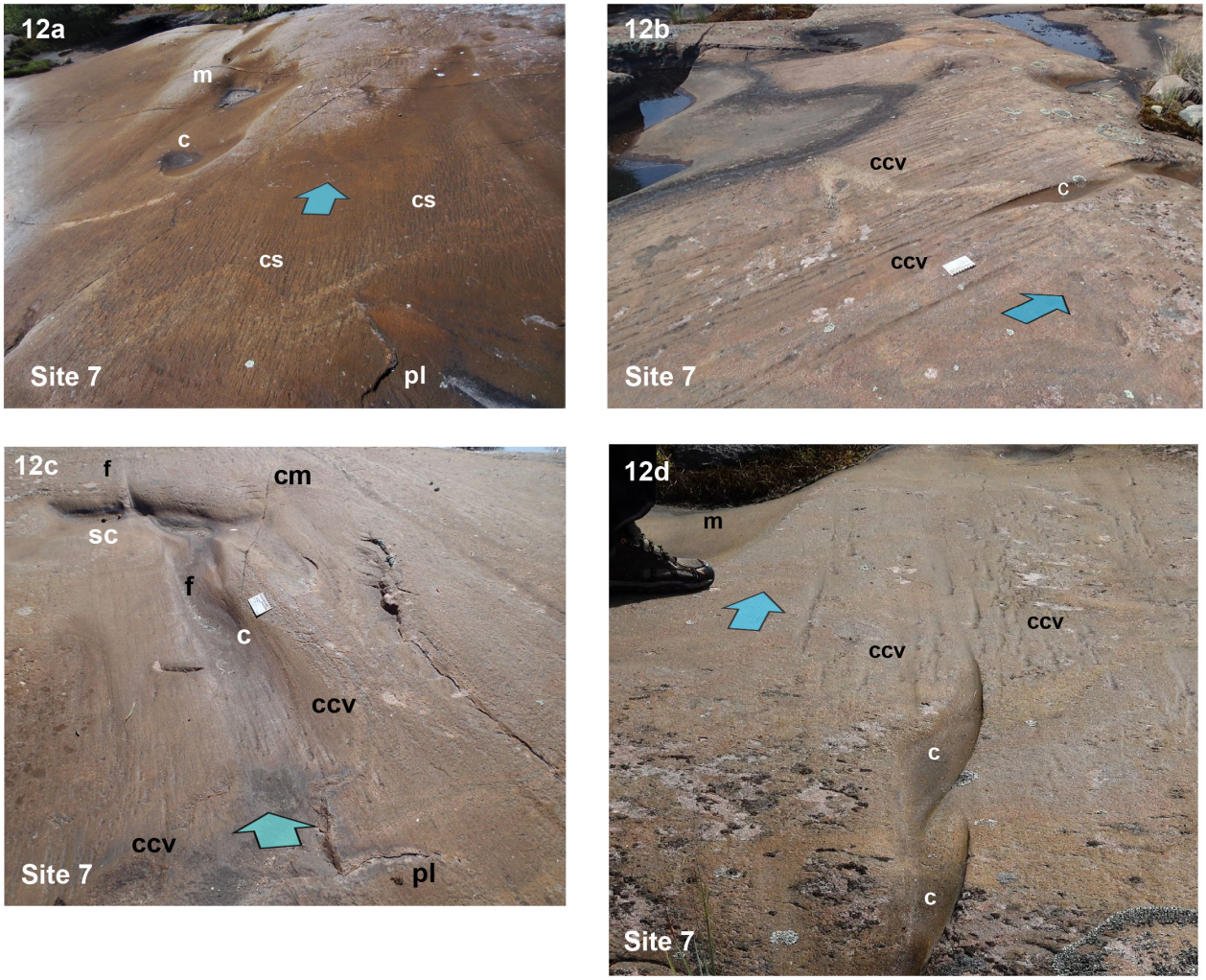

Figure 12: a) Fields of carrot-shaped (cs) erosion forms with commas (c), muschelbrüche (m) and minor plucking (pl). Note that the cs paleo flow (blue arrow) is at a slight angle to, and 'cuts' across the larger, comma (c) form. b) slight comma-shaped arms of a carrot form (ccv) and similarly-shaped forms with smooth comma (c) is the extended arm of a sichelwannen (out of view). c) carrot shaped forms (ccv) within and oriented towards a comma form (c); note also crescentic chatter mark (cm), furrow (f), sichelwanne (sc); carrot forms (ccv) occur near plucking with up flow and side facing scarps (pl). Scale card is 4.5 cm long. d) down flow view of comma form (c) and close association with comma-shaped carrot forms (ccv); notice to the right of the ccv label clusters of smaller ccv forms that have a right arm to the comma shape. Note muschelbrüche (m) 'top left' of the blue directional arrow. Photographs by D.R. Sharpe. NRCan photos 2022-509, 2022-510, 2022-511 and 2022-512.

Bedrock features are organized into flow sets: s-forms and sichelwannen, fields of pitted streaks, carrot marks (see description below), and are uniquely orientated near crescentic breaks/ steps (**Plates 11.1, 11.2**). At the pitting scale (mm-cm), we observe flow set variation involving crescentic breaks and s-forms. Tadpole-shaped pitted forms are self organized and aligned with mineral scale fine lamination (**Plate 11.8**) and their differential erosion (very delicate stair steps a few mm high). A detail study of a 3 m^2 area (**Plates 11.6, 11.7, 11.8**) shows that small relief (plucked breaks 12 cm high) locally deflected the orientation of lee side tadpole shapes before they realigned with the main flow (**Plate 11.6**). Such delicate features may inform on origin: ice abrasion or water erosion. This low obstacle was also marked by a crescentic break matching the fine gneiss layers (**Plate 11.7**).

8 **Outer Bottle Island** (45°55'07"N, 81°00'29"W; 176 m a.s.l.)

This site is on a low-relief coastal island where the structural trend is ~EW; erosion forms are also oriented NE (**Fig. 3**). The low relief most likely contributed to the formation of more longitudinal forms than transverse forms. Stoss-side

furrows, transverse troughs, sichelwannen, muschelbruch and commas occur on rising slopes, with spindle flutes, furrows and small rock drumlins are prominent on the upper rock surface. Rounded boulders occur between outcrop rises.

Pitting streaks were observed on the down flow rise in spindles and commas, and on upper rock surfaces. There is a modest amount of plucking where low relief rock drumlins occur at distal ends of the island.

9 **Bottle Island** (45°55'23"N, 81°00'53"W; 176 m a.s.l.)

A low-relief coastal island site where structure trends are ~EW while erosion forms were eroded from the NE. Predominant are low-relief sichelwannen, commas, furrows and small rock drumlins (**Plate 2.1**). Small transverse troughs and rounded plucking features were observed at low structural breaks (**Plate 5.1.6**). Other plucked blocks have up flow and down flow rock lips (perhaps requiring upward lift to become dislodged?). On the up flow (NE) side of the island, stoss-side and elongate furrows, and related rock drumlins were also observed.

10 **South Bustard Island (**45°52'33"N, 80°55'10"W; 176 m a.s.l.)

This moderate-relief coastal island shows ~NS structure trends (dipping to the west) and s-forms eroded by flow trending from the NE. Rock drumlins are prominent with scoured surfaces, furrows, cavettos and plucked distal ends. Sculpted forms (cavettos, furrows, flutes and fluting) are closely associated with plucking, some juxtaposed with flutes cross cutting the plucked face (**Fig. 13**). Striated surfaces are observed on longitudinal forms (e.g., commas, furrows) that crosscut one another. Potholes were also observed along structural fractures in the rock (**Plate 3**).

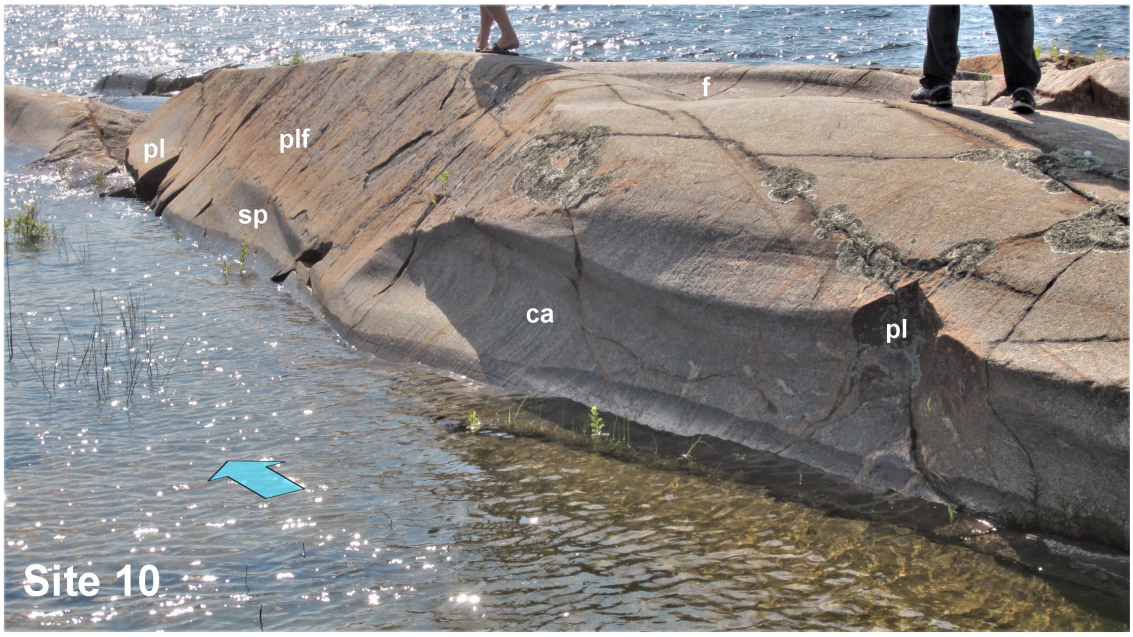

Figure 13: Sculpted forms (e.g., cavettos, ca), furrows, f) are closely associated with plucking (pl), some juxtaposed with spindle flutes (sp) cutting across a plucked face (plf). Blue arrow indicates flow direction. Photograph by D.R. Sharpe. NRCan photo 2022-513.

11. **North of Whistler Bay** (45°55'16"N, 80°44'36"W; 176 m a.s.l.)

Large fields of rock drumlins occur at this site, cutting across the folded structural grain of a burnt landscape, as revealed by aerial images obtained from a drone flight (**e.g., Plate 10.4**.). The pattern produced by these fields of rock drumlins with intervening valleys (transverse troughs) is observed as a strong linear feature on 1:50,000 aerial photographs (e.g., figure 4, Kor et al. 1991). Crescentic furrows highlight rock drumlins on the upflow, stoss-side rises of these eroded forms. Cavettos, furrows and spindle flutes ornament the walls of some inter-drumlin areas where meltwater lag deposits of large, rounded boulders occur.

12. **Whitefish Bay** (45°55'36"N, 80°56'00"W; 176 m a.s.l.)

This site occurs down flow of a 1991 study site (Kor et al. 1991, figure 8) that presented large fields of intersecting sichelwannen on the up-flow side of an upland. Terrain tapers down flow to a low-relief landscape. Transverse troughs related to the systematic fractures of the bedrock (**App. 6**) delimit many uplands. The Whitefish Bay site has a wealth of furrows down flow of low-relief sichelwannen, commas and spindle flutes (**Fig. 14**). Sichelwannen troughs trapped large rounded and percussion-fractured boulders (**Fig. 15**). Erosion streaks are common outside of s-forms, yet they also occur inside well-sculpted forms. Potholes and plucking are sparse at this site, but crescentic chatter marks are observed similar to those at site 7 (**Fig. 16**). An aerial view of the site (**App. 6**) illustrates the transition in forms as flow approached a rock rise, continued across the upland surface and proceeded to the distal end of the site. Boulders are trapped in long furrows, stoss-side furrows, fractures and on lee side steep slopes.

Figure 14: Long furrows (f) linked to comma forms (c) and sichelwannen (sc). Note large, rounded boulders (ro) on eroded surface (people for scale). Blue arrow indicates flow direction. Photograph by D.R. Sharpe. NRCan photo 2022-514.

Figure 15: Sichelwannen contain large, rounded boulders (ro) with percussion marks (pc), and angular boulders (a) are trapped in smooth rounded furrows (f) and crescentic troughs (sct). Boulder accumulations follow trough formation and are associated with the waning stage of a meltwater flood discharge. Blue arrow indicates flow direction. Photograph by D.R. Sharpe. NRCan photo 2022-515.

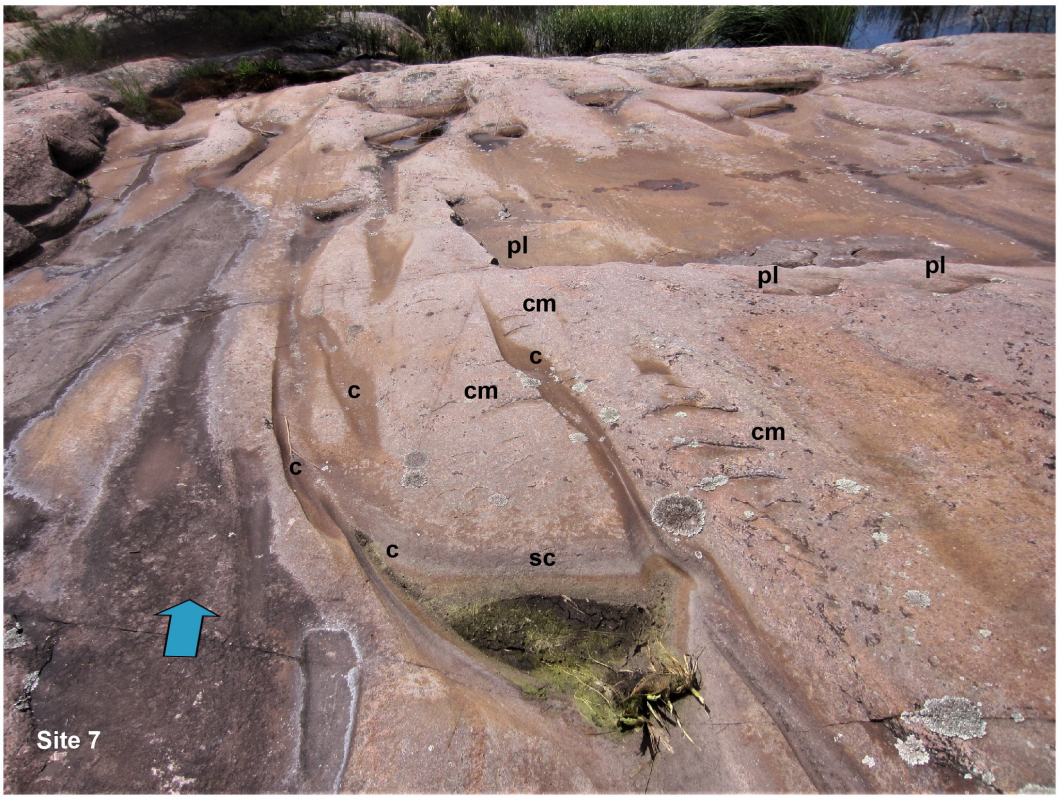

Figure 16: Sichelwannen (sc) arms extend down flow as commas (c) adjacent to crescentic chatter marks (cm) and plucking (pl), with up flow- and down flow-facing fractures. Blue arrow indicates flow direction. Photograph by D.R. Sharpe. NRCan photo 2022-516.

13. Lost Key (45°50'23"N, 80°43'05"W; 176 m a.s.l)

Stoss-side troughs lead to shallow sichelwannen and streaks are observed at this site where the outcrop rises to ~ 10 m in height. Potholes are prominent on steep down flow areas.

14. Sand Bay (45°56'40"N, 80°44'20"W; 176 m a.s.l)

This burn site provides access to new observations of rock drumlins, sichelwannen, spindle flutes, streaks, cavettos and troughs with boulder clusters in areas of sediment traps.

15. Inlet East of Fox Island (45°55'09"N, 80°48'08"W; 176 m a.s.l)

The site is a long inlet and ridge set parallel to the rock layers (**App. 8**), crossed by NNW flow.The inlet has cuesta-like geomorphology (see **Plate 9.1**). Down flow, the inlet (west shore) has stoss-side ramps, s-forms and rock drumlins (see **Plate 4.2**, **App. 8**). Up-flow, the inlet (east shore) is steep, has cavettos (>1 m), plucked forms and exposes the rock layers and bedding joints (**App. 8**). The bedding joints are not open as at sites 4, 5, 5a (e.g., **Plates 9.5, 12.7**).

16. Inlet East of Whitefish Bay (45°55'37"N, 80°55'42"W; 176 m a.s.l)

Flow direction is parallel to inlets and ridges (**Fig. 3**) and to long furrows (> 1m), which are all concordant with the gneiss layers and bedding joints (**Plate 9.6**). Many ridges have flat surfaces with fields of s-forms (**Plate 9.6**). Streamlined ridges have plucked and modified ends (**Plate 9.6**). Site erosion is shown in a diagram (**Plate 9.3**).

Structural geology and subglacial erosion

A preliminary assessment of the study area indicates that there is a link between geologic structure and the style of subglacial erosion (**Fig. 3**). At the mouth of Key River, the shoreline reflects elements shaped by lithology, structure of a large synform and the Key River fault line (**Plates 9, 10**).

Lithology: North of the Key River fault line and west of the synform hinge (sites 4, 5, 7, 11, 14), inlets are eroded; more specifically in rock unit 4 (intermediate to felsic rocks) and rock unit 5 (intermediate to mafic migmatitic rocks, **Fig. 3).** On the 'soft' bedrock of Germain Island (see **Plate 12.1**), amphibolite was vulnerable to pitting. Gneiss and pegmatite were more resistant (silica rich) resulting in differential erosion **(Fig. 21**). Weakly foliated, felsic intrusive rocks constitute higher ridges and islands. The topography near the hinge and east of the synform (**Fig. 3**) is characterised by long rock drumlins grouped by identical size in a series of parallel rows (**Plates 10.2 to 10.5**). The rock drumlin rows begin at the depression within eroded soft layers. Only the east-west fault lines of Key River and Henvey Inlet dissect this streamlined plateau (**Plates 10.1, 10.3, Fig. 3**).

Geological maps by Culshaw et al. 2004 show that strike and dip conform to the general structure of the regional synform (**Fig. 3; Plate 10.1**). A clear correlation is established between layer geometry and direction of subglacial water flow (blue arrow in **Plate 9**). **Table 3** provides details on the links between structural and subglacial erosion forms (**also see videos 1** and **6**).

INTERPRETATION

The agents of glaciogenic erosion are well known (Alley et al. 1997): abrasion, plucking (quarrying), and mechanical erosion by meltwater. Subglacial dissolution has also been recognized (Hallet 1996), but it is not a likely process to have eroded the very hard silicate rocks outcropping around Georgian Bay. The mechanisms of erosional processes responsible for the geometry of rock forms in the study area are less well known and our observations test this knowledge.

Overall, our observations and analysis support, and extend many of the interpretations of Kor et al. (1991) in which they emphasized the significance of broad, erosive subglacial meltwater flow. We focus on the central issue of how the variety, distribution and style of erosion forms relate to formative flow processes, as well as to the role of rock lithology and structure. Of note, the erosion forms and classification used in this study are similar to those used by Bryant and Young (1996) to describe and interpret forms related to coastal tsunami erosion.

Striations and crescentic fractures

Scattered striations (**Plate 7**) and crescentic fractures occur in the study area in combination with a wealth of sculpted erosion forms (**Fig. 16**). Striations are interpreted as ice abrasion forms that result from a combination of basal ice velocity, the pressure exerted by rock fragments on the bed, the shape of the bed, and, the amount of debris in the basal ice (Hallet 1981). Since Key River rock surfaces are adorned with s-forms, they were also likely eroded by subglacial meltwater flow (corrasion; Kor et al. 1991), during glacier lift-off from the rock surface. Sparse dragged tool marks on the rock bed resulted from ice re-grounding following meltwater flow. This sequence would explain light striations observed on sculpted forms. Ice grounding did not re-mould the sharp rims common on many s-forms (e.g., **Fig. 10**); thus, light striations ornament the sculpted forms rather than producing them (Gray 1981; Sharpe and Shaw 1989; Kor et al. 1991). These features and the recorded sequence of events support the concept that the ice lifted from the rock surface during meltwater floods with flow depth on the scale of meters (e.g., Shoemaker 1992). This meltwater flow (**Fig. 17**) removed debris-rich ice during scouring (Kor et al. 1991), and lightly abraded rock surfaces with sparse tools that remained in the re-grounded basal ice.

Several features appear to be the result of relatively high velocity ice flow recoupling with the rock bed. These include: (i) strong striations superimposed on s-forms; (ii) facets on some clasts with parallel striations on alternate facets, but different striation directions on these facets (**Fig. 18**), and, iii) bedrock fractures in brittle rocks, which record failure under extremely high glacial shear stress (**Fig. 19**).

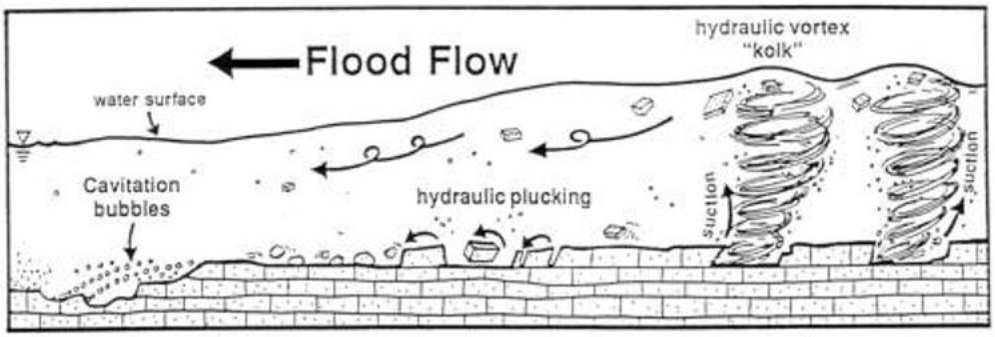

Figure 17: Model of fluvial erosion in high-velocity river flow (from Wilkinson et al. 2018) showing processes of fluvial erosion due to vortex erosion, hydraulic plucking and cavitation.

In the presence of strong evidence of meltwater erosion, is it also possible that both un-striated and striated spindle and comma forms are fluvial in origin despite the presence of 'striations'. Striations with short erratic patterns occur within and around smooth rock depressions (**Fig. 12**); are these abrasion striations or cavitation marks (e.g., Hjulstrom 1935)? There is some support that these striations are ice abrasion features (e.g., Eyles 2012) while others suggest erosion by cavitation (e.g., Bernard 1971; Gray 1981).

We infer minimal glacial abrasion (Shaw et al. 2020), or highly selected abrasion at Key River resulting in un-striated closed spindle flutes and minimally striated forms (e.g., Cavitation Island, **Plate 6.3**). We note that the shape and pattern of the striated spindle forms are identical to the un-striated spindle forms. These observations are consistent with spindle forms being glaciofluvial in origin and that abrasion was not a viable explanation for spindle formation, as is claimed by some (e.g., Boulton 1974; Rea et al. 2000).

Long, lee-side crescentic breaks (**Plate11.1**) within fields of s-forms at Cavitation Island are the result of cuesta-like differential fracture (plucking) of bedding joints of a 'finely laminated' gneiss broke. Similar forms at a smaller scale (mm-cm) observed between sets of elongate pitted forms and mineral lamination (**Plates 11.6, 11.7, 11.8**).

Small crescentic fractures occur facing up flow and down flow (**Figs. 12c, 16**) record evidence of ice erosion or quarrying (Hallet 1996; Krabbendam et al. 2017). Because these fractures (chatter marks to some) are closely associated with s-forms they were likely eroded as ice re-grounded on the rock bed. Some crescentic fractures (**Fig. 16)** show evidence of rounding, indicating that plucking and meltwater erosion occurred simultaneously. Hydraulic plucking is a significant, erosion process in many fluvial bedrock settings (**Fig. 17;** Whipple et al. 2000; Dubinski and Wohl 2013; Beaud et al. 2016); thus, the prominence of glaciofluvial erosion at Key River makes hydraulic plucking a plausible erosion mechanism as well as erosion by ice.

Figure 18: Multi-faceted striated clast strongly abraded during ice recoupling with the bed (see Hallet's theory on abrasion). Quarter for scale. Photograph by D.R. Sharpe. NRCan photo 2022-517.

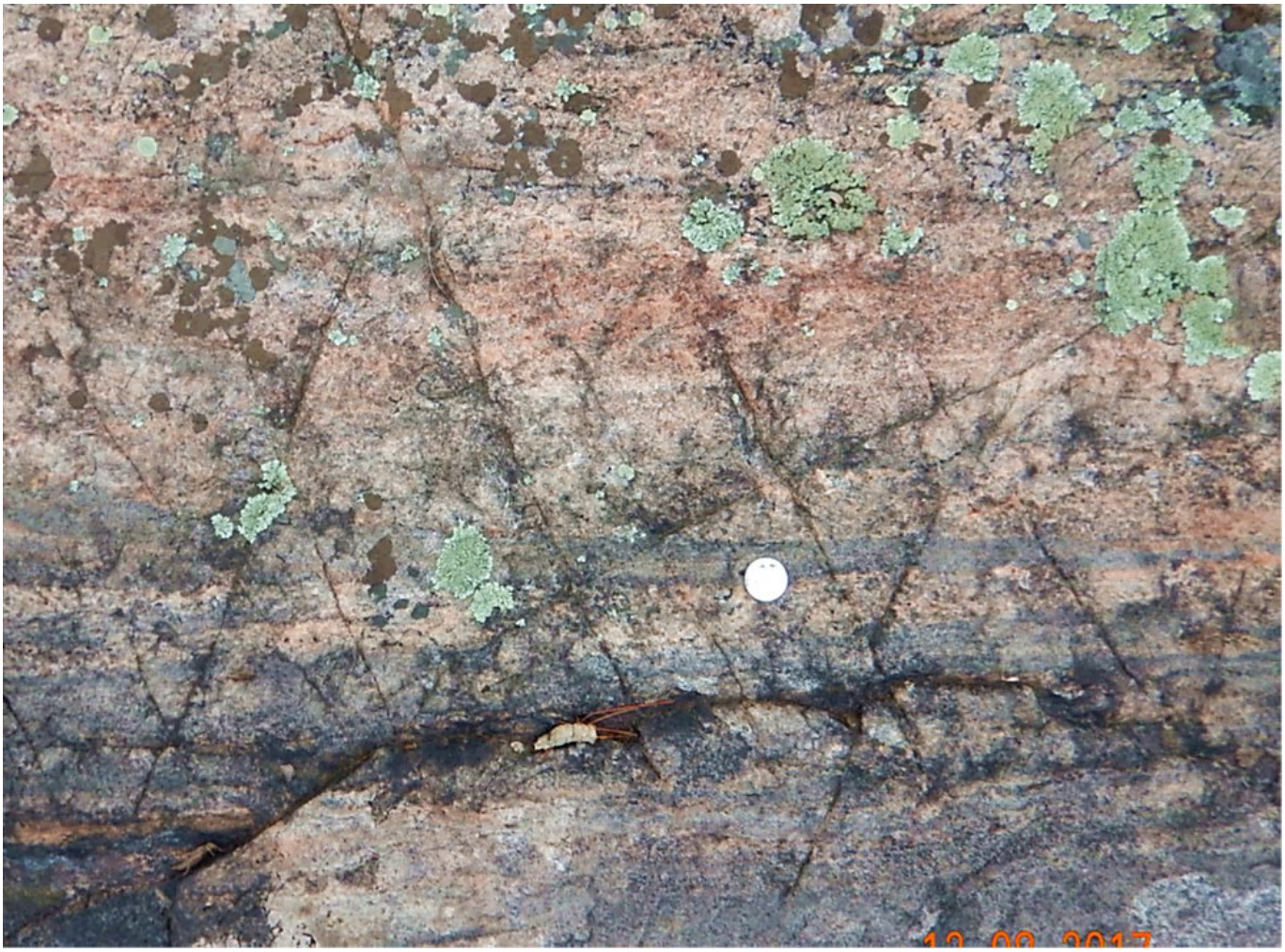

Figure 19: Bedrock failure indicated by crossing fractures with displacement of one fracture, "Plucking Island". Quarter for scale. Photograph by D.R. Sharpe. NRCan photo 2022-518.

The long breaks at Cavitation Island appear to be the result of differential erosion (cuesta-like) upon the bedding joints of a finely laminated massive gneiss. Of interest, a similar analogy is found at a smaller scale (mm-cm)

between the countless elongate pitted forms and mineral lamination (**Plates 11.6, 11.7, 11.8**). Cuesta form that face up flow are referred to as 'forward-facing escarpment' (Shaw et al. 2020).

S-form Origin

A recent review of subglacial s-form types by Shaw et al. 2020 identified three broad styles of erosion: i) obstacle marks (Allen 1971), ii) shallow basins, and, iii) forms at forward-facing escarpments. Obstacle marks and shallow basins are predominant types of erosion in the northern Georgian Bay region.

Obstacle marks

Flow against an obstacle (wall /bluff) is a common process in varied erosion settings studied by sedimentologists and engineers (e.g., Andrews 1883; Karcz 1973; Allen 1984; Paik et al. 2007). Obstacle scour (**Fig. 1**) leads to a set of transverse and longitudinal bed forms, obstacles marks, which include crescentic scours (furrows), remnant ridges, rat-tails and rock drumlins (Shaw et al. 2020). Flow past obstacles attached to the bed creates differential velocity and increasing fluid pressure along the forward-facing side of the obstacle with height above the bed (Allen 1982). This sets up a reverse eddy that separates from the bed and combines with divergent flow around the obstacle to produce a helical horseshoe vortex that wraps around the up flow face and each side of the obstacle (**App. 4**). Paired horseshoe vortices carry high velocity fluid that results in crescentic scouring of the bed (Shaw 1994). As the paired vortices re-join main flow past the obstacle, the eroded furrows become shallower and broader, while leaving a remnant ridge (rat-tail, rock drumlin) in the lee of the obstacle. These forms are illustrated as images (**Figs. 4, 9, 11, 16**) and as a conceptual process model displayed in Shaw (1994; **App. 4**). An understanding of these processes helps decipher our observed hierarchy in crescentic forms (larger forms intersected by smaller forms, **Plates 12.5, 12.6**); this indicates structure in the eroding flow and simultaneous erosion with different scales of flow turbulence (Allen 1982).

Shallow basins

Shallow basins comprise a family of finely sculpted and distinctive erosional marks forming low longitudinal or transverse depressions in rock surfaces (e.g., **Fig. 12; Plate 2.3**). They occur in three principal forms: spindle, muschelbrüche and sichelwannen, with a comma form variant. These forms commonly occur in an organized array on bedrock rises as shown in **Fig. 11** and **App. 2**.

Spindle flutes

Spindle flutes are subglacial meltwater erosion forms where they have superimposed light striation (Shaw 1988). They likely result from vortices impinging on the bed during turbulent meltwater flow (Kor et al. 1991; Shaw et al. 2020). A unique formative process explains narrow, shallow, spindle-shaped (open or closed) marks, which are generally internally unadorned, and form sharp bounding rims which point up flow and smoothly broaden down flow (**Plates 1.4; 5.1.3**). Similar forms, observed on the base of turbidite beds (Dzulinski and Walton 1965), have also been produced in flume experiments under turbulent flow regimes (Allen 1971).

Muschelbrüche

Muschelbrüche, mussel-shell-shaped, shallow depressions with sharp, convex up flow rims, and, indistinct, down flow margins merging imperceptibly with adjacent rock surfaces (**Fig. 12a**; **Plate 2.3**), are features unrelated to known ice erosion (Hallet 1981; Iverson 1991). They have no internal ornamentation and being identical to simple flutes (Allen 1982), they also relate to higher-velocity, process dynamics. For example, Elliot (2000) illustrates similar flute forms in marine rocks with sharp edges about 15 m wide in Upper Carboniferous strata. Normark et al. (1979) recorded similar forms, crescent-shaped depressions up to 500 m wide, scoured into the surface of Navy Submarine Fan sediments off the California coast. These forms require high-energy turbulent flow, which evidently operated with vortex flow structures striking the bed at multiple scales (Allen 1971). The lack of internal ornamentation on spindle flutes and muschelbrüche indicates no flow separation at the leading rims, no multiple vortex erosion, and the likely impingement of a single vortex on the rock bed as these two forms evolved (Shaw et al. 2020).

Sichelwannen

Sichelwannen (**Figs. 11, 15, 16**; **Plates 2.2, 2.5**) are identical to the flutes of turbidite sole marks (Allen, 1982) and likely have a similar origin. The convex proximal rim is invariably sharp and normally crescentic, a form element considered to indicate separation in the formative flow (Allen 1982). Sichelwannen display internal ornamentation with a primary furrow wrapping around a median ridge, and a secondary, much smaller, lateral furrows along the rim (**App. 2).** Sichelwannen are also asymmetrical in longitudinal section, as muschelbrüche, with steep slopes beneath the proximal rim, and gentle distal slopes of the primary furrow rising to merge with the surrounding bed (**Fig. 15**). A particular feature of Key River forms is that primary furrows extend < 100 m downstream (**Fig. 14**) and as a result the median ridge forms a rock drumlin (**Plate 2.2**)**.** This process-form model is similar to the formation of rock drumlins with residual ridges resulting from hairpin scours (Shaw 1994). The principle of equifinality appears to apply (Shaw et al. 2020), as the same form results from

different flow mechanisms with hairpin scours being related to horseshoe vortices while sichelwannen are related to flow separation.

The principal vortex pattern for sichelwannen, although similar to that for obstacle scour marks (**Fig. 4b; App. 4**), requires a different formative mechanism (Shaw et al. 2020) to explain its distinct features. Flow separation for sichelwannen occurs due to low pressure down flow from the rim, which causes the flow to turn back on itself; this 'separation bubble' is similar to that in the lee of ripples and dunes (Allen 1982). An open roller forms where the rim is orthogonal to flow, and a spiral vortex appears where the rim is oblique to flow, giving rise to crescentic scours (Koken and Constantinescu (2011). Thus, horseshoe-shaped vortices, which wrap around a median ridge, account for the internal features of sichelwannen and are to be expected with flow separation at a convex rim (Allen (1982, his fig. 7.25). Furthermore, lateral furrows result from a single, counter-rotating vortex spawn by the primary vortex in the main furrow (Allen 1982).

Comma forms (**Fig. 12**) are hydrid sichelwannen, in which one arm of the lateral furrow becomes dominant as the paired vortex roller on one side of the remnant ridge rejoins or breaks down in the main flow. Commas, as Sichelwannen, appear as isolate and conjugate features, commonly found together with muschelbrüche and spindle flutes (Shaw et al. 2020, figure. 4). Extending down flow from sichelwannen, comma arms are elongate furrows on the level, low relief portions of rock surfaces (**Fig. 14**). In aerial view, these furrows and furrows that extend down flow from crescentic (hairpin) scours, form streamlined bedrock common across the Georgian Bay region (**Fig. 4**).

Experimental spindle-form flutes, muschelbrüche and sichelwannen can be produced by fast-flowing, turbulent water over a plaster-of-Paris bed (Shaw 1996). These experiments act as representations for subglacial bedforms (Shaw et al. 2020, figures. 5A and B) because two sets of forms, experimental/ analog and subglacial, are identical and genetically the same, with common terminology. Both analog and field forms (sichelwannen) show convex upstream sharp rims, median ridges, principal and lateral furrows and longitudinal asymmetry **(Fig. 15**). These features also occur together on the same eroded bed with spindle flutes and muschelbrüche. Conjugate forms result in truncated residual ridges ('r' in **Plate 2.5**), tapering distally over a short distance to a sharp point.

Cavitation

The occurrence of non-traditional small-scale erosion forms with well-preserved s-forms (e.g., spindles, furrows, commas, sichelwannen and muschelbrüche (**Plate 6.3**), (**Table 2**) indicates formation in high-velocity meltwater flow. Pitted erosional streaks (**Fig. 12; Plate 11.6 to 11.8**) are interpreted to form due to cavitation; that is, erosion by high-velocity aqueous jets within turbulent flow. Micro-jets strike the bed with violent impacts as vapour bubbles collapse (Hjulstom 1935; Barnes 1956; Dahl 1956; Bernard 1971; Shaw et al. 2020). While the occurrence of cavitation in natural rivers has been debated (Carling et al. 2017; **Fig. 17**), it has been demonstrated in laboratory studies (Bourne and Field 1995) and is a well-known in engineering studies, to be a high-velocity, clear-fluid erosion process that damages hydraulic structures (e.g., Falvey 1990; Dular et al. 2004; Dular and Petkovšek 2015).

Pitted streaks are unlike the three classic forms of striations commonly found on abraded surfaces. Classic striations are: i) shallow, narrow, steadily increasing in width and depth, with abrupt termination; ii) similar form to first, yet steadily decreases in size, then terminates as it started; iii) form that starts abruptly and gradually tapers out (Iverson 1991a, figure 4). Pitted streaks observed in the study area may appear to be similar to type 3 striations, however, type 3 erosion forms are usually isolated and occur more or less randomly. Type 3 striations indicate the tendency of some clasts in ice to rotate, but it would be unlikely for a group of clasts (pitted streaks; **Fig. 12**) to behave as a cluster (Iverson per. Comm. 2020). Type 3 striations also tend to narrow to a point less rapidly along their lengths than pitted streaks, which tend to have a carrot shape that tapers down flow. If the observed pitted marks were eroded by clasts, the marks should have crescent-shaped fractures at their bottoms (which pitted marks do not), with their open ends pointing down-glacier (not observed). Such abrasion fractures form in tension along the trailing edge of clast-bed contacts (Iverson 1991a). None of these abrasion features were observed within pitted and nearby related streak-like forms in our study area. On the other hand, smaller forms (< 1mm) similar to pitted streaks have been produced in a laboratory experiment (Carling et al. 2017 figure 6). Hence, cavitation or hydraulic abrasion (corrasion) is a plausible mechanism for the origin of elongate erosion forms that we call pitted streaks.

Pitted streaks are associated with a series of s-forms (spindle flute, musclebruche and comma forms; **Fig. 12**; **Plate 11.4**) that likely formed due to the impingement of vortices on the bed of high-velocity meltwater flow (Kor et al. 1991; Shaw et al. 2020). Because vortices can generate cavitation (Kenn and Minton 1968), it seems that fields of fast-moving vortices in the meltwater flow may have created arrays of pitted forms. This is likely the case where arrays of pitted forms occur down flow of bed steps (**Plate 11**), a setting which likely produced vortices associated with hydraulic jumps. The arrays also form small flow sets (**Plate 11.6 and 11.8**), indicative of complex turbulent flow (Koken and Constantinescu 2011). That pitted forms ornament the surface of well-preserved, sculpted forms indicate a meltwater process link that they formed late

in the flow event. Engineering research by Dular et al. (2004, Dular and Petkovšek 2015) indicates that cavitation erosion becomes viable at flow velocities of >10 m/ sec or higher (particularly under enhanced subglacial pressure regimes). Such flow velocities add to the power of the proposed erosive meltwater flood event(s). We suggest that as the flood event waned and ice closed rapidly towards the bed (Nye 1976), flow velocities increased such that cavitation became a prominent late-stage erosion process. The observed flow sets, s-forms, fields of pitted streaks, and carrot marks are uniquely orientated near crescentic breaks/ steps (**Plates 11.6, 11.7**). This observation leads to the conclusion that the crescentic breaks are a result of bedrock removal (plucking) during a meltwater sculpting process that produced s-forms and pitted forms.

Plucking

Plucking appears to have been an important agent of erosion in the study area and plucked forms are intimately associated with the sculpted features observed in many of the study sites. Plucking is commonly interpreted as solely an ice erosion process (e.g., Krabbendan et al. 2011), yet the association of plucked forms with high-velocity meltwater erosional forms may involve a more complex process model. The prominence of hydraulic plucking in fluvial bedrock channels (e.g., Dubinski and Wohl 2013), prompts us to assess the potential for glaciofluvial plucking at Key River.

The common occurrence of plucking with ragged surfaces on the down flow end of streamlined rock ridges (**Plate 5.1**) is credibly attributed to ice quarrying (Hallet 1996). At several sites, plucked surfaces have also been rounded and smoothed (**Plate 5.1.5**). In addition, there is a close association with meltwater erosion forms that surround the plucked surfaces (**Fig. 13**; **Plate 5.1.2).** This rough-smooth form association appears to indicate the simultaneous action of ice and flowing water. Iverson (1991b) has shown that lubrication from water at the glacier bed appears to increase erosion as ice velocity increases. Variations in subglacial meltwater storage and discharge likely created ice lift-off and bed re-attachment events (Shoemaker 1991**;** Magnusson et al. 2011), creating the potential for alternating or contemporaneous meltwater erosion and ice plucking events.

The close association of widespread meltwater erosion forms with more isolated plucked surfaces (e.g., **Fig. 13**; **Plate 5.1.2**) provides support for hydraulic plucking (**Fig. 17**; Carling et al. 2009; Wilkinson et al. 2018). Although poorly understood, plucking is a dominant mechanism of erosion in bedrock river channels (Whipple et al. 2013). Hydraulic plucking could explain the observation that some blocks appear to have been lifted rather than dragged from eroded Key River rock surfaces. In settings where blocks appear to have been plucked lateral to flow (**Plate 5.1.4**), the plucked surfaces are rounded and smooth (**Fig. 13**). Krabbendan et al. (2011) invoke ice stream erosion to explain lateral plucking. However, rapid flow with vortex structures could create the water pressure fluctuations needed to induce hydraulic plucking (Röthlisberger and Iken 1981; Iverson 1991b). Lateral plucking by ice has been favoured where joint control is prominent (Krabbendan et al. 2017), whereas flume experiments indicate that velocity or pressure variations (hydraulic pumping) around eroded blocks provide a sufficient mechanism to lift blocks: pressure gradients in the sub-bed crack network are enhanced by fluctuations in turbulent-flow pressure fields (Wilkinson et al. 2018). As an example, Tinkler and Parish (1998) observed erosion of bedrock slabs of 10 cm or greater in thickness that can be related to an estimated flow velocity of 6.6 m/s at the entrance to hydraulic jumps.

It may also to be possible for late ice plucking to follow widespread meltwater flow events. Such large meltwater flood events would have most likely lifted ice and eroded temperate ice from the base of the glacier. The remaining thin ice was likely cold and temporarily froze to the re-grounded rock bed. Any renewed meltwater discharge, or ice flow, would have likely caused ice plucking, such as the observed crescentic fractures at Key River. Alternatively, some crescentic fractures (**Fig. 16**) may indicate drag as the lifted ice re-attached to the rock surface.

Long, lee-side steps (like small cuestas; **plates 11.6, 11.7, 11.8**) at Cavitation Island indicate differential erosion of rock joints and mineral lamination. Where slabs of rock were displaced from crescentic breaks and detached along jointing and gneiss layering, several explanations need to be explored: i) frictional ice drag; ii) hydrodynamic pressure fluctuation; iii) hydrodynamic lifting (e.g., Wilkinson et al. 2018); iv) Bernoulli lifting; iv) ex-foliation jointing of near-surface layers.

Frictional ice drag would have removed any fine s-forms and pitted forms, yet delicate pitted forms (cavitation marks) have remained in a pristine state since the last ice cover (**Plates 11.6, 11.7**). It could be reasoned that subglacial hydrodynamic processes are likely the main origin of these terrain features.

An added point, long lee-side steps (depth > 20 cm) relate to fracture sets in the gneiss (**Plate 11.1**) and some are independent of rock structure yet have related s-forms (**Plate 5.1.2**).

Ice Recoupling to the sub-ice bed

Several features provide specific evidence of ice lifting and recoupling to the bed following subglacial flooding, these include striations, facetted/ striated rocks, fracture forms, and indirectly, cavitation and boulder percussion marks.

i) Weak local striations are superimposed on s-forms (**Fig. 10a**; **plates 7.1, 7.2**) and do not crosscut or erode the sculpted meltwater forms. This indicates that ice re-grounding followed meltwater sculpting with little expenditure of abrasion energy.

ii) Clasts with parallel and cross-cut striations on one or more facets (**Fig. 18; plate 7.3**) indicate abrasion and rotation of a clast in basal ice before continued abrasion. Because many clasts in the area show glaciofluvial rounding (**plate 8**), facetted clasts are interpreted as re-grounding abrasion which survived additional clast striation/faceting.

iii) Brittle crescentic fractures in bedrock (**Fig. 19**) indicate failure under extremely high, late-stage glacial load or shear stress (**Plate 5.4**). Crescentic fractures in the rock (**Fig. 16**) are clearly different from joint fractures, and they also indicate late-stage loading, following hydraulic lifting.

iv) Boulders with percussion fractures (**plate 8**), and rock surfaces with cavitation marks (pitted streaks) may both indirectly indicate re-grounded ice. Both features indicate that high-velocity subglacial meltwater flow, which allowed boulders to bounce rapidly along the sub-glacier bed. Similarly, inferred cavitation marks, associated with well-formed, low-relief s-forms, which are not over-printed by abrasion (**plate 6**), indicate ice lifting and recoupling to the bed. These features indicate late-stage formation as flow velocities potentially increased as ice closure reduced cross sectional area prior to final waning-flow meltwater discharge.

Tsunami forms

The proposed bedrock forms of Kor et al. (1991) inferred to result from turbulent subglacial meltwater flow have been recognized as being analogous to forms created during tsunami events that sculptured near shore rock surfaces (**Fig. 20**).

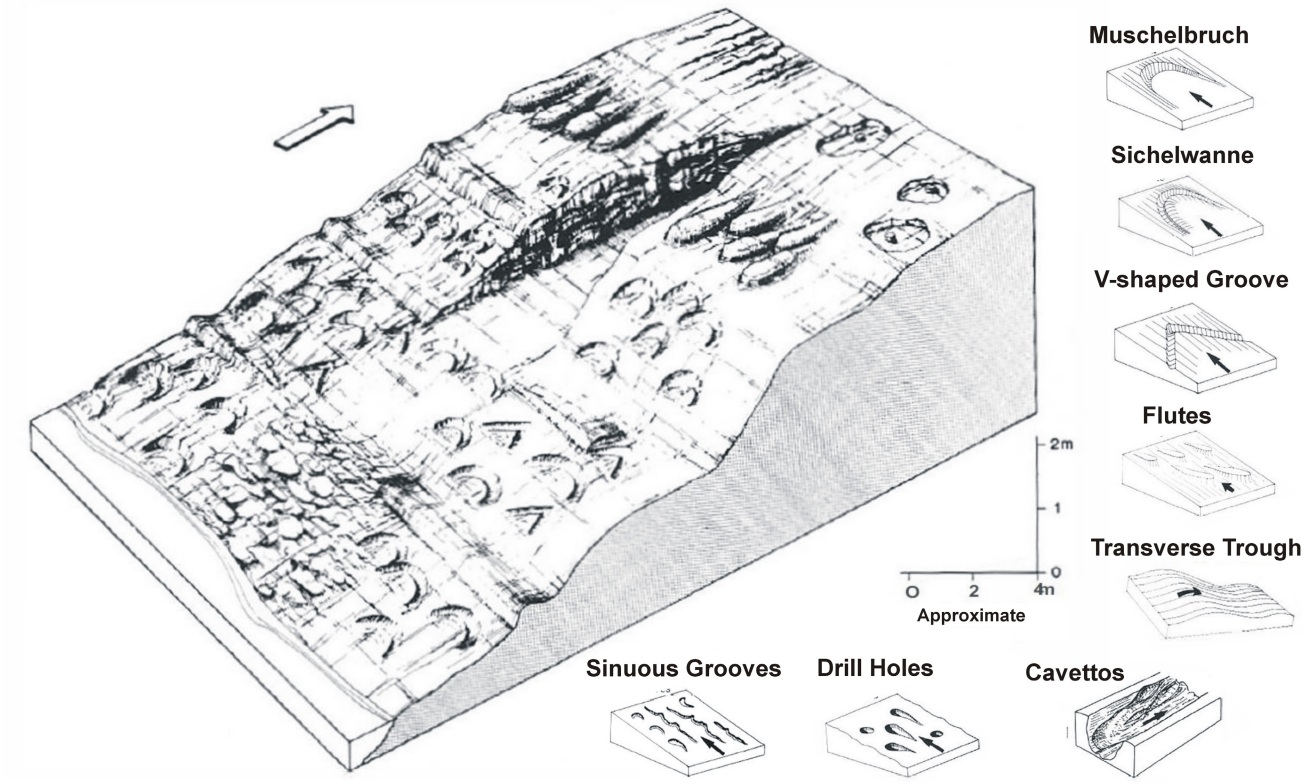

Figure 20: Schematic model for tsunami sculptured, smooth, small-scale, bedrock surfaces, analogous to that proposed by Kor et al. (1991) for subglacial meltwater flow. Major difference are the reversed orientation of many forms. Inset shows the model for unconfined tsunami flow producing a gradation of muschelbruch-sichelwanne "v" shaped forms upslope. (from Bryant an Young 1996, their Figure 16).

DISCUSSION

In addition to the influence of structural geology on the erosion forms, the extent, height, paleoflow and velocity estimates of the Georgian Bay erosional forms allow us to assess the likely scale and formative processes, and alternatives, as well as potential sources of water.

Large linear bedforms in glaciated terrain

Our observational data indicate that large linear rock forms (rock drumlins, furrows) are the product of meltwater erosion. This challenges the assertion that Key River forms are products of glacial abrasion (e.g., Eyles 2012; Krabbendan et al. 2016; 2017) under rapidly streaming ice. Our conclusion arises from longitudinal furrows, interpreted to be glacial grooves by Krabbendan et al. 2016, are meltwater erosion forms. In addition, no viable abrasion model has been presented that can explain the furrowed and crescentic-sculpted landscape around Key River.

Longitudinal furrows are clearly related to and transitional from crescentic troughs (**Fig. 14**; **Plate 1.2; App. 4; video 1**) and extend as arms of sichelwannen (and commas), specifically the scours at their up-flow ends. Crescentic scours are related to turbulent structures (horseshoe vortices) in meltwater flow (Shaw 1994; **App. 4**). Horseshoe vortices are routinely identified and simulated in engineering erosion studies (Paik et al. 2007). Longitudinal furrows occur at multiple scales, as hierarchy in turbulent flow structures. Small vortices produce spindle flutes and larger vortices produce long furrows associated with crescentic scours (Shaw et al. 2020).

This analysis contests Krabbendam et al. (2016) use of the term groove (their figure 3A), where they falsely represent crescentic troughs and furrows (adjacent to rock drumlins) as glacial grooves. Their selected oblique, low-level aerial photograph of crescentic troughs and furrows near Henvey Inlet (**site 1**; Kor et al. 1991) omits the critical crescentic form, which leads into the down flow longitudinal furrows **(Fig. 4**). Thus, the Krabbendam et al. (2016) omission implies that the furrow of the crescentic scour results in an abraded mega-lineated bedrock. The horseshoe/ hairpin vortex erosion model of (Shaw 1994) was not considered as an alternative to their abrasion model (Krabbendam et al. 2016).

The debris-rich-ice abrasion / streaming model of Boulton (1974) and rejected by Shoemaker (1988) does not explain the furrowed and crescentic-sculpted landscape. Nonetheless, Eyles (2012) and Krabbendam et al. (2016) adopted this abrasion model (Boulton 1974, figure 12) and declared that grooves were carved by narrow streams of dirty, debris-rich, basal ice. However, no theoretical, empirical, experimental or engineering support is provided for the proposed narrow-stream abrasion model (e.g., Eyles 2012; Krabbendan et al. 2016). The lack of debris in flood-eroded basal ice in the northern Georgian Bay region also minimized abrasion erosion because of insufficient tools (e.g., Hallet 1981; Shoemaker 1988). The idea that 'grooves are carved by streams of dirty (debris-rich) basal ice' (Eyles 2012; Krabbendam et al. 2016) is also counter to common reasoning; a deforming bed would more likely fill rather than erode a crescentic furrow. Only an improbable mechanism would cause rapid flow in a thin filament of debris-rich ice to erode a bed as it wrapped around the forward-facing slope of a rock obstacle. Thus, the sketch of common Georgian Bay field observations (**Fig. 1**; crescentic scours) by Andrews (1883), more likely involves vortex erosion than ice abrasion.

From the observed hierarchy in Key River crescentic forms **(Plates 12.5, 12.6**), we infer that there was structure and secondary flow vectors in a turbulent eroding flow indicating that erosion occurred at different scales of flow dynamics. This evidence of vortex structure in turbulent flow rules out the abrasion erosion model for crescentic-sculpted form in the study area.

Influence of structural geology on subglacial erosion

There is a clear link between geological structure and the pattern of subglacial erosion in the area. For example, the shoreline along the Key River fault is shaped into inlets and rises according to mafic-felsic lithology and layer geometry within a synform structure (**Figs 3, 21; plates 9, 10**). Softer rocks were susceptible to erosion and resultant depressions were exploited by vortex erosion. Higher ridges and islands characterised by long rock drumlins of harder felsic intrusive rocks deflected longitudinal vortices into adjacent troughs. Rock drumlin topography displays groups of identically sized forms in sets of parallel rows; this formed within soft-rock depressions as transverse troughs below rock rises. This rock drumlin orientation produced a lineated pattern to the streamlined plateau between the Key River and Henvey Inlet fault zone (**Plates 10.1, 10.3, Fig. 3**). Hence, feature orientation demonstrates regional flow coherence despite the structural complexity in northern Georgian Bay (**Fig. 3**).

The relationship between lithology and the style of rock erosion is illustrated at several sites. Structural control involving open joints, plucking and gneissic layering is evident (e.g., **Plates 5.1.2, 9.5, 9.7, 11.1, 12.7; Fig. 9; video 1**). Softer amphibolite rocks (**Fig. 21**), for example, are more easily eroded than gneiss and pegmatite; the form is also different because pitting (and foliation) occurs on amphibolite but not as readily on harder rocks. Fault lines and fracture zones become initiation points for rock rises to display an s-form sequence: transverse trough (tt), nested, overlapping sichelwannen (sc) with their longitudinal arms extending down flow to long furrows starting where the sichelwannen arms leave crescentic rough (f) (**App.6**).

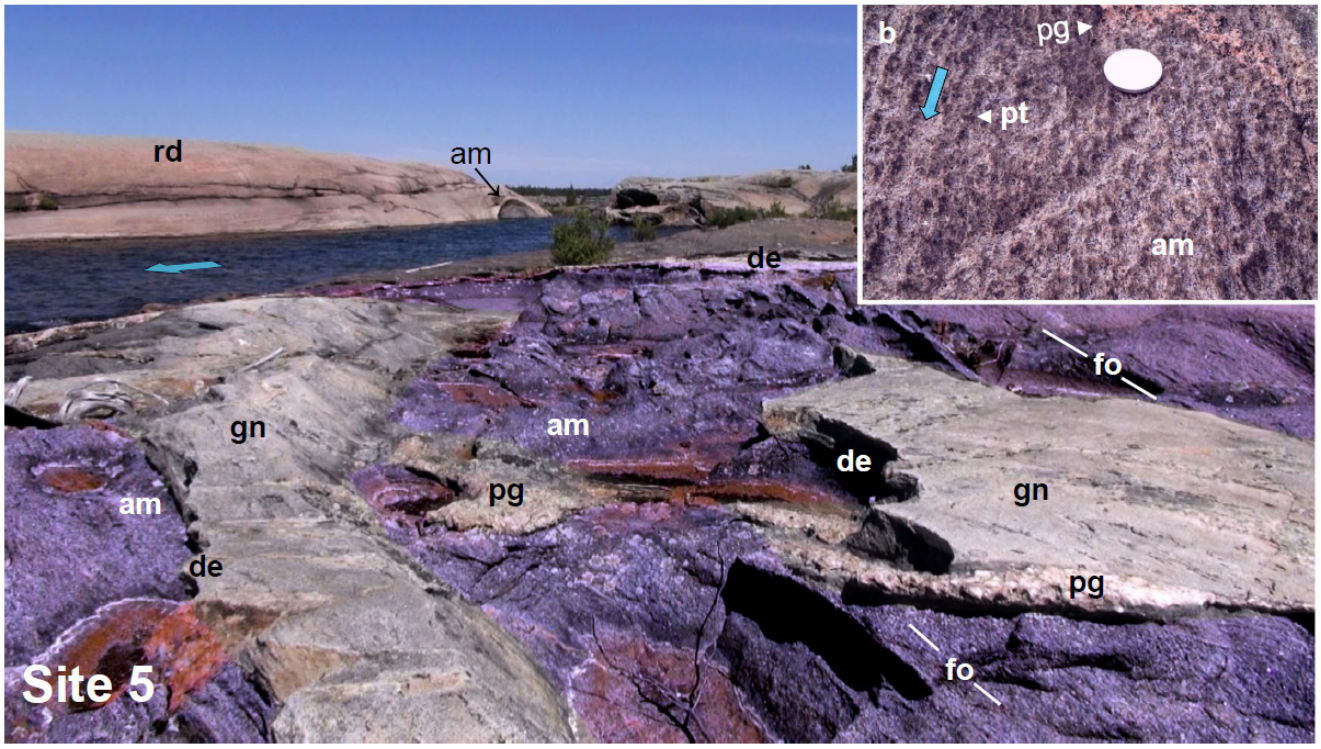

Figure 21: Differential erosion on 'soft' bedrock of Germain Island (see Plate 12.1 for location); amphibolite (am; colored in purple) was vulnerable to pitting erosion. Gneiss (gn) and pegmatite (pg) were more resistant (silica rich), resulting in differential erosion (de). Foliation (fo) is more apparent on amphibolite. Rock drumlin (rd) in the background indicates local flow direction (blue arrow). b) detailed view of flow orientated (blue arrow) with oval pitting cavities (pt) on amphibolite; note the positive relief of the small pegmatite vein (pg ►); quarter for scale. Photos courtesy of Guy Leduc.

Distribution and style of sculpted erosional forms

The distribution and arrangement of erosional marks at Georgian Bay closely conforms to bed relief, so that our findings support the idea that topography is an important factor in s-form type and organization (Kor et al. 1991). In areas of relatively high relief, we noted a collective asymmetry in style of erosion, related to interfluves between depressions orthogonal or oblique to paleo flow, best documented by drone aerial videos (e.g., Fox Island, Key River, Germain Island). At Fox Island (**Fig. 11**; **Plates 2.5, 2.6, video 3**), there is a predictable sequence of gentle, stoss-slope forms, to steeper lee-slope forms. This common motif trends from proximal rock rises with crescentic s-forms (**Plate 2**) transitional into longitudinal forms on distal slopes (**Plate 1**). The schematic representation of this sequence (**App. 2)** illustrates how the formative flow expended considerable energy eroding and, or, streaming around a topographic rise, then beyond the rise, energy in the flow was expended in producing elongate, straighter forms (e.g., Pollard et al. 1996). The transition from transverse to elongate forms is compatible with the expected behaviour of turbulent flow structures within continuous flow over a rise (Kor et al. 1991; Shaw et al. 2020). The relationship between the formative flow and s-forms (Shaw, 1994; Shaw et al. 2020) indicates that coherent flow structures, such as horseshoe vortices, develop across many scales (Allen 1971), a flow attribute that accounts for crescentic scour forms that range from ~1-1000 m in size (**Table 2).** Furthermore, forms that caused flow separation accentuated bed relief, thus increasing erosional rates, a feedback process that led to fields of multi-scaled sichelwannen (**Plates 2.5, 2.6**).

This interaction between the bed and flow structures also explains the geometry, location and scale of potholes (**Plate 3**; Kor et al. 1991). Potholes occur on both the down flow edge of large structural steps, Key River and Henvey Inlet **(Plate 3.1, video 5**), and, on small topographic steps. Potholes result when a flow vector that approaches a negative step in the bed

experiences flow separation and vortex generation at a hydraulic jump (e.g., Koken and Constantinescu 2011; Lanzerstorfer and Kuhlmann 2012). Both Key River and Henvey Inlet sites have long furrows (vortex erosion) leading into potholes, thus linking longitudinal furrows to vertical turbulent flow structures.

Based on extent and systematic topographic arrays (similar forms observed on similar slopes over a range of sizes), the formative flow structures provide information on scale, vorticity, separation, bifurcation, convergence (funneling), strength, and direction. These flow attributes may all be inferred from the erosional marks, sediment cover (scattered boulders) and their outcrop patterns in northern Georgian Bay. The inferred flow attributes imply meltwater erosion by powerful flow structures (vortices) operating at multiple scales (Allen 1971; Paik et al. 2010). Ornamentation of the sculpted forms by striation indicates that the meltwater flow was subglacial. Crescentic bedrock gouges may indicate that ice re-grounded on the bed with force; fractures on the crown of large boulders supports this inference of re-grounding. Thus, the Georgian Bay floods had a dynamic organization that produced a hierarchy of similar erosional forms at different scales, as indicated by rock drumlins that occur at the regional scale (>50 m wide), the local scale (10-15 m wide), the site scale (2-3 m wide), and the sub-site scale (<1 m wide) (Kor et al. 1991; **Fig. 4**).

Scale of the erosion events

The scale of the erosion events that sculpted the landscape in northern Georgian Bay region of Key River-French River can be derived from our field data and need to account for the following factors: i) extent and coverage of mapped forms; ii) paleoflow directions; iii) hierarchy of forms (multiple scales); iv) height of forms - depth of flow; v) velocity estimates.

Extent and coverage of mapped forms

We assessed, mapped and measured a wide range of s-forms in the north Georgian Bay region (**Fig. 2**) between Pointe-au-Baril and Killarney (**Table 2;** Kor et al. 1991). Distinguishable longitudinal, transverse and non-directional forms are present on most outcrops in the region, and at each recorded outcrop. S-forms cover more than 75% of outcrop surfaces. Our regional mapping of subglacial meltwater forms and their paleo flow indicators delimit a flow path at least 100 km wide (similar to Kor et al. figure 6). The flow width possibly extended westward to s-forms observed in the Manitoulin Island-McGregor Bay area[a] (Stanley 1934). The studied sculpted forms are remarkably consistent in size and style across this broad flow path, supportive of uniformity in the flow conditions within the meltwater flood. The internal structure of this regional flow was likely coherent and hierarchical and able to produce similar forms at both local and distant sites. This consistency in erosion form is supportive of the concept that the formative flow was a sheet flow (Shoemaker 1991; Kor et al. 1991; Flowers et al. 2004; Bjornson 2009). Although sheet flow is unstable and tends to channelize, a theoretical prediction by (-Shoemaker (1992) is observed by the channeled terrain of Georgian Bay and northern Lake Huron (**Fig. 2**), down flow of the study area. Some of these channels rise down flow as they approach escarpment ridges. This rising down flow channel form indicates formation under pressurized subglacial flow consistent with the French-Key River subglacial flow. This flow system most likely extended south of Georgian Bay to the water-sculpted terrain of the Bruce Peninsula (Kor and Cowell 1998) and the channelized sediment terrain of the Laurentian trough at the foot of Niagara Escarpment (Sharpe et al. 2018) and eastward (Brennand et al. 2006).

Form-flow coherence within the assemblage of forms and across a wide flow path are also compatible with the inference of a single regional event. This event scale may be correlated beyond the reported ~100 km wide zone to include the channelized landscape of Oak Ridges Moraine (Sharpe and Russell in review), eastern Ontario (Brennand and Shaw 1994) and the Kingston scablands (Shaw et al. 2020) and possibly Lake Erie (Munro-Stasiuk et al. 2005).

Paleoflow consistency

Kor et al. (1991) demonstrated consistency in s-form paleo flow direction across the ~100 km wide zone of mapped forms (their figure 6); mean paleo flow directions range from 213 to 223 at eight study sites. We obtained similar directional orientations at our 14 additional study sites where striations are less common yet occur with similar coverage as s-forms. Directional indicators also cluster tightly: s-forms (221 degrees, N=179), compared to 222 degrees (N=61) for striations (Kor et al. 1991).

Measurements of lineation on aerial photographs (linked to ridge and furrow forms on the ground, **Fig. 5**) show similar trends (**Fig. 22**) as those from small-scale forms, over a large area transverse to the flood. Channels present on the floor of Georgian Bay and northern Lake Huron have similar southwest flow orientations to the measured s-forms in the study area (**Fig. 22**). Further down flow on the Bruce Peninsula, striations were measured at mean directions of 220, s-forms at 237, and erosional rock and sediment drumlins, ~220-235 degrees (Cowan and Sharpe 2007; Kor and Cowell 1998).

[a] Stanley (1934) described >50 potholes in Huronian quartzite of the La Cloche Mountains, Whitefish Falls north of Manitoulin Island. These potholes are 0.5-4.5 m in diameter with visible depths up to 6 m.

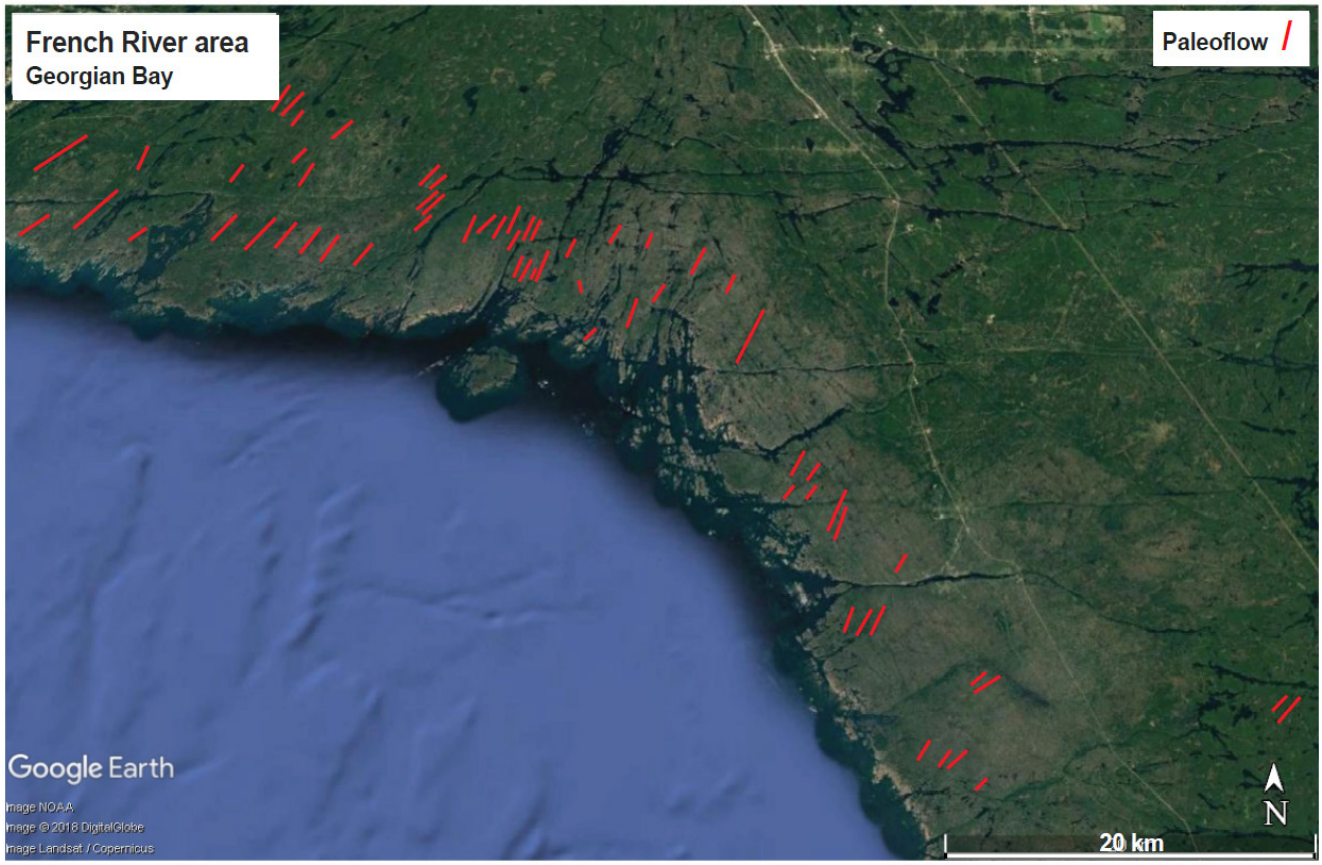

Figure 22: Paleoflow trends mapped based on lineations observed on Google Earth (crescentic scours, furrows and rock drumlin patterns; see similar map in Kor et al. 1991.

Height range of forms - depth of flow

Sculpted forms were observed to cover all rock surfaces up to a height of <25 m on low relief land adjacent to northern Georgian Bay. This height estimate is conservative and does not include s-forms that can be observed beneath the water. North of the study area, the slopes of the La Cloche (quartzite) Mountains rise more than 300 m above the level of Georgian Bay where the rocks also display sculpted forms. Hence, it is possible that minimum flow depth of a meltwater sheet flood was greater than 25 m. While the ice lid above the sheet flow could have potentially sagged to take up a portion of the 25 m flow depth, the bedform flow-depth relationship can help constrain the estimated flow depth. Bed structures in the 5 to 10 m range (dimensions of some sichelwannen/ rock drumlins) might equate to a 25-50 m flow depth, based on ~ 5 times bed form depth scaling (e.g., Paola and Borgman 1991). While these depths estimates are for open channel conditions, closed conduit flow appears to yield equivalent dimensions (Coleman et al. 2003).

Velocity estimates

Velocity estimates can be made using three criteria: i) boulders size and character; ii) plucking and, iii) cavitation features. Many boulders across the study sites are larger than ~25 cm, and they occur in clusters where many are rounded, and some show percussion marks (**Plate 8**). Kor et al. (1991) examined 158 boulders, most larger than ~0.3m, to estimate meltwater flow velocity. Flow competence removed most clasts less than 0.3 m diameter, and percussion marks on boulder surfaces indicate bed load transport by saltation for boulders < 1m. Relating these observations to empirical studies, yield velocity estimates of ~4 to 15 m/s (e.g., Elfstrom 1987; Maizels 1997).

Boulders

Boulders observed in the study area accumulated after the s-forms were sculpted. Rounding suggests fluvial mechanisms for transport of boulders; angular clasts were probably plucked from nearby outcrops with little transport. Ground and drone images show boulders preferentially deposited in s-form depressions (e.g., crescentic troughs /scours). The corollary is that most clasts smaller than ~ 25 cm bypassed these depositional traps and the study area. The widespread observation of boulder clustering in s-form depressions (**Fig. 15**) is consistent with related evidence (e,g., paleoflow directional consistency) that clusters and bypassed sediment were transported in a meltwater sheet flow event, rather than later re-organized by waves or lake ice. A sudden drop in sheet flood discharge is evidenced by deposition of boulders and cobbles, and smaller particle sizes (< 25 cm) were swept away, possibly in suspension flow.

There is a general lack of striations on rock surfaces, which is consistent with the likely bypassing of most sediment during meltwater discharge; it also appears to indicate a lack of debris in basal ice as it re-attached to the sub-ice rock surface.

Plucked forms, if due to hydraulic processes, foster a range of flow velocity estimates. Plucking of bedrock slabs of 10 cm or greater in thickness has been related to estimated flow velocity of ~6.6 m/s at the entrance to hydraulic jumps (Tinkler and Parish 1998; Wilkson et al. 2018). Plucked blocks of 0.3 to 1.0 m in size are present in the study area, so that meltwater flow velocities of >10 meters/s are possible or likely to have occurred. At several sites (e.g., Henvey, Pluck and Bootle islands) rounded plucked surfaces indicate that glaciofluvial flow continued after plucking events.

Cavitation
Proposed cavitation forms, mapped across the study area, may relate to flow velocities of >10 m/ sec (Dular et al. 2004), and likely much higher velocities under subglacial pressure gradients (Röthlisberger 1972). However, the erosive meltwater flood event(s) likely involved hydraulic ice lifting and drop-down events (Shoemaker 1991). Thus, as the flood event waned and ice closed rapidly towards the bed (exponentially according to Nye 1976, in tunnels), flow velocities may have increased rapidly to many 10's m/sec. This theoretical scenario may explain why cavitation forms appear to be a preserved late-stage erosion process in the study area. The general lack of small forms, (except cavitation forms) ornamenting large s-forms, appears to indicate rapid termination of the erosional flow (Shaw et al. 2020).

Event summary
Based on the above landscape assessment, the scale of the erosion events that sculpted the landscape in northern Georgian Bay region of Key River-French River involved regional, deep, high-energy subglacial meltwater floods as the primary agent (e.g., Shoemaker 1992). Ice erosion by abrasion, plucking and re-grounding played a lesser role in the erosional regime; yet, the full role of ice erosion may be masked by the prominence of meltwater-sculpted forms on the present day rock surfaces[b]. Nevertheless, the mapped forms indicate massive erosional meltwater floods that were up to 100 km across, <25 m deep, with consistent paleoflow indicators (~213-223 degrees). Vortex structures in turbulent meltwater flow produce a hierarchy of forms (multiple scales), which help to explain the width and depth estimates of the mapped meltwater erosional features.

Water source

The case for Georgian Bay floods is not limited by water sources. Glacial hydrologic theory (Shoemaker 1991) shows that the required large volumes of stored subglacial and supraglacial water were likely available. The topography north of the study site provided the appropriate pathways, a saddle in the Abitibi Upland, connected to probable large reservoir sites in the James Bay Lowland and Hudson Bay region (Kor et al. 1991; Shoemaker 1999). Storage reservoirs were likely of considerable extent in late glacial times, such that the ice sheet adjusted to reduced basal shear stresses from stored subglacial water (e.g., Alley et al. 2006); stored subglacial water (e.g., Siegert et al. 2007; Livingstone et al. 2013) tends to lead to a relatively thin and flat ice sheet that was susceptible to large drainage events (Shoemaker 1992).

Plucking by ice or hydraulic action?

Plucking, observed on the lee side of many rock drumlins and remnant ridges, was not prominent in previous descriptions of Key River sculpted rock forms. The association of plucked forms and s-forms may be very important in assessing the role of the two main agents of erosion (ice and water).

Plucking (or quarrying) is dependent on i) glaciological variables, sliding velocity and basal effective pressure, and ii) lithologic controls, resistance to fracture and the existence of pre-existing cracks (Hallet 1996). Patterns and style of jointing provide critical information as much of the bedrock in the study area is poorly jointed. However, it may be possible to fracture (pluck) unjointed bedrock, if differential effective stresses on a rock step are very high (e.g., Hallet 1996). Some consider rock fractures to be exceptional (e.g., Gordon 1981), yet joints represent a significant mechanical weakness compared to unfractured rock. In most cases, joints are considered to control whether glacial plucking occurred (Rea et al. 2000) or not, as supported by several field studies (e.g., Sugden et al. 1992; Dühnforthet et al. 2010).

Key River observations indicate that plucking is associated both with and without pre-existing fractures (**video 6**). The relationship between concave down flow (crescentic) fractures and down flow-facing rock steps may be related to fractures with jointing being less significant (**Fig**. **23**). At the Plucking Island site, the spacing of incipient crescentic rock failure

[b] For example, ice plucking may have created step drops in relief, so that flow separation in turbulent meltwater led to the common formation of sichelwanne, which require flow separation to form.

near a down flow step was ~10-20 cm, whereas straight joint spacing was closer to 0.5-1.0 m in the same streamlined rock mass. Hydraulic plucking may have been involved in addition to ice plucking.

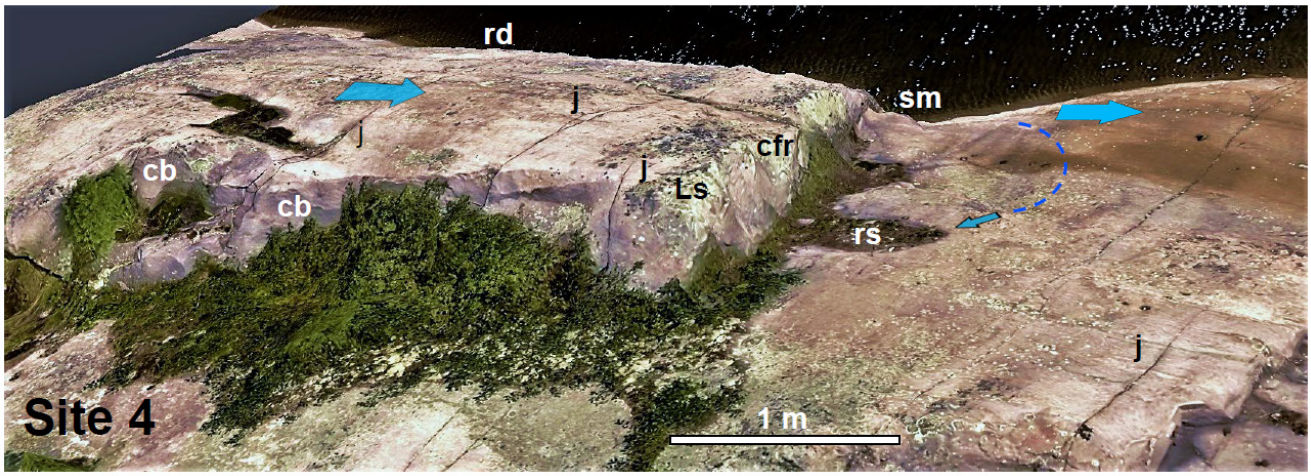

Figure 23: Photogrammetry survey of a rock drumlin (rd) at Plucking Island (site 4). Main joints (j) and the steep lee side slope (Ls) of the rock drumlin are orthogonal to the main flow direction (blue arrow). S-forms (rs) at the foot of steep lee side (Ls) indicate a local roller or reverse flow (dashed blue lines). Crescentic plucked breaks (cb) and crescentic fractures **(cfr**) are common on the lee side; note, one smooth lee side (sm) segment. Photo courtesy of Guy Leduc.

In several places (e.g., Henvey Inlet; steps with half potholes; Plucking Island; Bottle Island), glaciofluvial rounding followed plucking; this indicates a close relationship between plucking and meltwater flow. Although poorly understood, hydraulic plucking is a dominant mechanism for channel erosion in rock-floored rivers (Whipple et al. 2013). Hydraulic plucking is commonly observed in coulees eroded in basalt in the Washington Scablands (Baker 1978; 1988). Experimental flume results with fractured slabs of plaster rock show that plucking results from non-uniform flow, particularly rapidly varying flow with hydraulic jumps and with free-surface flow undulations (Wilkinson et al. 2018). Particle, image-velocity analysis of flow during a plucking event indicates that structures in the flow (vortices) smaller than the eroded blocks aid the plucking process. Varying velocity / pressure gradients near eroded blocks (rock steps) provide the mechanism to lift blocks. Pressure gradients in the sub-bed crack network are also enhanced by these turbulent fluctuations (Wilkinson et al. 2018), in effect creating a hydraulic pumping action. These experimental results are consistent with previous studies of slab uplift in energy-dissipating spillways under plunging jets and hydraulic jumps with high inertial energy (Whipple et al. 2000).

Krabbendam et al. (2011) suggest that lateral plucking explains considerable block removal on rock walls parallel to ice flow. Removal of joint-bounded blocks from such rock walls involves a component of vertical rotation. Thus, lateral plucking results in horizontal erosion at right angles to ice flow within groove/ridge topography. This erosional topography, observed at Bastard Island, has cavetto forms as well as lateral pluck elements (**Fig. 13**). These features tend to occur on down flow ridge flanks where the pressure field was variable in a lee-slope position. More generally, plucking erosion on Bastard and Germain islands relates to how flow over asymmetrical ridges expends energy.

The relationships between hydraulic pressure fluctuations (Röthlisberger and Iken 1981; Whipple et al. 2013), the formation of down-flow-concave fractures (Wilson et al. 2018), and plucking, as identified in rivers, in engineering work and in lab experiments (see Wilkinson et al. 2018), all provide support for the competence of hydraulic plucking. Ice plucking also needs to be considered as subglacial meltwater flow led to abrupt ice re-grounding following lift-off events in the French-Key River area.

Ice re-grounding features

Direct field evidence for ice flotation (e.g., Magmussen et al. 2011) and re-grounding, while sparse, provides key information on ice sheet behaviour, debris content, loading, and late-glacial flow events.

Meltwater sheet flow events are likely to have resulted in a transitory surge, increased ice flow, and flattening and thinning of the glacier (e.g., Kamb et al. 1985; Shoemaker 1991). As subglacial flood pressure lowered the ice roof closed, and the remaining glacial load influenced the bed. As ice closed on the bed, sheet flow became unstable, forcing flow to break down to channel flow. During these discharge events most of the sediment from the base of the ice and the rock surface

was removed. However, sparse lag boulders remained with some of the more prominent boulders displaying fractured crowns potentially due to rapid loading by the glacier.

Closure of the moving re-grounding ice added a shear component at the bed in the form of crescentic fractures, crushing and drag effects such as striations, and conchoidal fractures on rock surfaces. Transverse lee-side bedrock fractures (plucking) (**Figs. 12c, 13**) may also be a product of ice re-grounding and drag deceleration, although these plucking features are closely associated with high-energy meltwater flow that produced s-forms.

Theory and field observations indicate a sheet-to-channel flow, re-grounding event sequence. The observed landscape reinforces the concept that most sediment was removed from the base of the glacier by subglacial floods prior to re-grounding, in addition to the fact that hard silicate Shield rocks yield modest amounts of detritus from glaciogenic erosion.

EVENT SEQUENCE

Three stages of landscape development occurred at Key River, events during main ice flow and then as the last glacial episode waned and meltwater accumulated on, under and around the ice sheet:

1) Abrasion-conduit stage (Nye channels) during main glacial conditions.
2) Late-glacial sheet-floods (potholes, s-form fields, streaks, hydraulic plucking), followed by channelization (mainly down flow).
3) Recoupling stage (striations, fracture and plucked forms, cavitation marks, boulder clusters, clast percussion fractures, striated rock facets and fractured rock surfaces).

1) Abrasion-conduit Stage

Key River terrain consists of regional, rectilinear bedrock structures (Corrigan et al. 1994; Culshaw et al. 2004). This fracture and joint structure, enhanced by sub-glacial erosion (ie., Key River), serves as ~ EW linear structurally-controlled, drainage way. Subglacial meltwater was likely active in Nye channels during a "grounded ice stage" of unknown duration (Röthlisberger 1972). Thus, enhancement of structural channels and trenches between islands would have originated from subglacial abrasion and meltwater erosion in linked cavities and channels, and similarly in discontinuous fractured-controlled depressions on islands and uplands. These structural trenches thus became enlarged over time. Presumably, structural drain ways represent cumulative erosion during multiple glaciations related to ice abrasion, quarrying and to water erosion, then functioned as conduits in later glaciations.

Ornamentation of these drainage ways by s-form, potholes, and plucking indicates that conduit development came before most mapped erosion features (e.g., Key River. **Figs. 7, 8; Plate 10.3**). This observation is analogous to other examples of subglacial "channel erosion" preceding sheet flow (e.g., evidence from the drumlinized sounds (channels) in Puget Sound, Washington (Booth 2004); evidence from large-scale fluting on the downstream rim of Athabasca tunnel channels in Alberta (Shaw et al. 2020). In these cases, as in other examples (Finger Lakes, Mullins et al. 1990; Victoria Island, Brennand and Sharpe 1993; Lake Simcoe, Brennand and Shaw 1994; Russell et al. 2004); Kingston Channeled Scablands, Shaw et al. 2020), formation of significant streamlined landforms occurred related to a pre-existing channel side-slope facing into regional flow.

2) Sheet Flood Stage

From theory (Shoemaker 1991), empirical observation (Seigert et al. 2007; Bjorson 2009) and from modelling (Lelandais et al. 2018), pressurised subglacial meltwater flow (floods) over a hard rock bed is anticipated to exhibit distinct stages during drainage: sheet, channel and linked-cavity flow. Energetic subglacial sheet flow overrides topography but is directed toward lower hydraulic potential (channel outlets) and is expected to strip basal ice of bed debris while sculpting the rock surface (s-forms). At the same time, extensive decoupling accelerates and increases the strain within the overlying ice, followed by enhanced flow and progressive exhaustion of water reservoirs. These events reduced basal water pressure and lowered the ice roof, before grounding the moving ice onto more prominent, raised-bed rock surfaces.

The continuous, consistent and widespread occurrence of s-forms, pothole and plucking across a full range of topographic and structural settings in the Key-French River area, supports the expectation of a meltwater sheet flow event. Aerial (drone) videos show detailed assemblages of s-forms from site to site across the region (**App. 3. 1-7**). The flood left a consistent, observable pattern across low-relief topography (e.g., Henvey Flats), where transverse forms tend to cluster on NE, steeper, upflow (stoss-side) slopes, and, longitudinal furrows occur on SW, low-relief, lee-side slopes (Kor et al. (1991). This spatial pattern of s-forms produced the consistent SSW paleo-current directions across a wide range of sites ~100 km in width. These observations and the lack of 'flow margin' features support the inference of a regional meltwater sheet flow.

Large cavettos and potholes observed on steep lee-side bluffs and oblique channels attest to the scale and depth of this broad flood stage. The locations of potholes on the tops of ridges (e.g., Stanley 1934) between structural waterways is also significant to the sheet flow evidence. Flow-depth scaling of s-form geometry indicates meltwater flow depths (<25 m), consistent with a sheet flow event.

Support for subglacial sheet flooding in the French-Key River area is further provided by river hydraulic research with respect to the role of hydraulic plucking. Such studies show that hydraulic pressure fluctuations with lift indicators can form concave fractures (e.g., Wilkinson et al. 2018) as observed in the study area (video 6 Plucking Island). Rounding on Key River plucked erosion surfaces is indicative of meltwater modification in which fluvial corrasion followed ice-hydraulic plucking.

During flood discharge, most sediment was removed from the base of the ice and the rock surface. The remaining sparse distribution of trapped boulders across a large study area also supports the proposed sheet flow. Flood stage flows removed most clasts < 30 cm in diameter. Such flow competence indicates transport by-passing of clasts (< 30 cm) across the area, except at points of reduced fluid drag, constriction, traps, such as sichelwannen troughs (**Fig. 15; Plate 8**).

The French River sheet flow evolved to channelized flow, which is marked by the channel forms with rising down flow thalwegs across the floor of Georgian Bay and northern Lake Huron (**Fig. 2**). Deeply eroded waterways such as Key River and inter-island depressions (**Plate 12a**) helped to channelize flow as the sheet started to collapse. On the margins of these channel areas, small (cm-m scale) channels **(Plates 4.3 11.5**) climb over down-flow rock rises as part of the final transition from sheet to channel, to linked-cavity flow. This transition occurs following main hierarchical flow regimes and represents the classic progression of flood regimes from larger, flood-stage forms to smaller, waning-flow stage forms.

The Georgian Bay meltwater discharges are estimated to have been comparable to those associated with the drainage of glacial Lake Missoula (Baker 1973), with a catastrophic flow discharge in the order of $l0^7$ m^3/s (Carling et al. 2009).

3) Ice Recoupling

Evidence of ice-recoupling to the bed following waning subglacial sheet-flow supports the theoretical predictions of accelerated movement, stretching, and thinning of the glacier (Shoemaker 1991), as well as stripping of most basal debris. As subglacial flood pressure lowered, the ice roof sagged, and the glacial load affected the bed. Upon closure, the ice contacted sparse boulders; some display fractured crowns due to loading, while many boulders show percussion fractures from fluvial transport.

The grounding ice was also moving, adding shear to its closure, which may have left crescentic fractures, crushing and drag features such as striations and up-flow conchoidal fractures on some rock surfaces. Transverse, lee-side bedrock fractures (plucking; **Plate 5**) may also be a product of ice re-grounding and drag deceleration. Some rounded plucking features help support the role of hydraulic plucking considering the strong association of plucking with well-preserved s-forms.

As floodwaters waned, ice closed quickly (Nye 1956) and the velocity of remaining floodwaters increased rapidly before the re-grounded ice sheet impacted the bed (Shoemaker 1991). Cavitation marks found in close association with meltwater erosion forms indicate rapid sediment removal and preservation of delicate pitting forms that were not over-printed. These events imply late-stage cavitation under high flow velocities during ice closure. Light post-flood striations also resulted from this ice closure.

4) Summary

As theory and field observation led us to a sheet-to-channel flow, re-grounding sequence, what is remarkable is that more re-grounding features are not present. This observation reinforces the concept that most sediment was stripped from the base of the glacier by subglacial floods, even though hard silicate Shield rocks yield modest amounts of detritus from glacial erosion. Other than limited striations and crescentic fractures, there is little post-closure glacial alteration, suggesting that the flood event was a prelude to stagnation and deglaciation. Immediate ice stagnation on flow termination is indicated by prominent boulder accumulations that have not been eroded from bedrock surfaces by post-glacial lakes.

TABLES

TABLE 1: Georgian Bay Terrain Elements

1.0 Longitudinal s-forms

1.1 Cavettos
Cavettos are curvilinear, undercut channels eroded into steep, commonly vertical or near-vertical rock faces (**Plate 1.1**) (Johnsson 1956). The upper lip is usually sharper than the lower one, although both may be sharp.

1.2 Furrows
Furrows are linear troughs, much longer than wide, which carry a variety of s-forms and remnant ridges on their beds and walls (**Figs. 5, 6, 15**; **Plates 1.2, 3.1**). Rims are remarkably straight when viewed over the full length of furrows but are usually sinuous in detail (Kor et al. 1991); they are commonly sinuous as a result of sculpting into the trough walls by smaller, included s-forms.

1.3 Stoss-side furrows
Stoss-side furrows (Kor et al. 1991) are shallow, linear depressions on the stoss side of bedrock rises, giving a regular, gently curving, sinuous contour to the slope (**Plate 1.3, 4.1**). They have rounded rims and are open at both ends, leading down flow to furrows.

1.4 Spindle flutes
Spindle flutes are narrow, shallow, spindle-shaped marks much longer than they are wide and with sharp rims bounding the up flow side (**Plate 1.4;** (Allen 1971). They are pointed in the upflow direction and broaden down flow. Whereas open spindle flutes merge indistinctly downflow with the adjacent surface, closed spindles have sharp rims closing at both the up flow and down flow ends. Spindle flutes may be asymmetrical, with one rim more curved than the other.

1.5 Remnant ridges (rat tail, rock drumlin, bedrock fluting, or mega-lineations)
Remnant rock ridges occur between lateral and crescentic furrows; they form smooth, rounded linear ridges at multiple (mm to km) scales (**Plates 1.2, 1.5a**). The have blunt rounded proximal ends that taper to pointed ends down flow (**Plate 1.5**) They have been variously described as rat tails; rock drumlins; bedrock flutings (**Figs. 4, 5; Plates 1.5, 1.6)**; or mega-lineations (Shaw et al. 2020; **Plate 10.3**). They are common in nature and are attributed to formation by turbulent flow structures related to horseshoe vortex erosion (Shaw et al. 2020).

2.0 Transverse s-forms

2.1 Comma forms
Comma forms are similar to sichelwannen but with only one arm well developed; the other arm is either missing or poorly formed (**Figs. 4, 12, 14a; plate 2.1**) (Shaw and Kvill 1984). Comma forms are part of a continuum with sichelwanne and may be considered transitional between transverse and longitudinal forms.

2.2 Sichelwannen (singular sichelwanne)
Sichelwannen are sickle-shaped marks (**Figs. 1, 4, 8, 11, 16; plate 2.2**) (Ljungner 1930) resembling the classical transverse erosional marks of Allen (1971, fig. 1). They have sharp rims (r) convex-up flow, and a crescentic main furrow, extending down flow into arms wrapped around a residual, median ridge. Smaller, lateral furrows may flank the main furrow.

2.3 Muschelbruche (singular muschelbruch)
Muschelbriiche are mussel-shell-shaped, shallow depressions with sharp, convex up flow rims and indistinct, down flow margins merging imperceptibly with the adjacent rock surface (**Plate 2.3**; Ljungner 1930). Sichelwannen are identical to classical flutes of turbidite sole marks (Allen, 1982). Although both are gentle, the proximal slope is normally steeper than the distal slope, otherwise, there are no distinguishing internal form elements.

2.4 Transverse troughs
Transverse troughs are relatively straight troughs arranged perpendicular to flow, with lengths much greater than widths (**Figs. 4, 5; plate 2.4**). They commonly have a steep, relatively planar up flow slope or lee face below a relatively straight rim. The down flow or riser slope is gentler and normally eroded by shallow, stoss-side furrows, which produce a sinuous slope contour. Large transverse troughs are normally compound forms enclosing numerous, smaller scale s-forms.

3.0 Non-directional s-forms

3.1 Potholes (vertical)
Potholes are near-circular, deep depressions that may show spiralling, rising flow elements inscribed on their walls (**Figs. 7, 22**) (Gilbert 1906; Alexander 1932).

3.1.1 steep lee side **(Fig. 6; plate 3.1)**
3.1.2 flat uplands **(plate 3.2)**
3.1.3 flat lowlands **(plate 3.3)**

3.2 Undulating surfaces
Undulating surfaces are smooth, non-directional, low-amplitude undulations found on gentle lee slopes of rock rises (present but not illustrated here; see Kor et al. 1991).

Note: We have added two additional styles of forms to the s-form classification of Kor et al. 1991; these include asymmetric forms and pitted surfaces.

4.0 Asymmetric-forms

Asymmetric forms occur in particular settings (e.g., bed relief or obstacles) relative to the formative flow, creating an erosional asymmetry to affected rock surfaces.

4.1 Stoss-side ramp
Stoss-side ramps (**Fig. 8; plate 4.1**) are smooth to furrowed, low-relief slopes that face into the formative flow. They commonly occur with evenly-spaced, stoss-side furrows that create a wavy plan view (horizontal line) where the ramp meets a water plane.

4.2 Stoss-side oblique ramp
On stoss-side slopes that are oblique to flow, sets of transverse forms (e.g., transverse troughs, commas, sichelwannen) and longitudinal forms (furrows, rock drumlins) are commonly found **(Figs. 8, plate 4.1**).

4.3 Lee-side ramp
On lee-side slopes with oblique flow, plucking and sets of longitudinal forms (e.g., cavettos, fluting; furrows) (**Fig. 10a, b**).

5.0 Pitted forms

Pitted surfaces occur as small (fingernail to thumb print size), smooth, rounded depressions transverse or parallel to flow, on low relief surfaces (**Figs. 10, 12, 14; plates 6.1-6.3**).

***5.1* Pitted surfaces**
Pitted surfaces occur as small swaths of smooth, rounded depressions (~1-5 mm) transverse to flow, interrupting striated surfaces at breaks in slope (**plate 6.1**). Sometimes associated with differential erosion due to lithological change.

5.2 Pitted streaks (tapered)
Pitted streaks have pits in alignment with a tapered depression (~1-2 mm) down flow of the first or single pit (**Plate 6.2**). Vague streaks have the appearance of striations yet they are intimately associated with s-forms (**Plate 6.2c**).

5.3 Pitted streaks in fields
Pitted streaks are single pits with a tapered down flow depression (~1-2 mm) which occur in fields with all forms parallel to former flow (**Fig. 12b**,**c,d**; **plate 6.2b**). These forms are found in association with spindle flutes, commas and shallow furrows (**plate 6.3**).

Several other features occur within the described eroded rock surface; these will likely provide additional insights to the formative agents of erosion and their settings. These include striations, plucking features and boulders.

6.0 Striations

Striations, small, shallow (~ 1-2 mm), elongate depressions in the rock surface, are common on Key River eroded rock surfaces, particularly outside of smooth, sculpted forms showing differential erosion (cms to meters).

6.1 Linear striations on s-forms
Short (~ 1-10 cm), elongate depressions (~ 1-2 mm) are found on raised rock surfaces (**Fig. 10b**; **Plate 7.1a, b**).

6.2 Curved striation
Short (~ 1-10 cm), curved depressions (~ 1-2 mm) are found on undulating rock surfaces (**Plate 7.2**).

6.3 Striated clasts
Short (~ 1-10 cm), elongate depressions (~ 1-2 mm) are found on clasts resting on eroded bedrock surfaces; often with multiple sets (**Plate 7.3**).

7.0 Plucked forms

Plucked forms occur in a variety of styles; block, sheet, sculpted, crescentic and modified. Plucking occurs mainly on lee, some stoss surfaces, and on steep and gentle slopes. They are intimately associated with forms in the study area.

7.1 Lee side:

7.1.1 blocks plucked from down flow side of small, highly sculpted surfaces (**Fig. 13**; **Plate 5.2, 5.3**)
7.1.2 blocks plucked from down flow side of steep, highly sculpted surfaces (**Plates 5.1.1, 5.1.5**)
7.1.3 sheets plucked from down flow side of highly sculpted surfaces (**Plate 5.4**)
7.1.4 plucking on the sides of rock rises with oblique an eroding flow (**Figs. 13**).
7.1.5 plucked surfaces can be modified (rounded) (**Plate 5.1.6**)
7.1.6 crescentic block plucking despite the presence of nearby fracture planes (**Plate 5.3**)

7.2 Stoss side: stoss-side surface may have shallow, sheet-like plucking (**Plate 5.1.4a**)

Note:
This classification emphasizes the negative erosional forms that represent zones of high relative erosional rates. But distinctive positive forms also result from this differential erosion. The median ridges of sichelwannen and residual ridges between diverging furrows are streamlined forms with a broad, rounded upstream portion and a tapered tail. These are defined as rock drumlins (also rat tail, bedrock fluting, or mega-lineations) and belong to the class of erosional drumlins (Shaw and Sharpe 1987).

A similar classification of rock erosional forms has been developed for features related to tsunami erosion (Bryant and Young 1996, figure 16) and linked to our forms (in brackets). Longitudinal forms include: flutes (rock drumlins), sinuous grooves (furrows), cavetto (cavetto); transverse forms sichelwannen (sichelwanne), muschelbruche (muschelbruche), comma marks (commas), transverse form (transverse trough), v-shaped groove (not recognized), and non-directional forms: impact marks (percussion marks), drill holes (pits), potholes (potholes), hummocky topography (undulating surface).

TABLE 3: Structural geology and subglacial erosion

Rock Structure	Schematic block diagram	Plates	Figures	Sites
1.Layers dip diagonally toward to the flux	Plate 9.1	1.3, 1.6, 4.2, 5.1.2, 5.1.3, 4.3, 9.5, 9.6 & 9.7		4, 5, 5a, 7, 15
2. Layers dip diagonally opposite to the flux	Plates 9.2	10.2, 10.3, 10.4 & 10.5		East of site 11
3. Layers are parallel to the flux	Plate 9.3	9.6		16
4. Layers are sub horizontal		1.5a, 1.5b, 2.2, 1.3, 5.1.2, 8.1, 8.4, 8.5a		1 & 7
5. Granite & gneiss are mildly layered.		1.2, 2.5, 2.6		6, 8, 9 & 12
6. Steep grabens of the fault lines.	Plate 9.4	3.1a, 3.1b		2, 3 & 13

1. Layers dip diagonally toward to the flux

West of the synform hinge (sites 4, 5, 5a, 15; **Fig.3**), layers dip into flow (**Plate 9.1**). Inlets are eroded into softer, dark layers (sl**)**. Lee sides of the ridge are steep and often carved by long cavettos (c) (**Plate 9.1, 4.3**). Stoss sides formed ramps (r) covered with s-forms (s) (**Plate 9.1, 4.2**). At site 4, site 5 (**Plate 9.5, 9.7**), site 5a (**Plate 9.6)** and site 15, many of the rock layers were delaminated by ex-foliation joints (ej; **Plates 9.1, 9.5, 9.6** & **9.7**). Plucking (p) occurs mostly on the lee side of ridges (**Plate 9.1**).

On Cavitation Island (site 7), layers are sub-horizontal and dip diagonally into flow. Interestingly, the topography of the island has a low relief and is depicted well in a block diagram (**Plate 9.1**), with smaller scale. Ex-foliation joints and plucking are located on the lee side of small ramps.

2. Layers dip diagonally opposite to the flux

East of the synform, layers dip down flow (**Plate 9.2**); softer layers (sl) in dark mark transverse troughs at the head of the rock drumlins rows (rd) (**Plates 9.7**).

3. Layers are parallel to the flux

Plate 9.3 illustrates flow parallel to dipping layers (**Plate 9.6**) at site 16 (**Fig. 3**). Softer layers (***sl*** in **Plate 9.3**) often correspond to inlets (**Plate 9.6**); plucking occurs at the end of ridges (p); s-forms parallel to the ridge are nested as a field (sf).

4. Layers are sub-horizontal

The layers at flat Henvey Island (site 1, **Fig. 3**) are sub-horizontal due to proximity to the synform hinge line. Relief is low and carries large sichelwannen. As on Cavitation island (site 7), layers are sub-horizontal and represent a small version of a block diagram (**Plate 9.1).**

5. Granite & gneiss are mildly layered

Where bedrock is more homogeneous, topography is more uniformly characterized by fields of s-forms (sites 6, 8, 9 & 12). Of interest, though site 12 is near site 16, we notice a major difference in geomorphology which corresponds to sudden changes in geology (unit 52b, site 12; unit 52c, site 16; (**Fig. 3**), where felsic intrusive rocks are strongly foliated.

6. Steep grabens of the fault lines

Plate 9.4 illustrates flow crossing a graben with fault depressions (f), potholes (***ph***) on the lee side, ramp of rock drumlin rows (***dr***) on stoss slopes. Long rock drumlins are ubiquitous on these plateaus (**Plates 10.2** to **10.5).**

PLATES

PLATE 1: Longitudinal forms

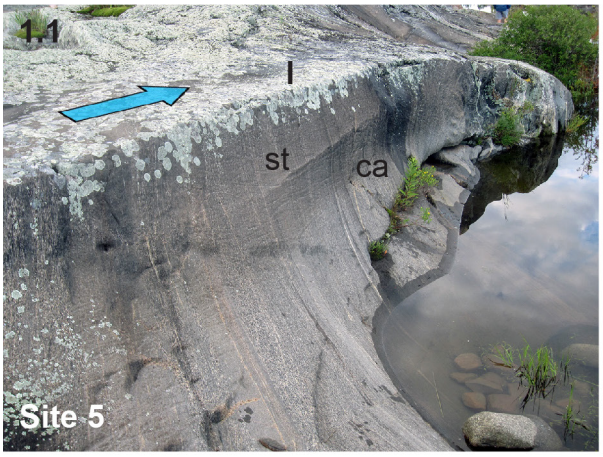

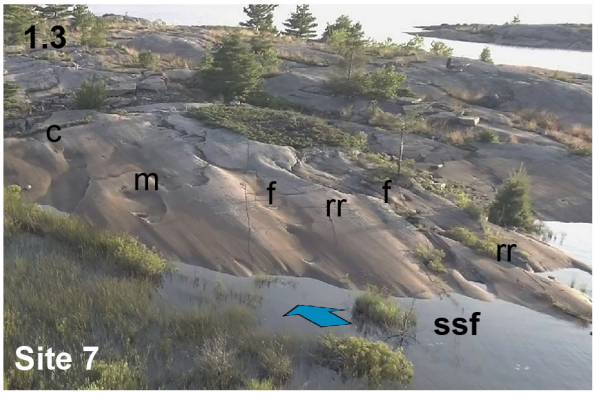

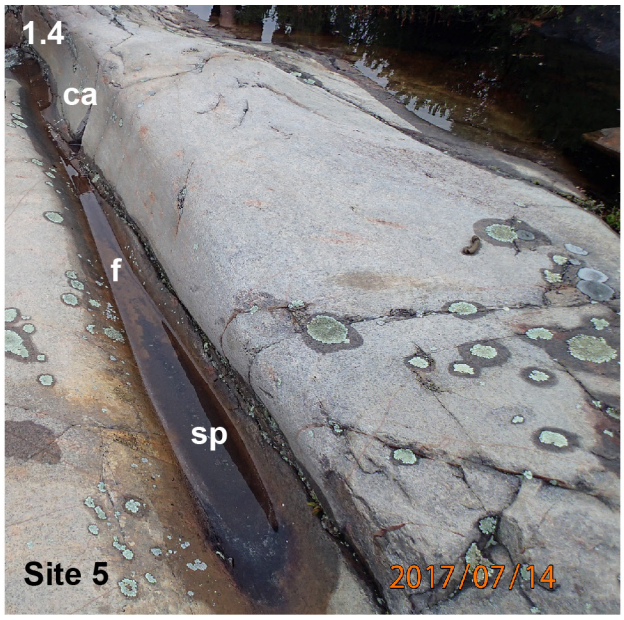

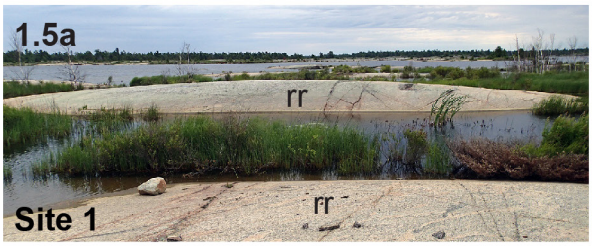

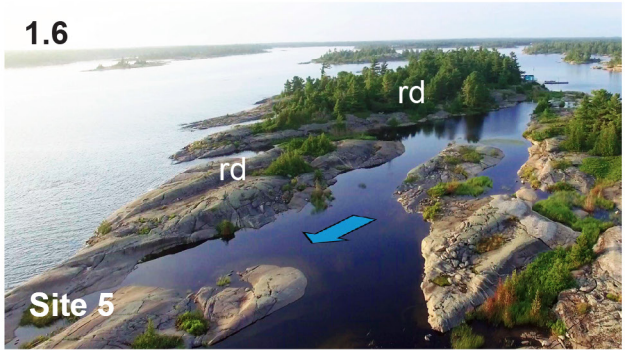

1.1 Cavetto form (ca) shows a slightly overhung rock face with a sharp upper lip (l) separating two sculpted surfaces marked with short, disorganized striation/ scratches (st). Photograph by D.R. Sharpe. NRCan photo 2022-519.

1.2 Furrows: long, narrow furrows (f) extend for > 10 m across low-relief outcrop; furrows extend as down flow arms from comma (c) or sichelwannen (sc) forms. Erosional remnants (rr) occur between erosional arms (furrows). Photograph by D.R. Sharpe. NRCan photo 2022-520.

1.3 Stoss-side furrows (**ss**f): form depressions leading down flow to furrows (f); they form an undulating trace against the waterline on Cavitation Island. Erosion of ssf leads to remnant ridges (rr), including rat-tails. They (ssf) occur in association with transverse forms, such as musclebruche (m) and commas (c). Photograph by D.R. Sharpe. NRCan photo 2022-521.

1.4 A **spindle flute** (s) extends down flow into a furrow (f) and cavetto (ca), illustrating continuity of longitudinal forms. We infer spindle erosion by vortex impingement on the bed forming a longitudinal vortex flow structure. Photograph by D.R. Sharpe. NRCan photo 2022-522.

1.5 a) Remnant ridges (**rr**) occur between furrows as; b) **rock flutings** (fl) on Henvery flats, elongate (> 5m) remnant ridges, longer than rat tails, with lateral furrows (f) and spindle flute (sp); symmetrical remnant ridges or rock drumlins, common in the Henvey Inlet area. Photographs by D.R. Sharpe. NRCan photo 2022-523 and 2022-524.

1.6 Field of **rock drumlins (rd)** occur at several scales on the south end of Germain Island. Photo courtesy of Guy Leduc.

PLATE 2: Transverse forms

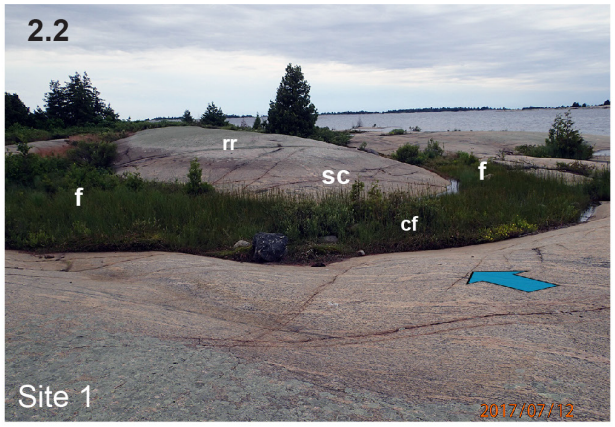

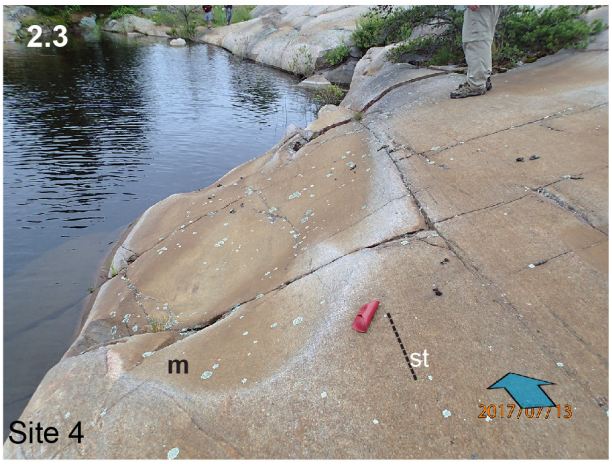

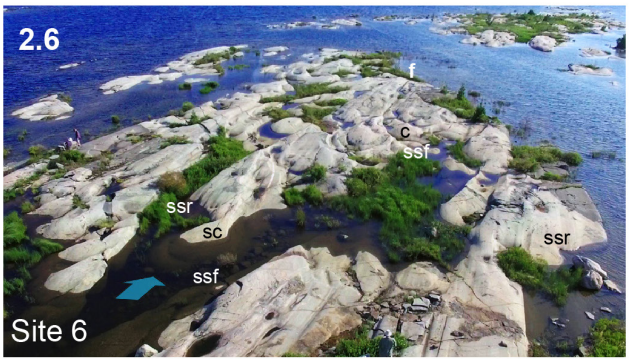

2.1 Comma forms (c): are prominent on Bottle Island, in this case with a furrow arm (f) extending down flow from a comma in a low-relief setting. Note lack of striation on rock surface. Photograph by D.R. Sharpe. NRCan photo 2022-526.

2.2 Sichelwannen (sc): in Henvey Inlet area they are defined by crescentic furrow (cf) up flow and lateral furrows (f), highlighted by vegetation surrounding a remnant ridge (rr) or rock drumlin. Similar forms are present at multiple scales (~1, 10 100, 1000 m) in the Henvey Inlet area, likely related to nested structures in the formative flow. These descriptions are in direct contrast to those by Krabbendan et al. (2016) who, using low, oblique-angle photographs (their figure 3) to describe /interpret glacial grooves with no mention of widespread transverse /crescentic forms. Photograph by D.R. Sharpe. NRCan photo 2022-527.

2.3 Muschelbruch (m): are usually found on low-relief rock surface; note smooth interior surface and weak striation (st) outside the form. Red glass-case (scale) shows direction of s-from flow oblique to striations (st). Photograph by D.R. Sharpe. NRCan photo 2022-528.

2.4 Transverse troughs (tt): on Plucking Island occur at structural and/ or topographic breaks with 'arms' (f) eroded around the ends of the rock rise. Photograph by D.R. Sharpe. NRCan photo 2022-529.

2.5. Fields of sichelwannen (sc) (and their incomplete partner, commas (c)), are common across the study area; they form nested arrays likely related to turbulent structure in the formative flow. Note complete absence of sediment on the eroded rock surfaces and few, if any, striations present. Photograph by Guy Leduc. NRCan photo 2022-530.

2.6. Fields of erosion forms: occur at the distal end of Fox Island. Stoss-side ramps (ssr) and stoss-side furrows (ssf) occur up flow of sichelwannen (sc) and commas (c), before leading down flow to elongate furrows (f). Note hierarchy of forms: nested array likely related to turbulence in the formative flow. Photograph by Guy Leduc. NRCan photo 2022-531.

PLATE 3: Non-directional -vertical forms

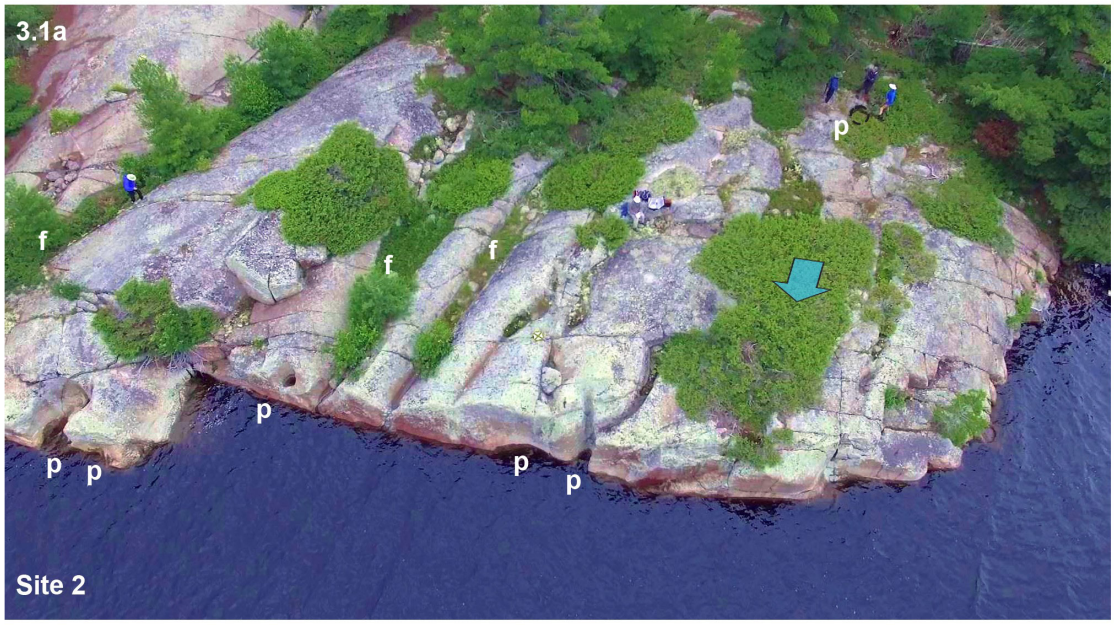

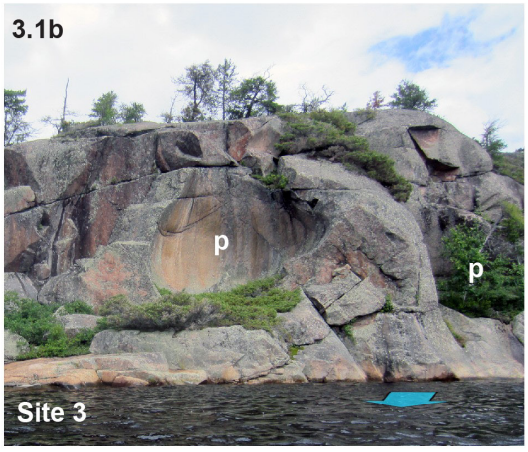

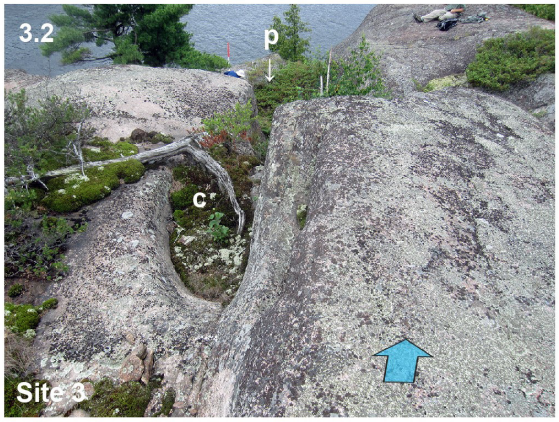

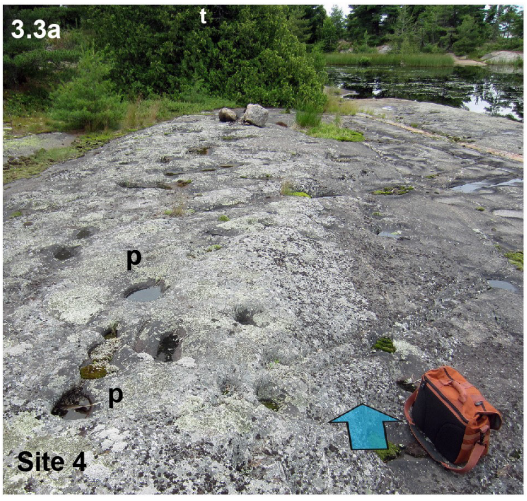

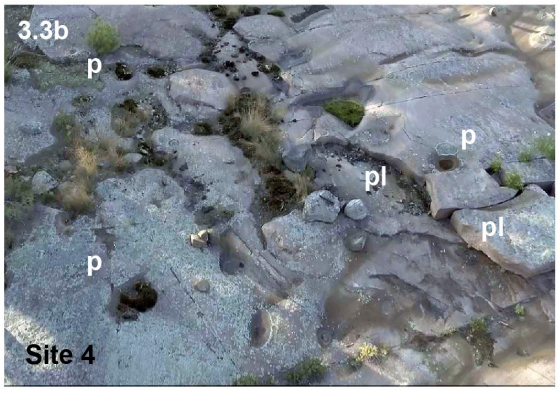

Vertical forms, mainly potholes, occur at down flow breaks in slope, yet, they also occur in low relief settings prominent along Key River and Henvey Inlet.

3.1 **a)** Aerial view of Henvey Inlet study site, with potholes (p) at break in slope. Note longitudinal furrows (f) that indicate paleo flow orientation of vortex streams from the NE. Photo courtesy of Guy Leduc. **b)** Large (< 10 m across: < 10 m deep) potholes (p) occur at steep ~east-west, lee-side structural steps along Key River. Photograph by Guy Leduc. NRCan photo 2022-532.

3.2 **b) Flat uplands:** Potholes also occur on the flat uplands above steep lee-side steps. Comma forms trough structures (**c**) occur where the flat uplands meet steep lee-side step above; trough leads into the large pothole in **3.1b);** this indicates a transition from upland flow forms, potholes to larger potholes at the steep step. Photograph by D.R. Sharpe. NRCan photo 2022-533.

3.3 **c) Flat lowland terrain**: potholes (p) on flat terrain: a) these potholes occur in groups of small forms (<20 cm across) on level terrain on Plucking Island; b) incipient potholes (p) at a small break in slope where plucked (pl) forms are present. Photographs by D.R. Sharpe. NRCan photo 2022-534 and 2022-535.

PLATE 4: Asymmetric forms

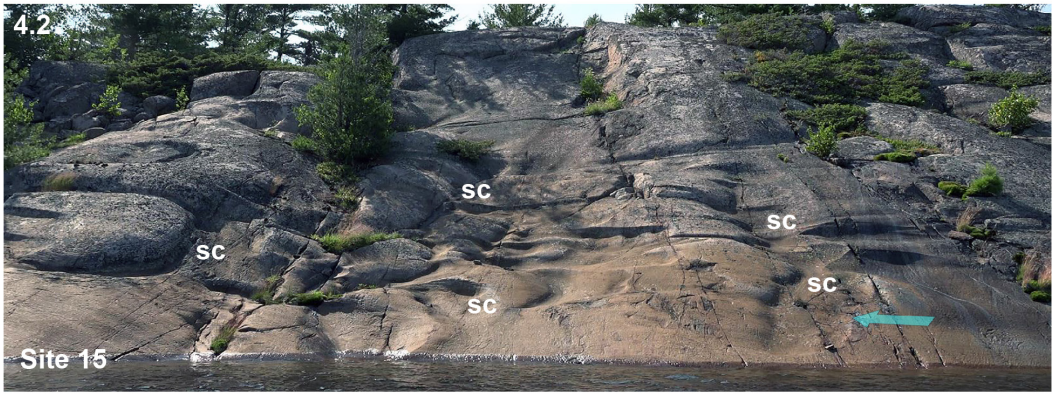

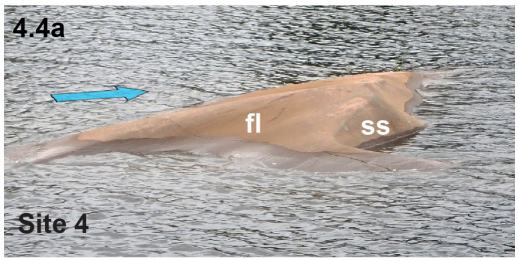

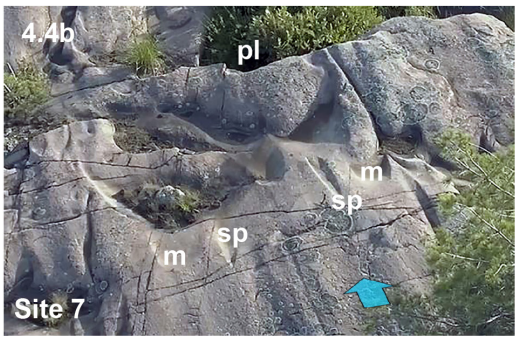

4.1 Stoss-side ramps (ssr) are present on the up flow side of rock rises, such as the northeast end of Plucking Island where weak stoss-side furrows (ssf), furrows (f) and striation (s) are found up flow of transverse forms, sichelwannen (sc) and commas (c). Photo courtesy of Guy Leduc.

4.2 **Stoss (east) side forms:** on the east side ~NS bedrock rises, there is preferential erosion in fields of transverse forms, mainly sichelwannen (sc) as shown along the eastern flank of the Fingerboard Islands. Photograph by D.R. Sharpe. NRCan photo 2022-536.

4.3 **Lee (west) side forms:** on the west side ~NS bedrock rises show lateral plucking (pl) and cavettos (ca), common along the west side of Germain Island. Photo courtesy of Guy Leduc.

4.4 **a) Lee side forms**: a low, streamlined rock rise shows a smooth sculpted faces (ss) on the down flow (lee) side of streamlined (fluted, fl) erosion form, Pluck Island; Photograph by D.R. Sharpe. NRCan photo 2022-537. **b**) lee side forms may include, plucking (pl), spindle flutes (sp) and muschelbruch (m). Photo courtesy of Guy Leduc.

PLATE 5: Plucked forms

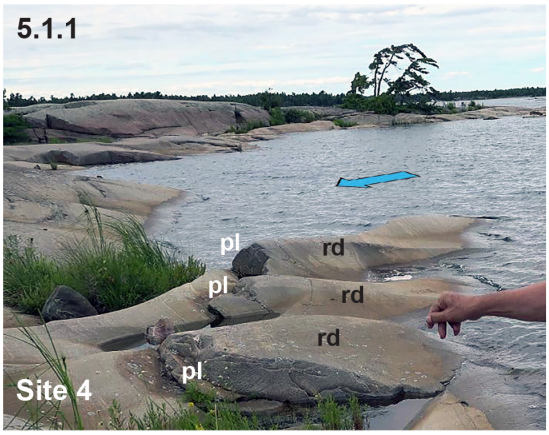

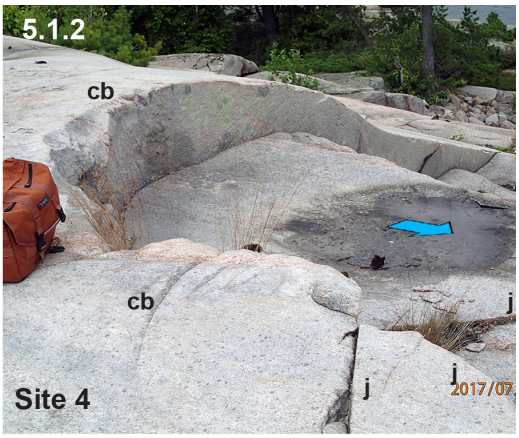

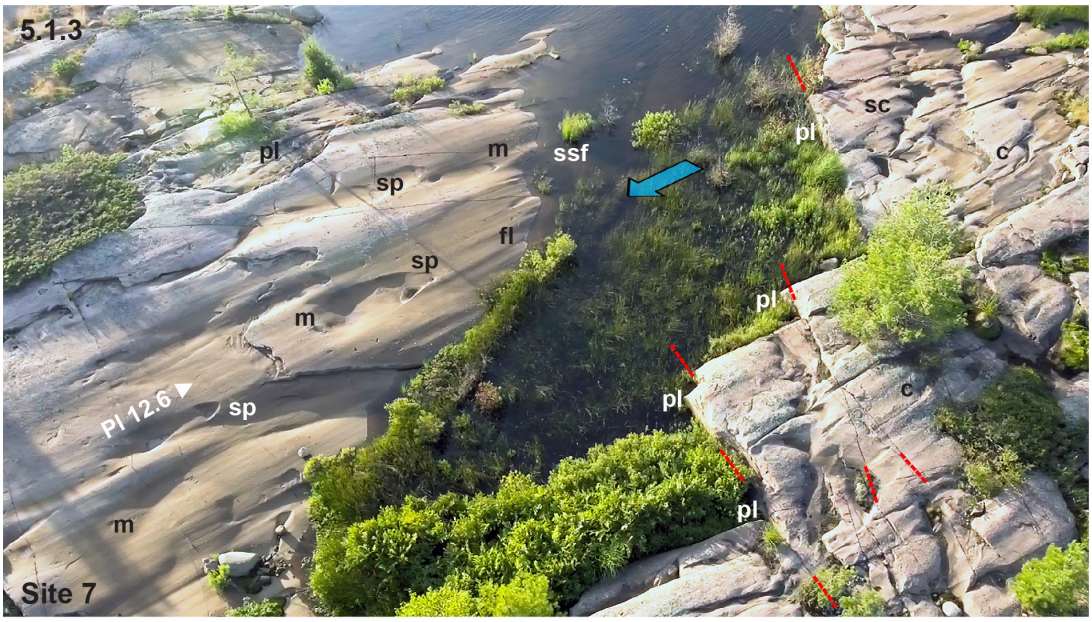

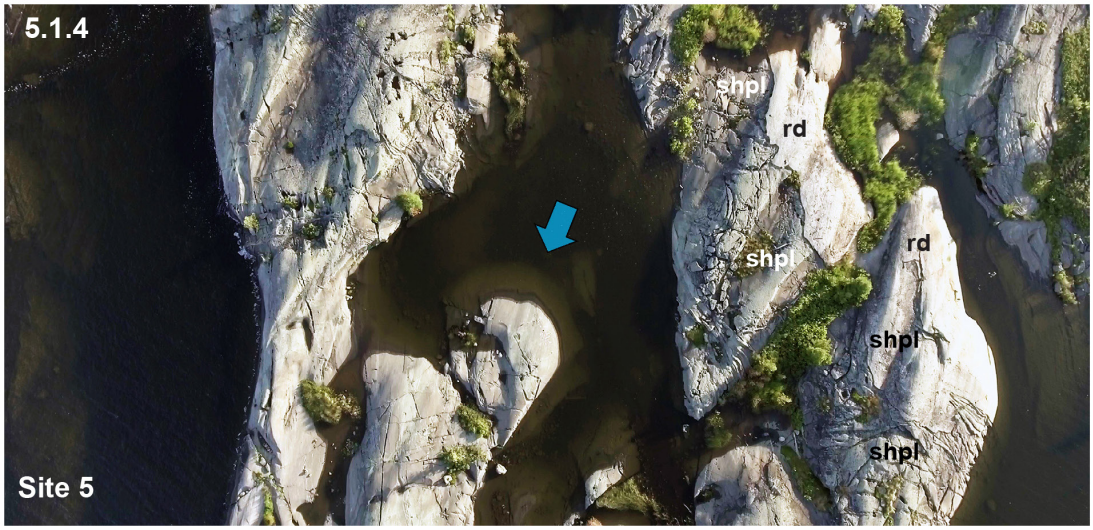

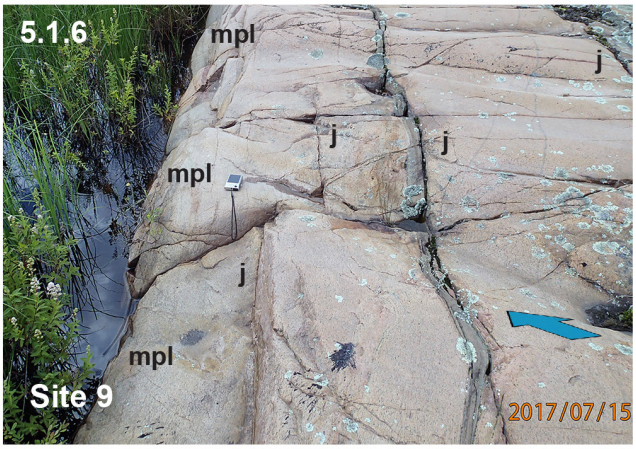

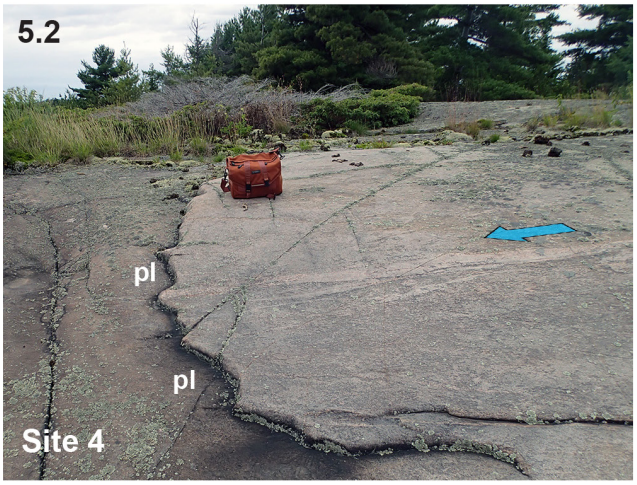

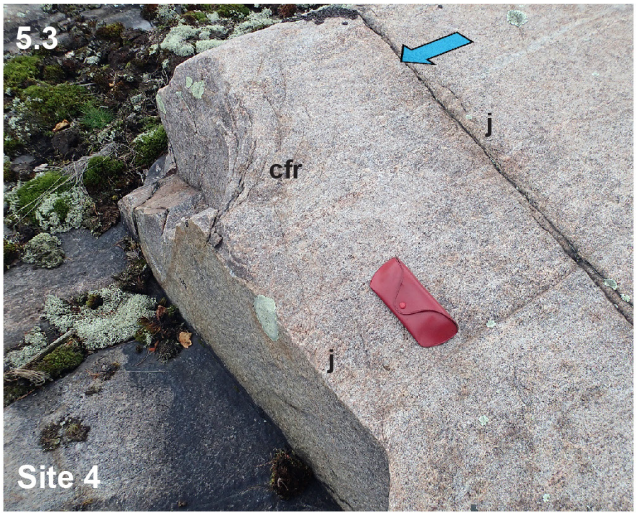

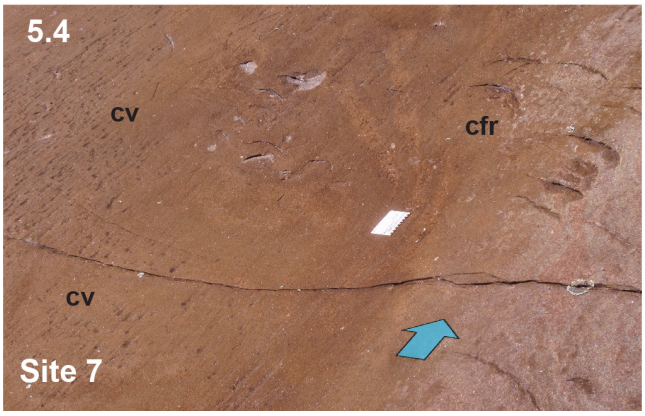

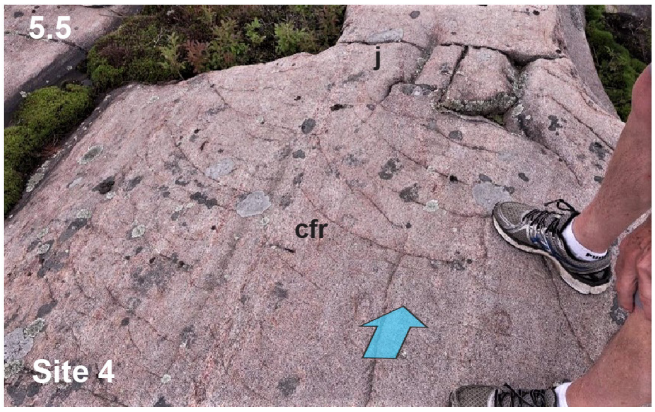

5.1.1 **lee side**: simple plucking (pl) occurs on the down flow end of streamlined rock ridges (e.g., rock drumlins, rd). Photograph by D.R. Sharpe. NRCan photo 2022-538.

5.1.2 **block**: large, arcuate-walled blocks have been eroded on the down flow end of Pluck Island; note that joints (j) do not align with crescentic break pattern (cb). Photograph by D.R. Sharpe. NRCan photo 2022-539.

5.1.3 **steep steps**: plucking (pl) is prominent on the down flow side of structural breaks (vegetated); note that down flow of the plucking zone, the outcrop is highly sculpted with muschelbruche (m), spindle flutes (sp), rock fluting (fl), sichelwannen (sc), comma (c) and stoss-side furrows (ssf) at Cavitation Island. Photo courtesy of Guy Leduc.

5.1.4 **sheets**: thin plucked sheets (shpl) are prominent on the down flow side of a rock drumlin rise (rd), Germain Island. Photograph by Guy Leduc. NRCan photo 2022-540.

5.1.5 **sculpted**: plucking (pl) occurs as ragged sculpted forms on the lateral (west) side of the flow direction of erosion. Photograph by D.R. Sharpe. NRCan photo 2022-541.

5.1.6 **modified**: plucked (mpl) forms show a modified (smoother) form in many case, such as this example from Bottle Island. Flow was right to left across a susceptible, joint (j) -controlled break in slope that has lost its ragged (plucked) surface. Photograph by D.R. Sharpe. NRCan photo 2022-542.

5.2 **stoss side**: stoss side plucking (pl) occurs as thin crescentic sheets on gentle rises in rock slope on Pluck Island. Photograph by D.R. Sharpe. NRCan photo 2022-543.

5.3 **crescentic fracture**: crescentic fractures (cfr) are common on Plucking Island; note that these fractures have been eroded on the down flow side of bedrock steps, but not always along the prominent nearby jointing plains (j). Photograph by D.R. Sharpe. NRCan photo 2022-544.

5.4 **Crescentic fracture and carrot forms:** up flow-facing crescentic fractures**(cfr)** occur in close association with possible carrot-shaped cavitation forms **(cv)**. Scale card is 8 cm long. Photograph by D.R. Sharpe. NRCan photo 2022-545.

5.5 **Crescentic fractures and joints**: crescentic fractures (cfr) are distinct from jointing (j) pattern exhibiting a planar shape at top side of the image. Photograph by D.R. Sharpe. NRCan photo 2022-546.

PLATE 6: Cavitation forms

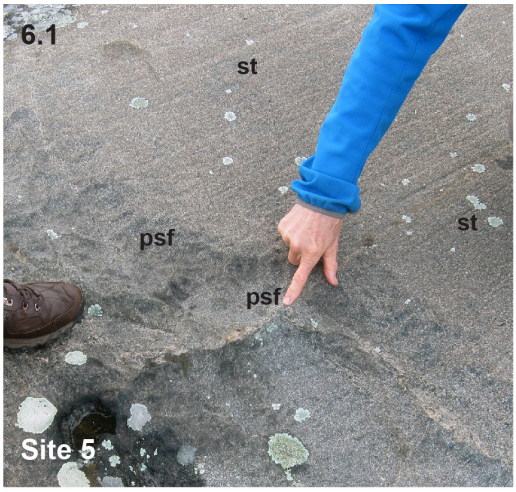

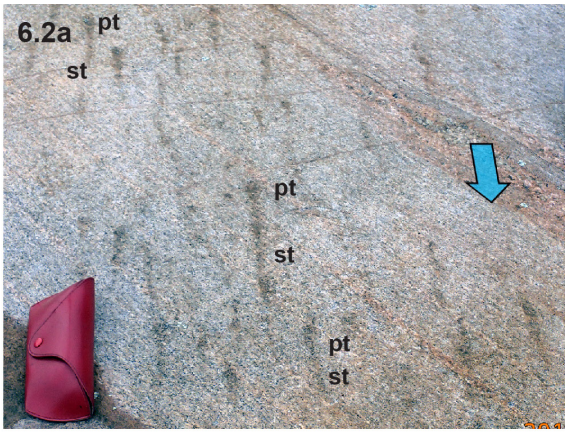

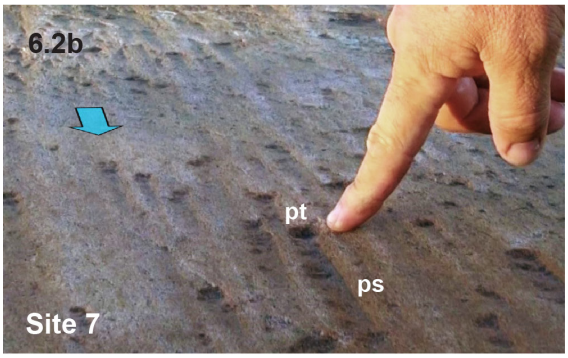

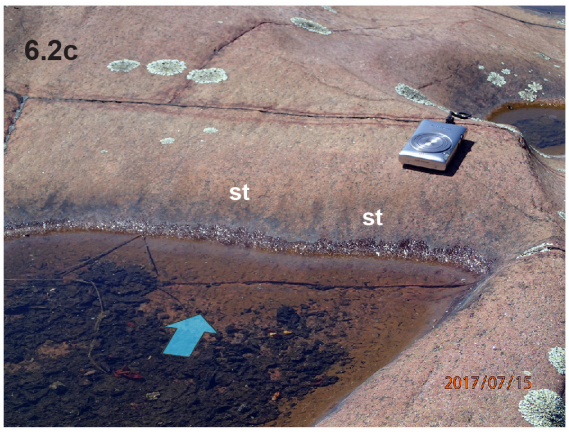

6.1 pitted surfaces (psf): an irregular, pitted erosion surface occurs down flow of an abraded surface with striation (st) on Germain Island. Photograph by D.R. Sharpe. NRCan photo 2022-547.

6.2 streaks: a) erosion pits (pt) occur in oriented streaks (st); a pit (pt) with a tapered down-flow depression are common on Pluck Island; b) pitted streaks (ps) in places show a leading pit (pt) and a series of smaller pits in the tapered down flow depression; c) streaks (st) can be difficult to distinguish from striations when pitting is absent. Photograph by D.R. Sharpe. NRCan photo 2022-548, 2022-549 and 2022-550.

6.3 streaks and s-form: pitted streaks (ps) in fields with tapered depressions also occur with other s-forms, commas (c), furrows (f) and spindle flutes (sp); these arrays cover wide areas of low relief on Cavitation Island. Photo courtesy of Guy Leduc.

PLATE 7: Striation

7.1 a) Striations occur in combination with other erosion forms, s-forms with a sharp rim (r) down flow of a striated (st) rock surface at Germain Island; note smooth (sm) lee side surface. Are these striations or cavitation marks? b) Striations with short erratic pattern occur within and around smooth rock depressions, furrow (f) and spindle flute (sp). Photographs by D.R. Sharpe. NRCan photo 2022-551 and 2022-552.

7.2 Striations with slightly erratic pattern and forms appear to diverge as vectors around and trending from a smooth rock depression. Photograph by D.R. Sharpe. NRCan photo 2022-553.

7.3 Striated clast observed on Henvey flats; note that the clast is sub-rounded and has two striae directions on the clast. Photograph by D.R. Sharpe. NRCan photo 2022-554.

PLATE 8: Boulders

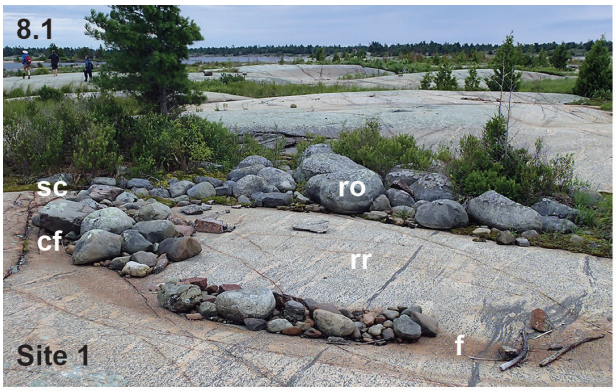

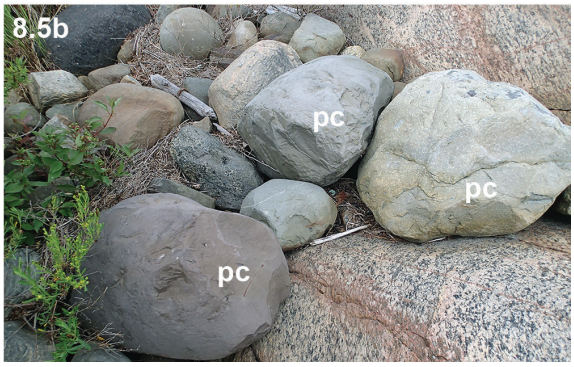

Boulders are sparse across the study area but are concentrated in depressions, such as illustrated below. Blue arrows indicate general flow.

8.1 rounded: boulders in the study area are commonly rounded (ro) to sub-rounded such as those found trapped in sichelwannen (sc) depressions and furrows (f) near Henvey Inlet. Note remnant ridge (rr) framed by eroded crescentic furrow (cf). Photograph by D.R. Sharpe. NRCan photo 2022-555.

8.2 angular: in places down flow of plucked bedrock surface, angular boulders (a) are intermixed with rounded boulders (ro). Photograph by D.R. Sharpe. NRCan photo 2022-556.

8.3 stoss-side: boulders may occur in stoss-side crevasses. Photograph by D.R. Sharpe. NRCan photo 2022-557.

8.4 lee-side: boulders occur most often in lee-side depressions such as the transverse (sichelwannen, sc) and longitudinal forms (furrows, f) on Henvey flats. Photograph by D.R. Sharpe. NRCan photo 2022-558.

8.5 textured: textured boulders provide information on a number of issues in the study area.

8.5a elephant texture: large boulders show elephant-skin structure. Photograph by D.R. Sharpe. NRCan photo 2022-559.

8.5b percussion: many study sites have boulders with percussion marks (pc), on rounded to sub rounded clasts. Photograph by D.R. Sharpe. NRCan photo 2022-560.

PLATE 9: Bedrock structure and erosion forms (blue arrows indicate flow direction)

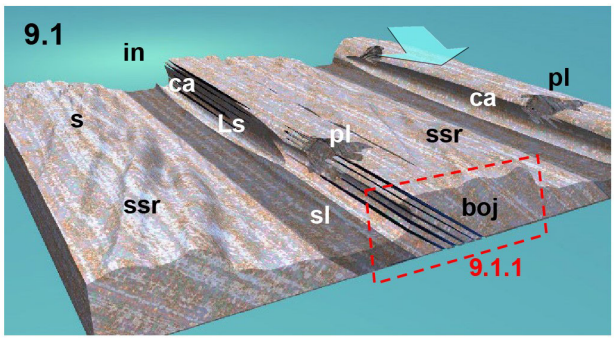

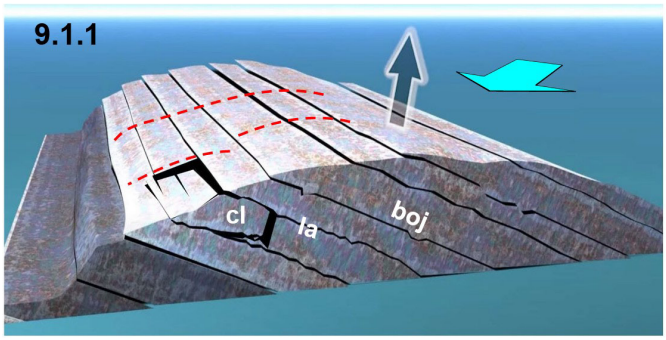

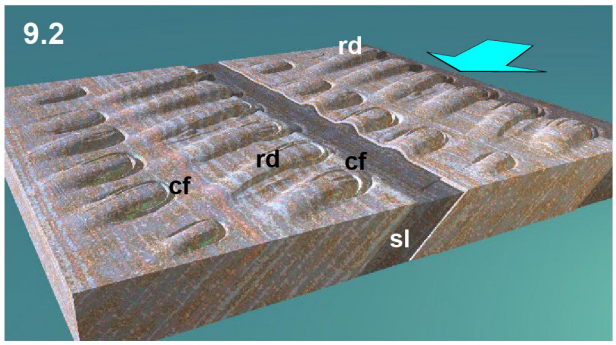

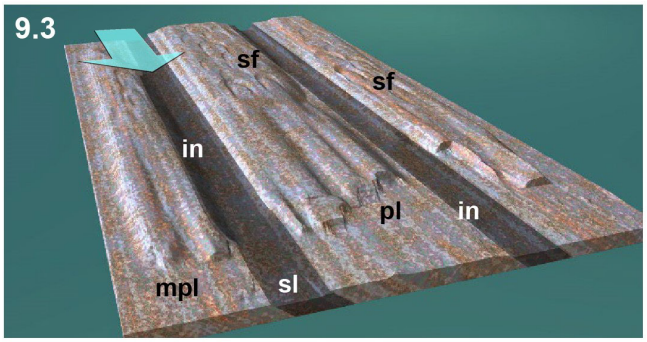

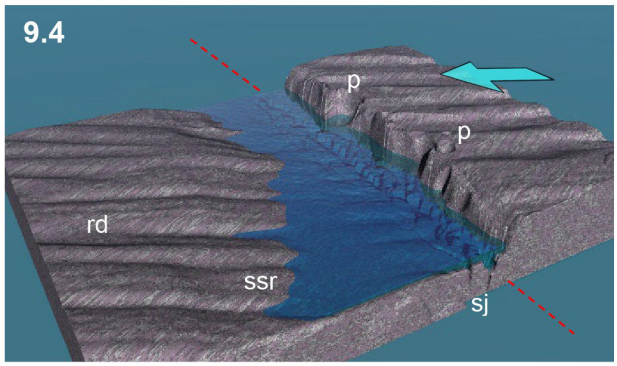

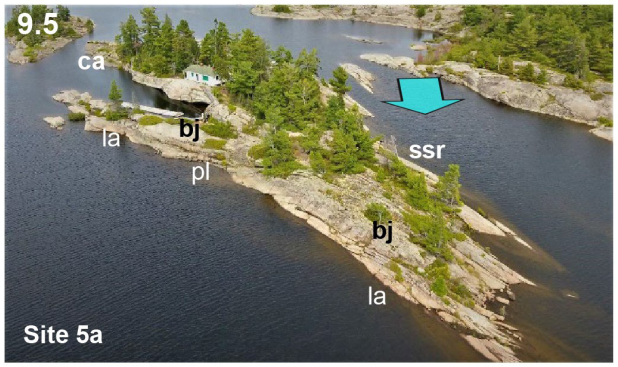

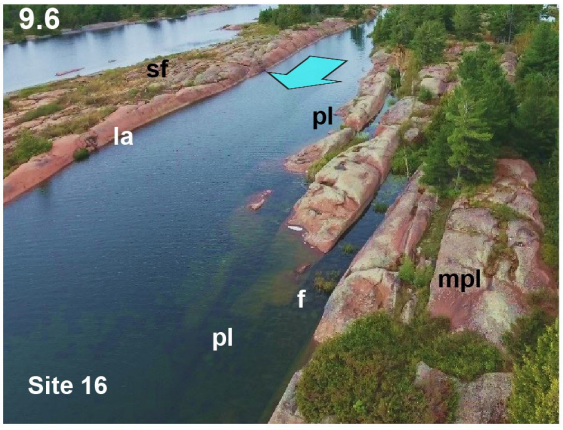

9.1 Schematic block diagram of rock layers dipping diagonally into flow. Softer, dark layers (**sl**) erode to form a linear depression expressed as an inlet. Stoss side of the ridge forms a ramp (ssr) covered with s-forms (***s***). Lee side of the ridge (Ls) is steep and carved with cavettos (**ca**). Bedding open joints (boj)) occur along lee side layering. Dashed red rectangle indicate Plate 9.1.1.

9.1.1 Detailed schematic block diagram of bedding open jointed (boj) ridge. Bedding open jointed (boj) occurs within existing rock layering (la). The force arrow shows a plausible lift effect (Bernoulli) due to main flow (blue arrow). Tension joints (red dashed lines) form orthogonal to the Bedding open jointed (boj). Bedding jointing causes some blocks to collapse (cl).

9.2 Schematic block diagram of layers dipping diagonally down flow. Softer layers (**sl**) form shallow transverse troughs marking the head of rock drumlins (rd) with crescentic furrows (cf), which occur in 'rows'. See Plates 10.2 to 10.5 for aerial view of this erosion terrain.

9.3 Schematic block diagram of layers parallel to flow. Softer dark layers (**sl**) eroded to form inlets; plucking (pl) and modified plucking (mp) mark the end of ridges; s-form field (sf) occurs parallel to the ridge. See Plate 9.6 for aerial view.

9.4 Schematic block diagram of flow crossing a steep step, a fault line (ft); potholes (p) occur on the lee side; rising ramp (ssr) of rock drumlins (rd) occurs on stoss side of step depression.

9.5 Site 5a conforms to diagram 9.1 with ramp (ssr) on the stoss side; on steep lee side: cavetto (ca), plucking (pl), beddind joints (bj) are concordant with rock layers (la). Photo courtesy of Guy Leduc.

9.6 Site 16 is represented by diagram 9.3. Flow direction parallels furrows (f), inlets, s-forms field (sf)) and the azimuth of rock layers (la). Plucking (pl) and modified (mp) occur at the end of streamlined ridges. Photo courtesy of Guy Leduc.

9.7 Site 5 conforms to diagram 9.1; the rock layers dip diagonally to the flow; gentle stoss-side ramp (ssr) with s-forms (s); steep lee side (ls) bedding open joints (boj) concordant with rock layers (la). Two geologists are looking at boulders trapped inside an opening joint 40 cm high. Photo courtesy of Guy Leduc.

PLATE 10: Bedrock structure and erosion forms (blue arrows indicate flow direction)

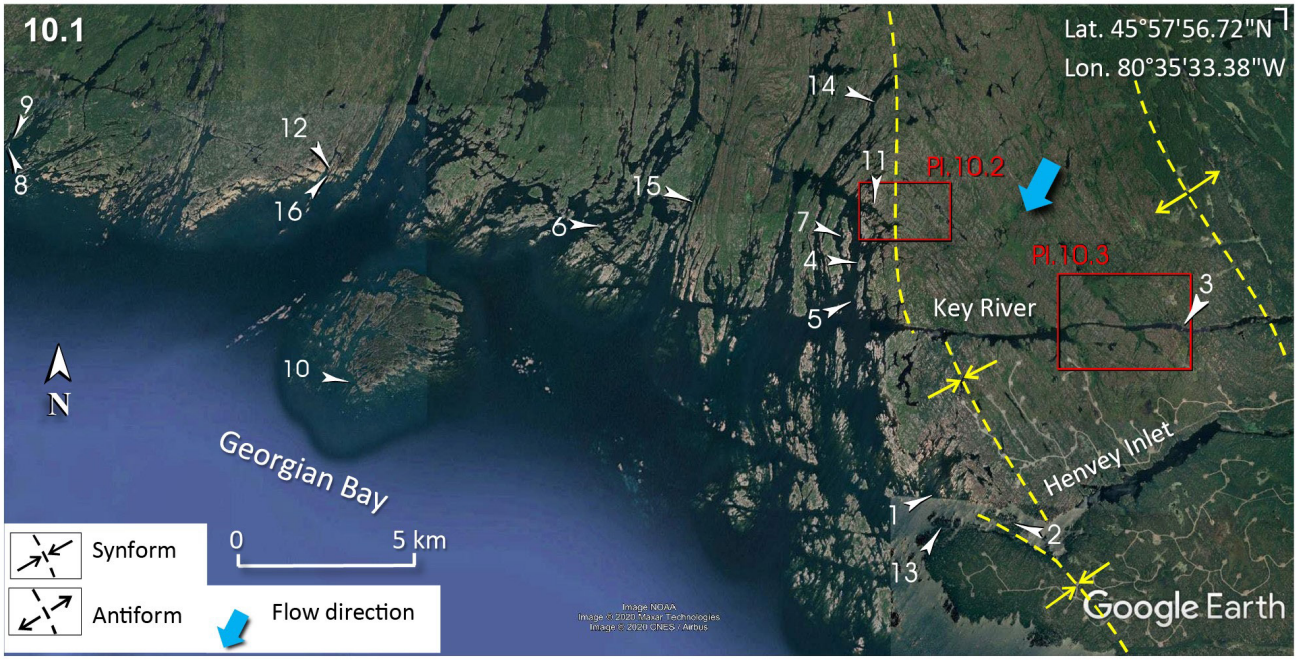

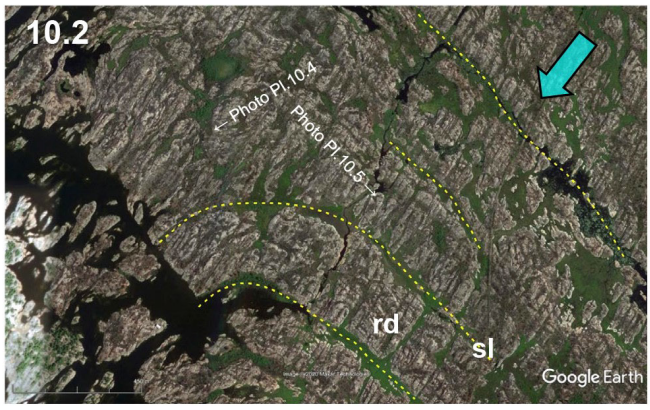

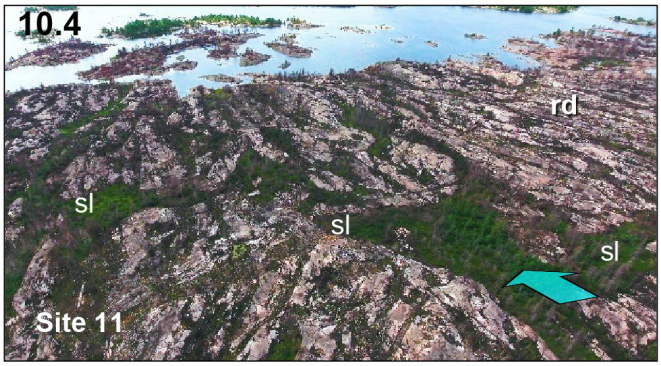

10.1 Study area with synform / antiform location, flow direction, plate 10.2, 10.3 and 16 study sites (numbered arrows) on Google Earth image.

10.2 Streamlined terrain at the synform fold (curved dashed yellow lines) showing location of softer rocks (sl) forming linear depressions and down flow, stoss-side rock drumlin (rd) sets at the topographic step or ramp. Location of plates 10.4 and 10.5 on Google Earth image. Flow from northeast (blue arrow).

10.3 Streamlined terrain occurs down flow of softer rock (sl) linear depression, as stoss-side rock drumlin (rd) at the topographic step. Location of site 3, Key River on Google Earth image. Flow from northeast (blue arrow).

10.4 Down flow aerial view of terrain at the synform fold (site 11) shows soft rock depressions (sl) and rock drumlin terrain (rd) down flow (blue arrow) of depressions. Photo courtesy of Guy Leduc.

10.5 Transverse to flow aerial view of terrain at the synform fold shows soft rock depressions (sl) and rock drumlin terrain (rd) down flow (blue arrow) of depressions. Photo courtesy of Guy Leduc.

PLATE 11a Cavitation Island (blue arrow indicates the main flow direction.)

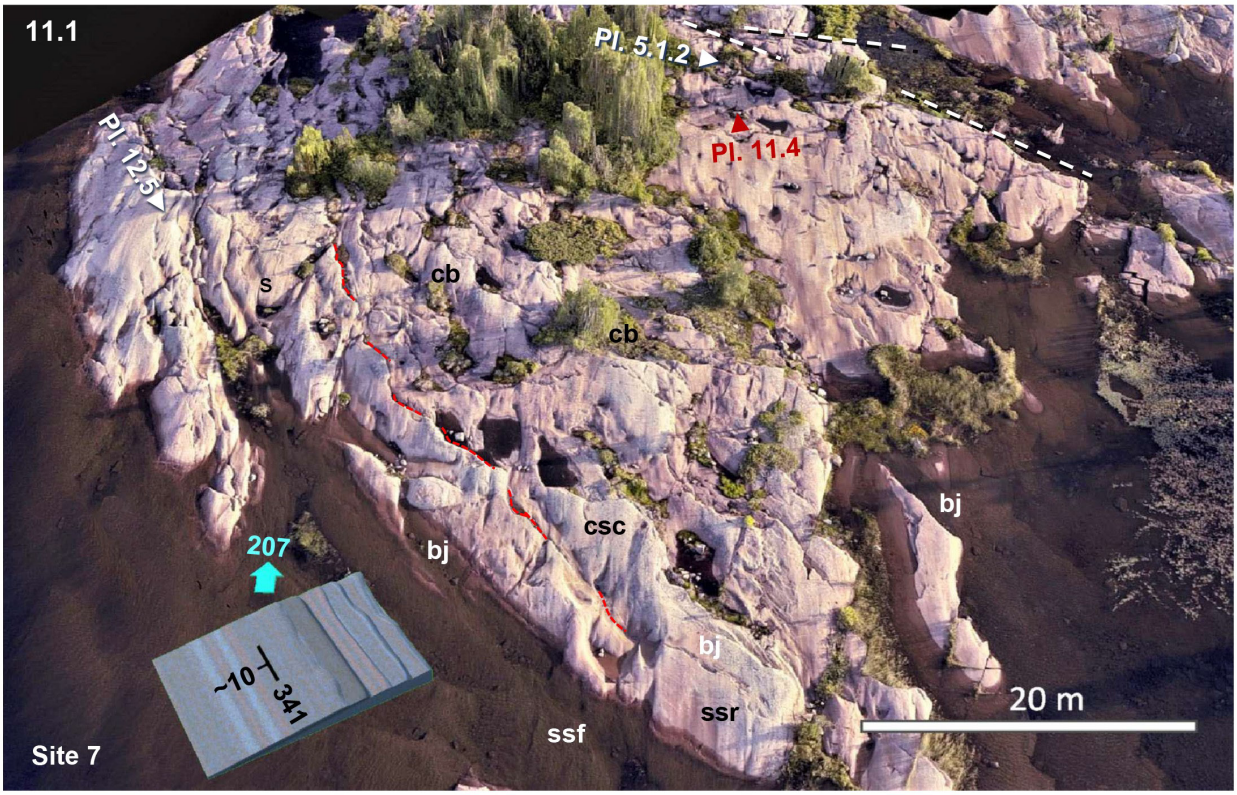

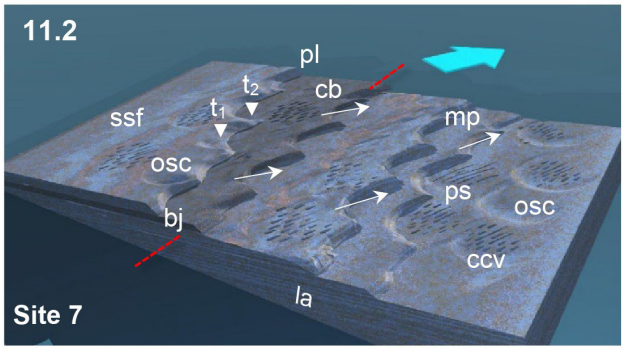

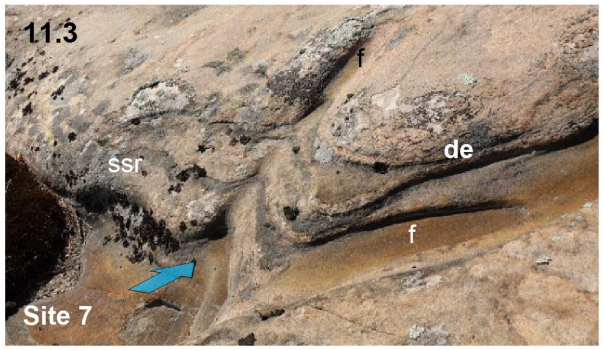

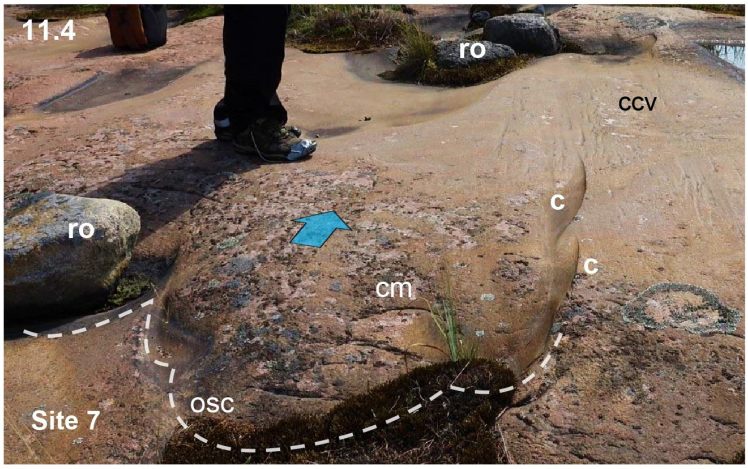

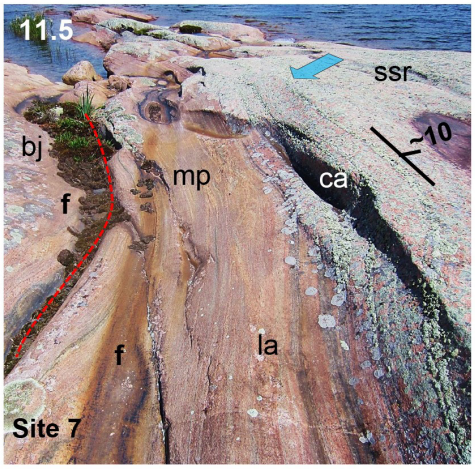

11.1 Photogrammetry survey of a low relief stoss-side ramp (ssr). The overall topography resembles a “fish scales” texture related to sculpting the stoss side and plucking the lee side. Flow is diagonal into dipping rock layers (lower left, block

diagram), yet stoss side furrows (ssf) are common. Lee-side plucking is related to structure where bedding in the gneiss eroded to a long chain of crescentic breaks (cb, red dashed lines) and bedding joints (bj) are mostly modified by s-forms (s), in particular sichelwannen (csc). Some straight brakes (white dashed lines) are the result of systematic fractures. Direction view (►) of Plates 11.4, 11.5 and 5.1.2. Photo courtesy of Guy Leduc.

11.2 Block diagram showing formation of "fish scale" terrain; stoss-side sculpting (ssf) and lee-side plucking (pl) and bedding joints (bj) forming long breaks (red dashed lines) mostly modified by s-forms (mp). Overlapping sichelwannen (osc) modified the long breaks. Layer (la) sections thinned (t_1) by s-forms were removed easier than the thicker ones (t_2), one of the processes leading to crescentic breaks (cb). Fields of pitted streaks (ps), tadpole/carrot forms (ccv), s-forms and crescentic breaks (cb, white arrows) represent organization and distribution within the flow.

11.3 Differential erosion (de) of the gneiss layers in furrows (f) and on the steep stoss-side ramp (ssr). Photograph by D.R. Sharpe. NRCan photo 2022-561.

11.4 Sets of overlapping sichelwannen (osc, white dashed lines) occur against rock rises; round boulders (ro) are trapped in s-forms; comma cavitation marks (ccv) are in aligned with larger commas (c) forms; and, crescentic chatter marks (cm) occur on local high points. Photograph by D.R. Sharpe. NRCan photo 2022-562.

11.5 Low relief stoss-side ramp (ssr) in close alignment with the sub-horizontal bedding of a massive gneiss finely laminated (la). Long depressions (red dashed lines) occur along bedding joints (bj), plucked (mp) and modified by furrows (f) and cavetto (ca). Photo courtesy of Guy Leduc.

Plate 11b. Cavitation Island study site 7; cavitation marks and local relief

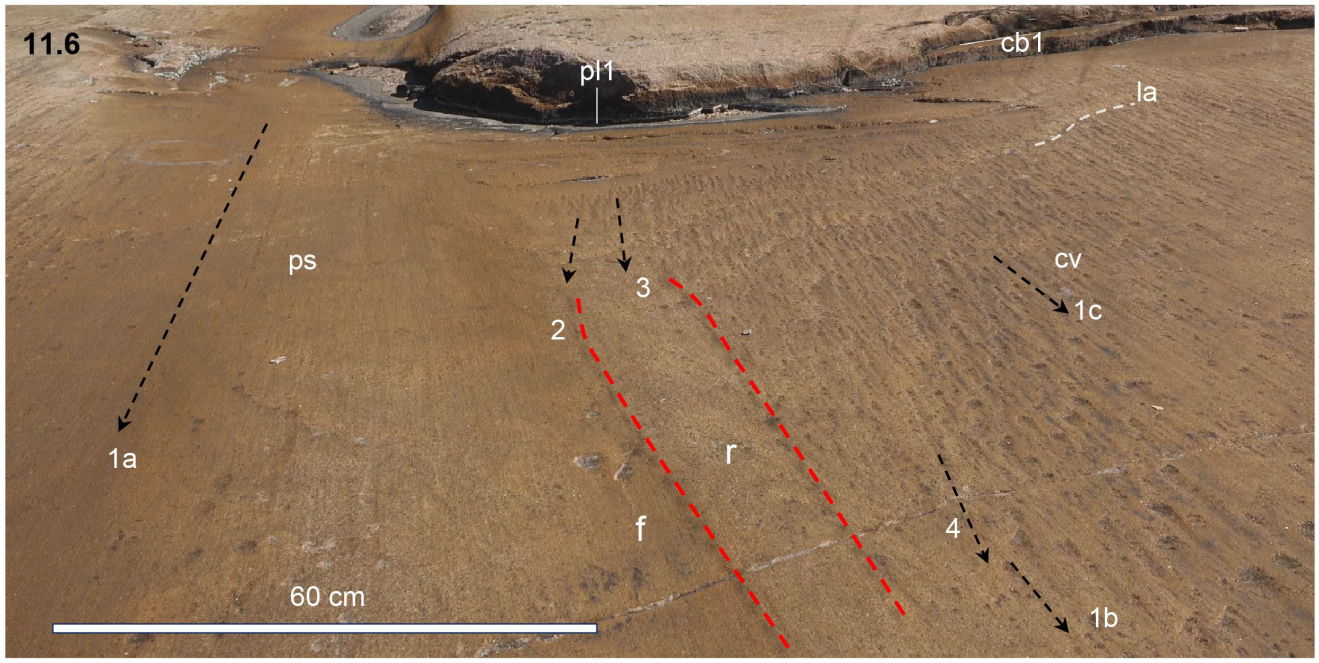

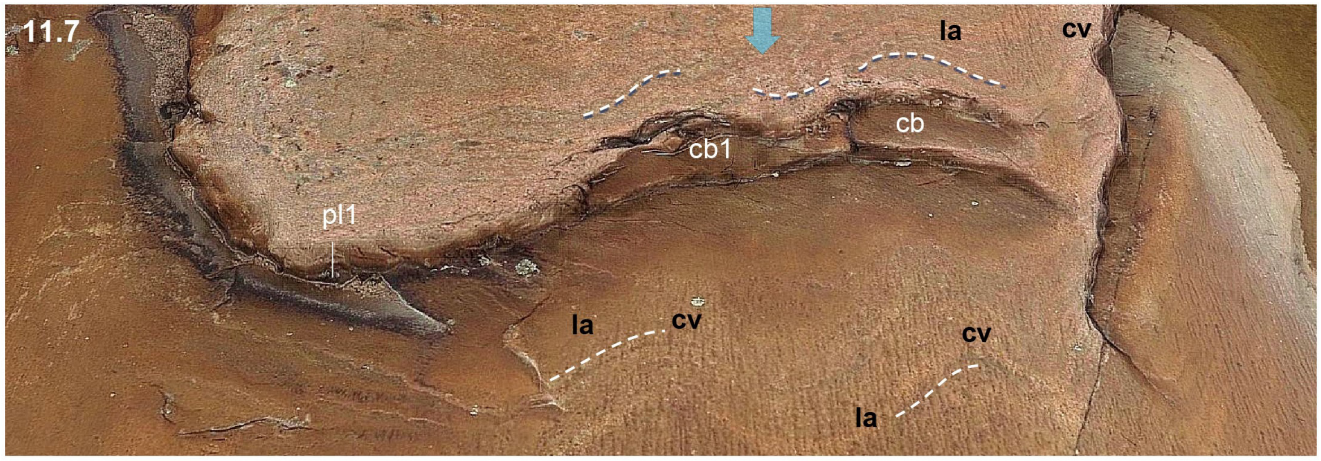

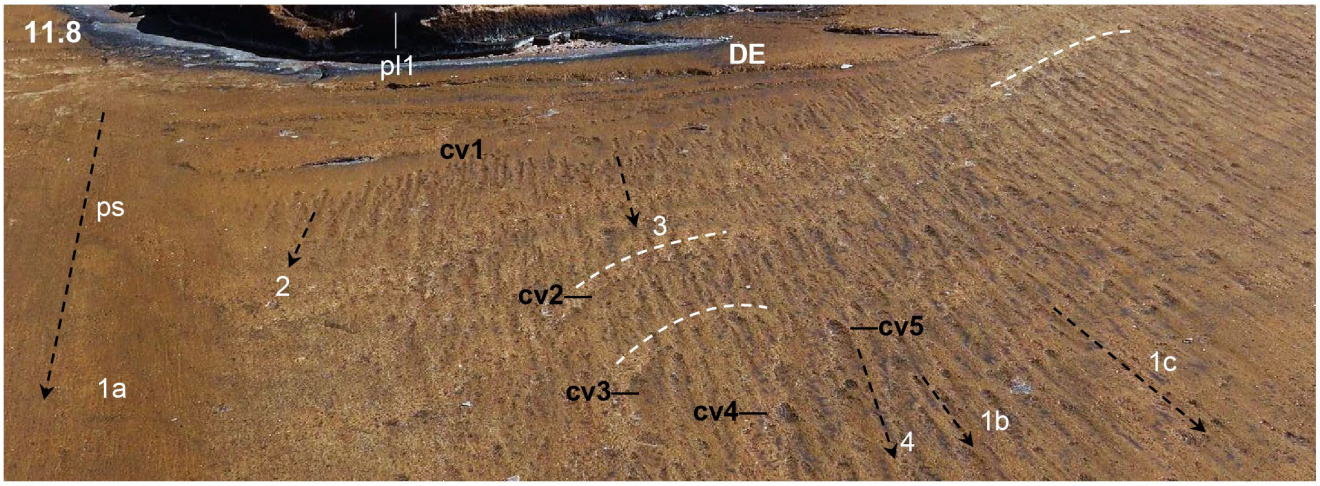

11.6 A rock step with low-relief plucking (pl1) and crescentic breaks (cb1) appears to alter flow vectors into small flow sets. General flow direction (arrows 1a,1b,1c) is indicated by long pitted streaks (ps) (arrow 1a) and tadpole/carrot cavitation marks (cv) of arrows 1b and 1c. Away from the lee-side rock step, pitted erosion marks are gradually re-orientated (arrows 2, 3, 4) to the main flow. A subtle furrow (f) and ridge ((r) red dashed lines) parallel main flow of the

1b, 1c flow set. Sets of tadpole/carrot marks are aligned along subtle erosion boundaries of rock layers (white dashed line (la)). Note that carrot pits and tails become larger down flow from label cv. Labels pl1 and cb1 are feature marks for Plate 11.7 and 11.8. The location of this site is indicated in Plate 5.1.3. Photograph by D.R. Sharpe. NRCan photo 2022-563.

11.7 Photogrammetry 3D survey, nadir view, of the low relief of Plate 11.6 (see marks pl1, cb1). Crescentic breaks (cb, cb1) represent plucking controlled by bedding joints and gneiss layers (white dashed lines (la)). Rows of tadpole/carrot cavitation marks (cv) are aligned along gneiss layers (white dashed line (la)) and occur immediately down flow of the rock step. Blue arrow indicates the main flow direction. Photograph by D.R. Sharpe. NRCan photo 2022-564.

11.8 Detail view of Plates 11.6 and 11.7 (feature mark pl1). General flow direction is indicated by long pitted streaks (ps) (arrow 1a) and tadpole/carrot cavitation marks of arrows 1b, 1c. Gneiss layers were differentially eroded into subtle steps (DE). Fine tadpole/carrot cavitation marks (cv1) align with a flat lower layer/step with flow directions gradually shifting (arrows 2 to 3). Cavitation marks (cv2) align with gneiss layers (white dashed lines). Label cv3 indicates a pitted surface with an upper edge aligned with layer (dashed white line). Large head carrot cavitation marks (cv4, cv5) are located down flow. Notice the large carrot mark cv5 (flow direction arrow 4) is at a slight angle to main flow 1b and 1c. Photograph by D.R. Sharpe. NRCan photo 2022-565.

PLATE 12a: Germain Island (study site 5): clusters of rock drumlins

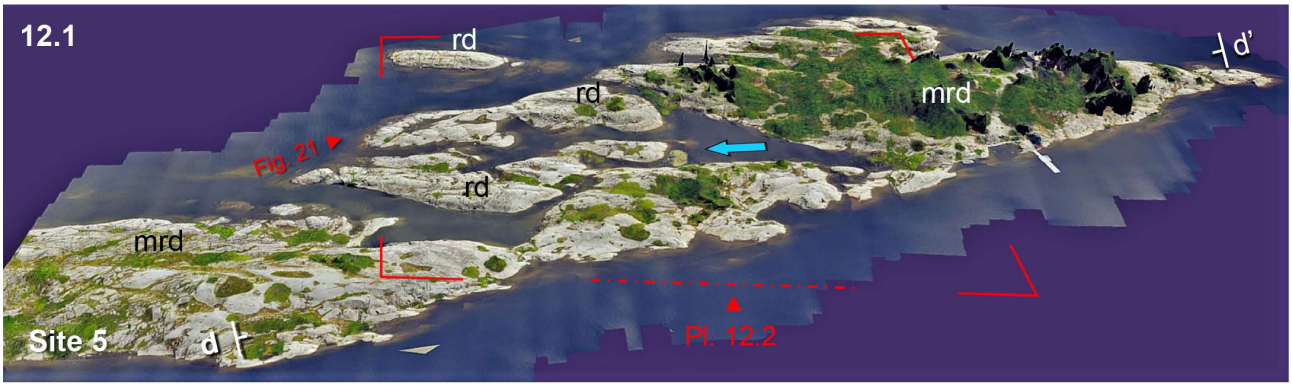

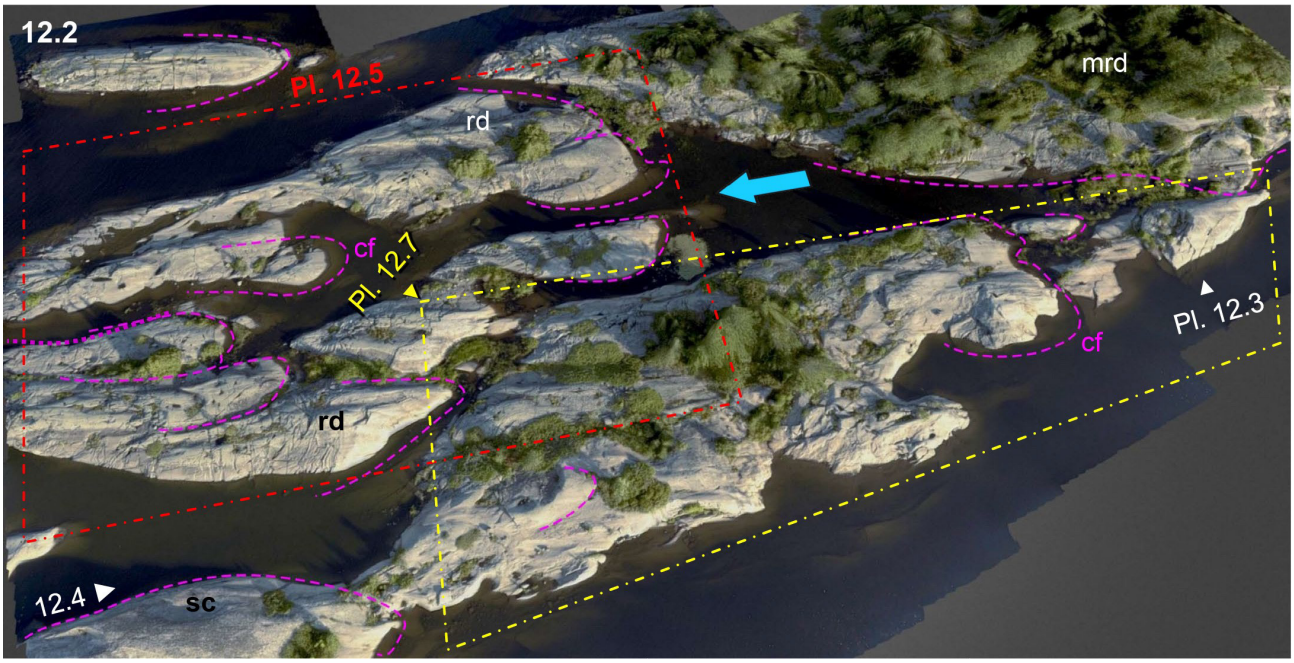

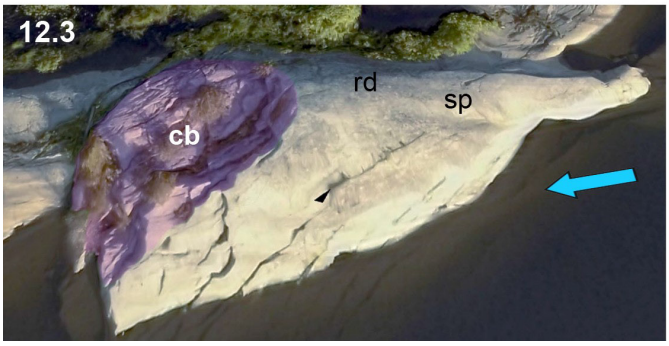

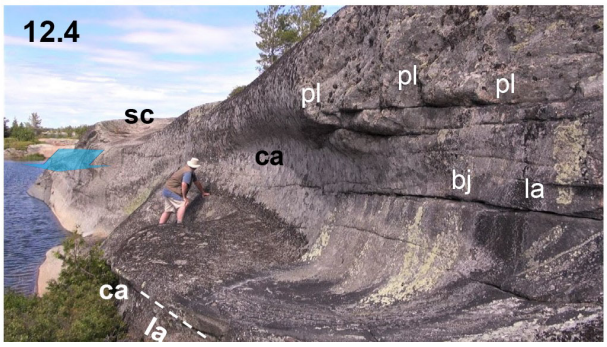

12.1 Photogrammetry survey of north Germain Island shows two clusters of rock drumlins (mrd) and solitary rock drumlins (rd); Plate 12.2 is framed in red; flow direction (blue arrow); distance (d-d') is 500 m. Photo courtesy of Guy Leduc.

12.2 Photogrammetry survey shows a series of rock drumlins (rd) with stoss-side, crescentic furrows (purple dashed lines (cr)), sichelwanne (sc) and rock drumlin cluster (mrd). Area of Plate 12.7 in yellow dashed line (view direction ►); area of Plate 12.5-12.6 in red dashed line (nadir view); Plates 12.3 & 12.4 (view direction ►) Photo courtesy of Guy Leduc.

12.3 Rock drumlin (rd) with bowl-shaped, lee-side plucking (colored purple (cb) and crescentic breaks at the erosion edge. Note spindle flute (sp) on top of rock drumlin. Photo courtesy of Guy Leduc.

12.4 A ~3 m high cavetto (ca) occurs down flow from large and small sichelwanne (sc) arm (see plate 12.2); bedding joints (bj) match the gneiss layering (la) below plucked forms (pl). Photograph by D.R. Sharpe. NRCan photo 2022-566.

PLATE 12b: Germain Island (study site 5)

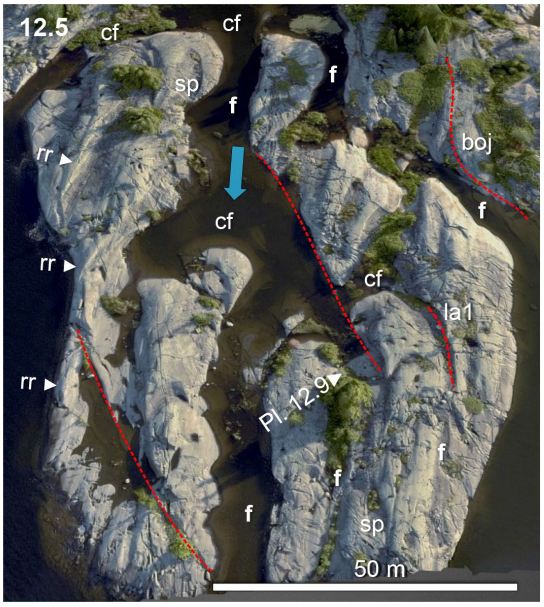

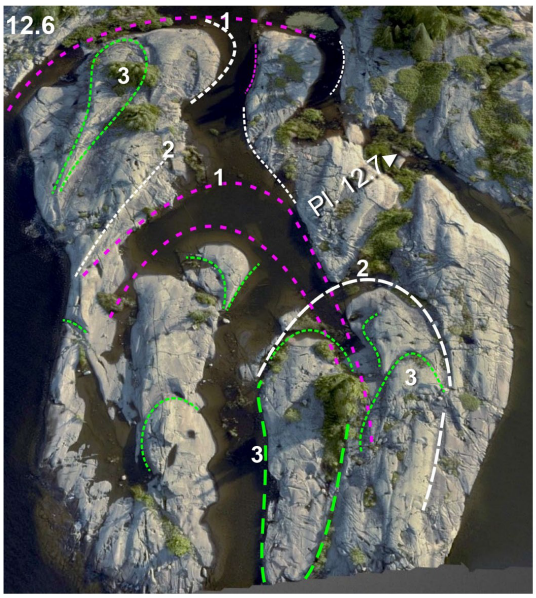

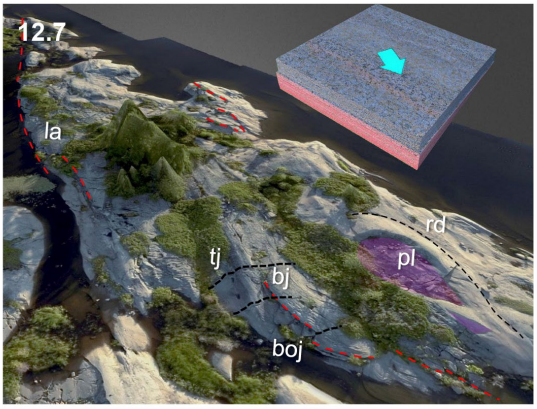

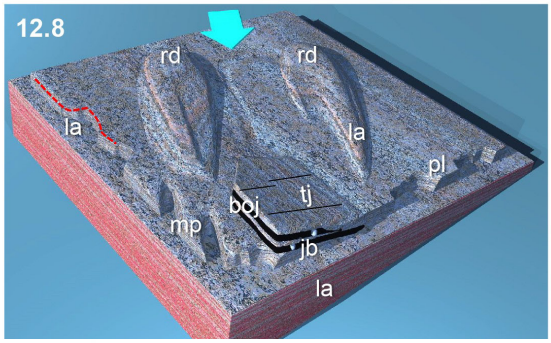

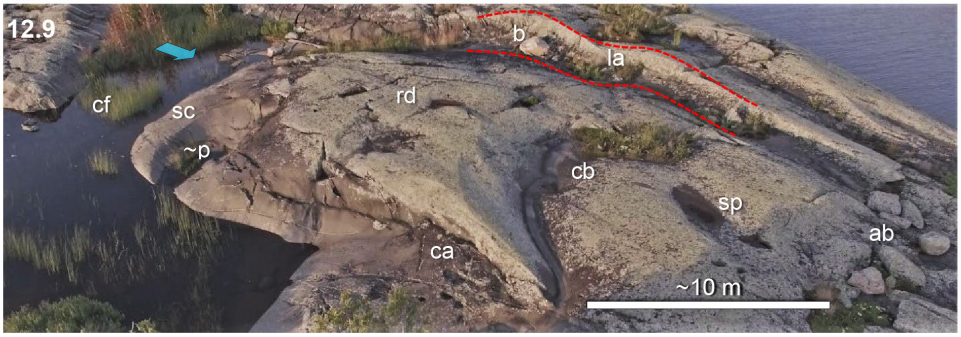

12.5 Photogrammetry survey (nadir view) of rock drumlins field/ cluster; crescentic furrow (cf); furrow (f); spindle flute (sp) sculpted individual rock drumlins and resulted in remnant ridge (rr) tails. Red dashed lines indicate gneiss layers that produce discontinuity in the sculpted erosion forms, such as bedding open joints (boj; see Plate 12.7). Location of Plate 12.9 (direction view ►). Blue arrow shows flow direction. Photo courtesy of Guy Leduc.

12.6 Same image as Plate 12.5 illustrates overlapping erosion features. 1) rock drumlin clusters defined by deep stoss-side crescentic furrows (purple dashed lines); 2) arms of crescentic furrows intersect 1 and join to form larger furrows /channels that divide rock drumlin clusters into smaller drumlins (white dashed lines); 3) final flow within the rock drumlins field created elongation of remnant ridges (green dashed lines); Location of Plate 12.7 (direction view ►). **Note: double armed sichelwannen occur at Fox River (Plate 2.5 and Fig. 11b).** Photo courtesy of Guy Leduc.

12.7 Photogrammetry survey, east side of Germain Island. Upper right, block diagram shows flow direction relative to vague gneiss layers (red dashed lines (la)). Bedding joints (bj) and bedding open joints (boj) with tension joints (tj); (see Plates 9.1.1 & 9.7) occur on the lee side of the ridge. A rock drumlin (rd) has a streamlined cavity, within the streamlined ridge (colored purple (pl)). Photo courtesy of Guy Leduc.

12.8 Block diagram showing an idealized rock rise landform array with included rock structure: gneiss layers (red dash lines (la)) form local bedding open jointing (boj); boulders (jb) are stranded in lee-side fractures and tension joints (tj); rock drumlins (rd), plucked (pl) and modified plucked forms (mp) are common forms.

12.9 Crescentic furrows (cf) define the stoss-side of large rock drumlins (rd), which are incised by well-defined sichelwanne (sc); small crescentic breaks (cb) occur up flow of a spindle flute (sp) surface; erosion along gneiss layers (red dashed lines (la)) allows for an enhanced deep arm of a sichelwanne (sc) to form; a possible pothole (~p) occurs on the upflow side of the rock drumlin, this may link to a crescentic furrow (cr) which extends down flow to a cavetto (ca); note large angular boulders (ab) on the lee side of rock drumlin and a round boulder (b) on the rock drumlin side. Photo courtesy of Guy Leduc.

APPENDICES

APPENDIX 1: Classification forms (Kor et al. 1991, figure 2).

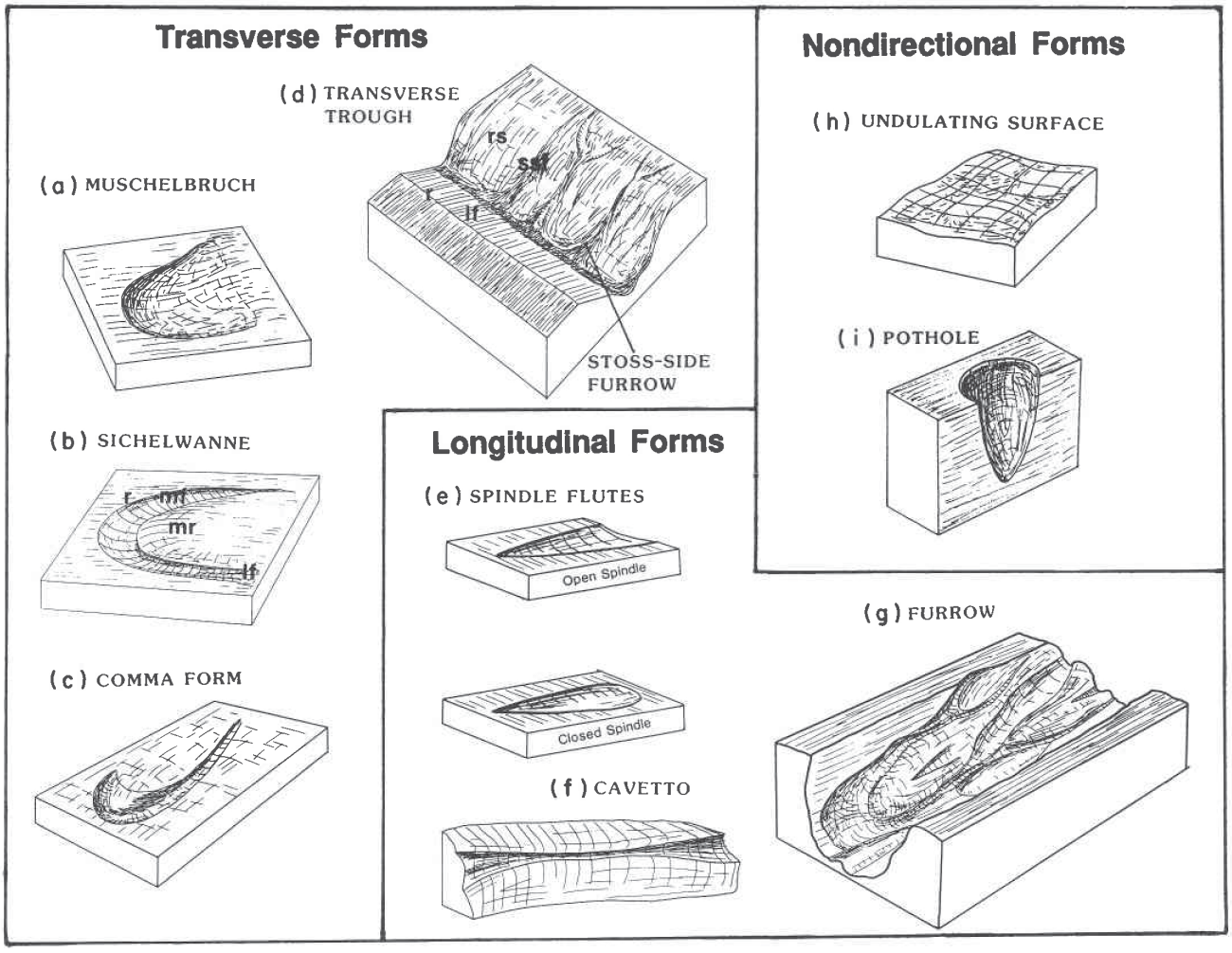

APPENDIX 2: Longitudinal array of s-forms on rock drumlins (from Kor et al. 1991, fig. 4).

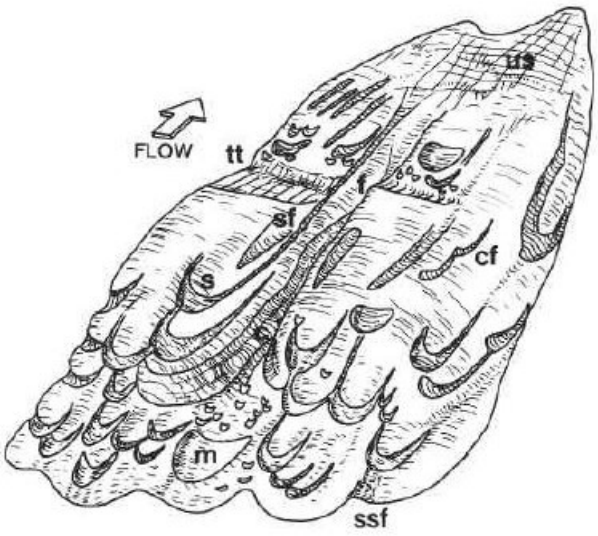

APPENDIX 3: Seven Videos
https://www.youtube.com/@Geodoxa

Playlist: *Georgian Bay bedrock erosion: evidence for regional floods 2023*
Intro: https://youtu.be/8pGhIdQobA4 (followed by 6 videos)

Drone video clips

Seven videos provide an overview of the main Key River sites with explanations, animations and interpretations of the bed forms and stages of evolution of the landscape and subglacial erosion features.

1. Introduction: Georgian Bay bedrock erosion: evidence for regional floods
2. Henvey Flat Island-part 1 of 6: rock drumlins with up flow crescentic scours
3. Outer Fox Island:- part 2 of 6: sichelwannen and commas with down flow furrows
4. Germain Island- part 3 of 6: nested rock drumlin motif
5. Henvey Inlet and Key River: part 4 of 6: potholes at cliff break on slopes linked to furrows
6. Plucking Island: part 5 of 6: plucked forms related to s-form types
7. Cavitation Island: part 6 of 6: cavitation streaks in association with s-forms

APPENDIX 4: Erosion by a horseshoe vortex and crescentic (hairpin) erosional mark. (from Shaw 1994)

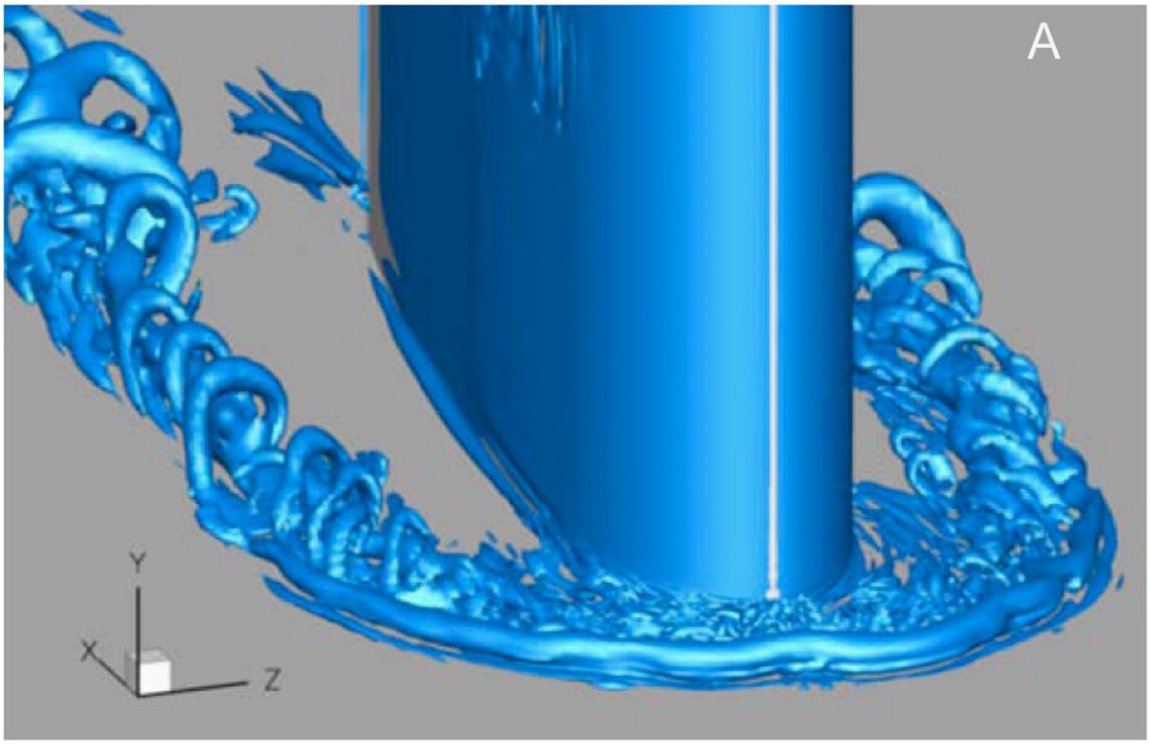

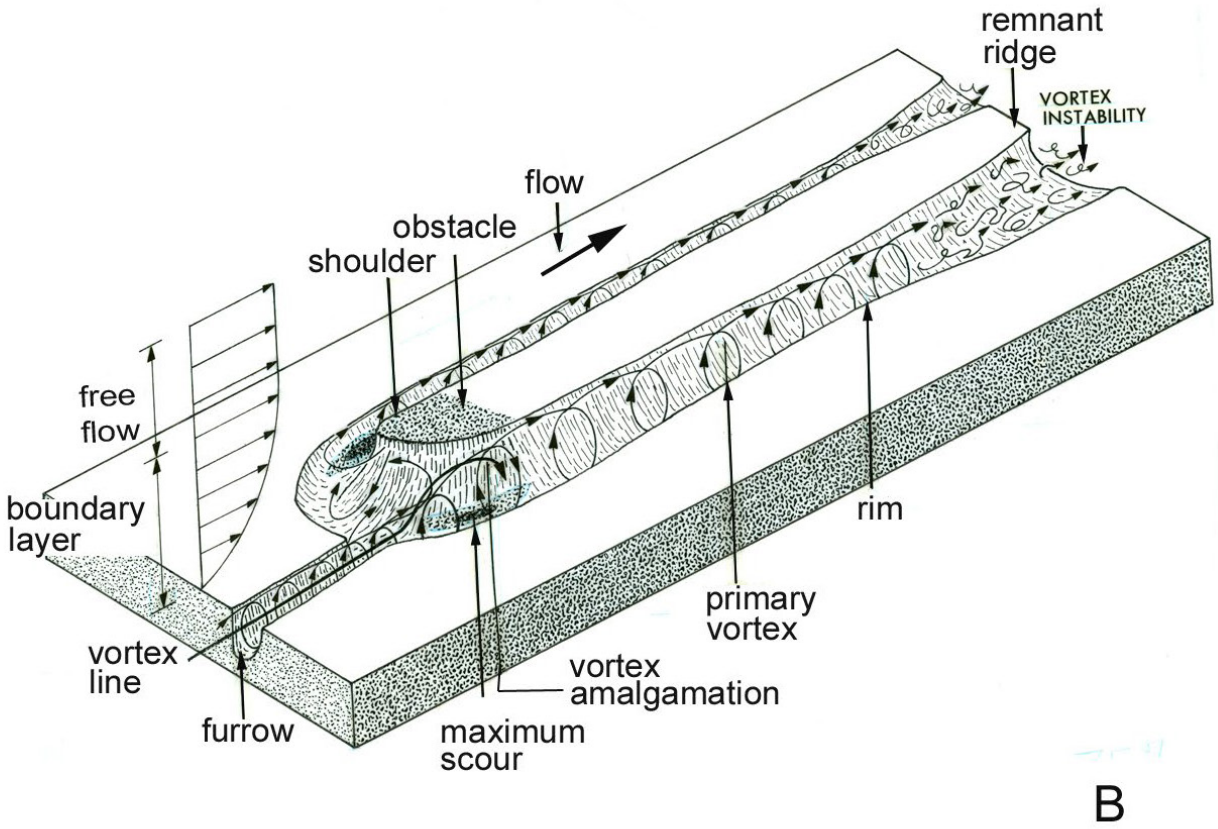

APPENDIX 5: Sketch of potholes at a structural step such as along Key River. As flow (blue arrow) approached the negative step, a hydraulic jump is established, and vertical vortices formed to erode potholes above and at the break in slope.

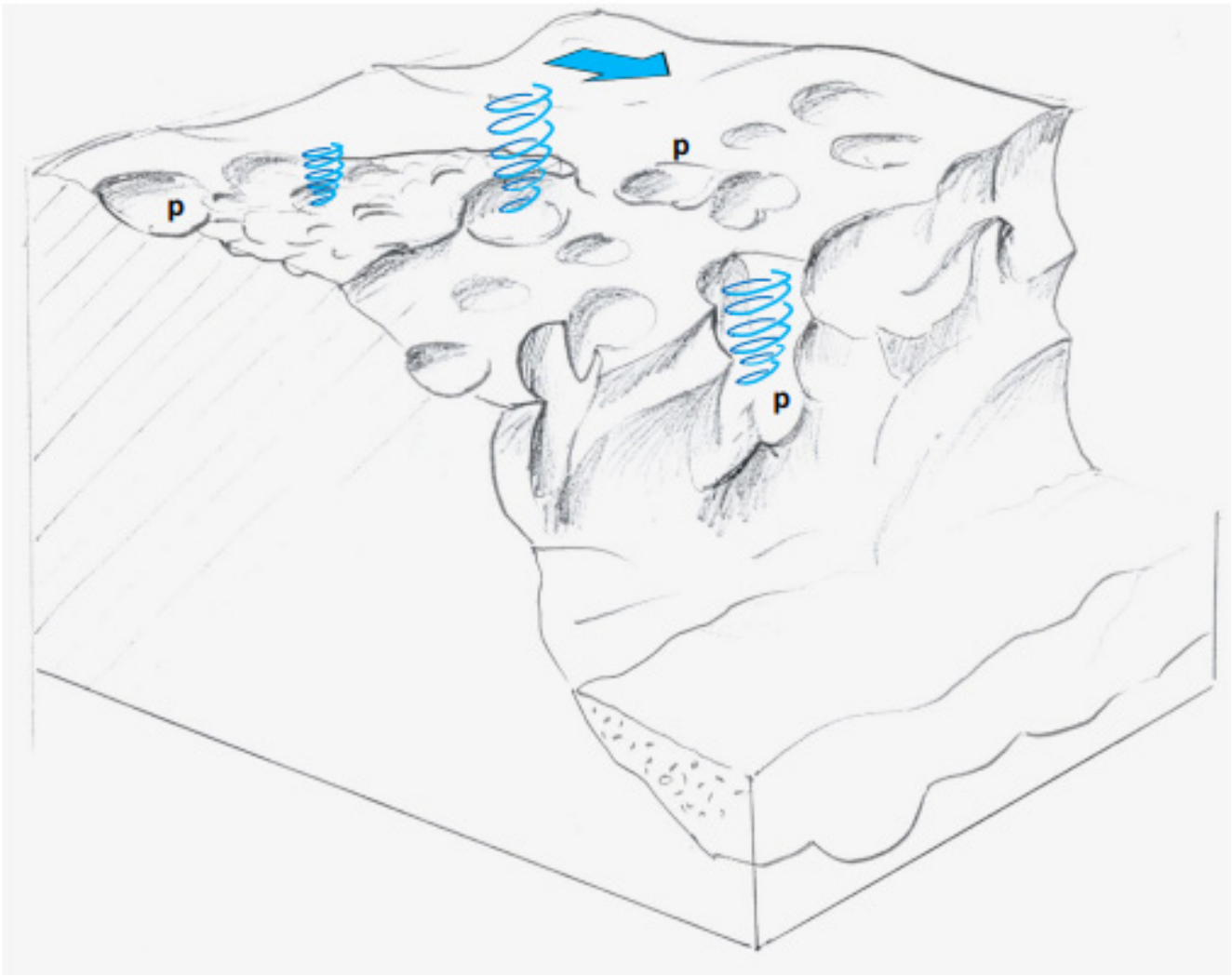

APPENDIX 6: As flow approaches a rock rise at Whitefish Bay, s-forms start to develop at the break in slope, perhaps at a structural break (white dashed lines); a transverse trough (tt) may form, then flow overrides the rise to form stoss-side furrows (ssf) that lead to commas (c) and crescentic furrows. These weak furrows evolve into sichelwannen (sc) from offset nested comma arms; long furrows (f) extend from the arms of sichelwannen (see detail b). Boulders gather in long furrows (b.f), in stoss-side furrows (b.ssf), in fractures (b.fr) and on lee side steep slope (b.Ls). See also figures 4 and 7. Photos courtesy of Guy Leduc.

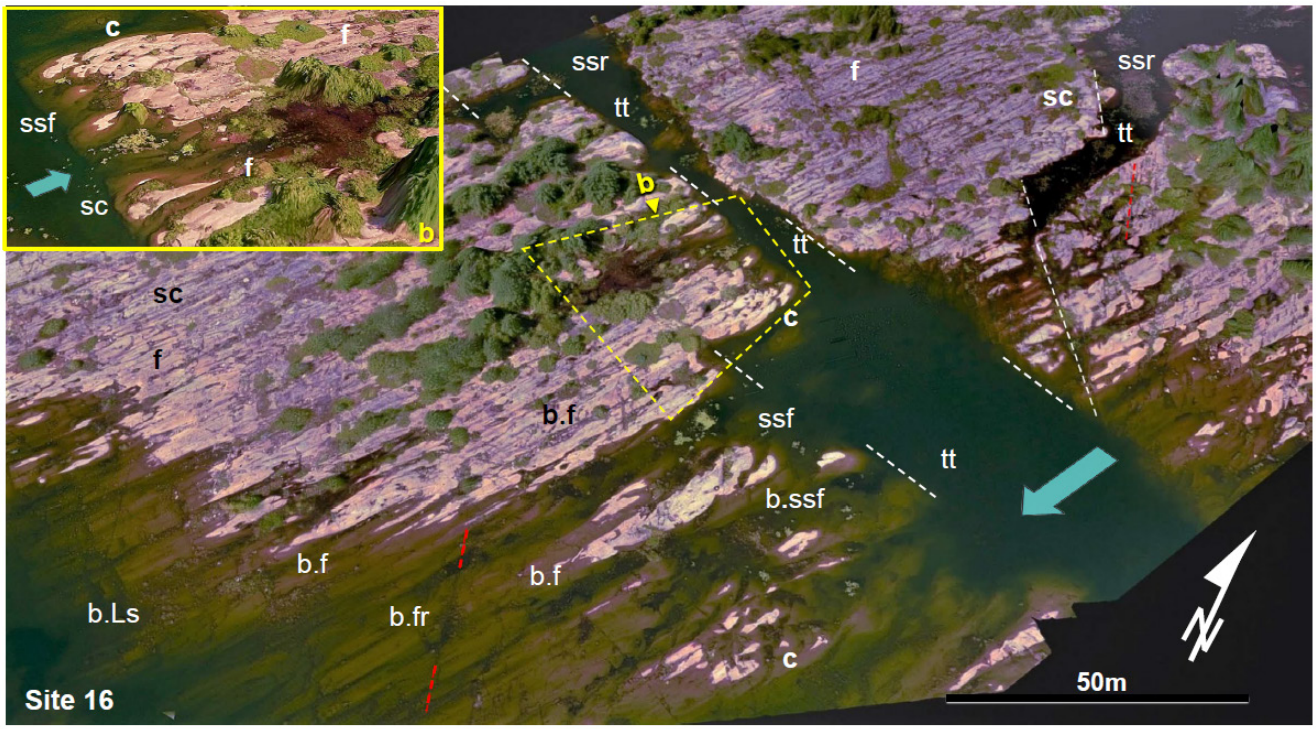

APPENDIX 7: Photogrammetry surveys of Plucking Island, site 4 (blue arrows indicate flow direction). **7.1** Drone image of the island indicating the surveyed area (Plate 7.2). Bedding open joints were observed at one location (◄boj). **7.2** Photogrammetry of the three detailed sections (Plates 7.3; 7.4; 7.5). **7.3** The height of the island shows the arrangement of s-forms down flow across a rise: stoss-side ramp (ssr), plucking (ssp) and stoss-side crescentic pluckings (1-2 m; ssc) were observed. These forms give way to Sichelwannen (sc), furrow (s) and spindle flutes (sp) which indicate the most prominent flow direction. Side and top plucking cavities have been modified by ongoing erosion (mp) in the flow. The full lee side of the land high was intensively plucked (pl). **7.4** Section up flow of the high (Plate 1.3). Main linear joints (j) cross the outcrop (W-E). Crescentic breaks and fractures (cb) are often smoothed by continued erosion. At the bottom of a lee side steep slope (Ls), we see sichelwanne (rs→) due to reverse flow (**video 4**). **7.5** Rock drumlin capped with a sichelwanne (sc). The longitudinal lee side is plucked (pl) with many crescentic breaks and fractures (cf) often smoothed by later flow. See Plate 5.1.4 looking up flow and Plate 5.5 looking down flow. Photos courtesy of Guy Leduc.

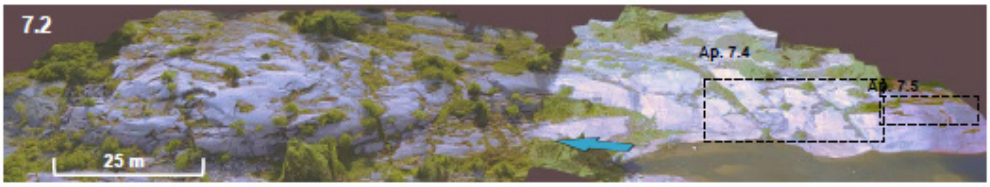

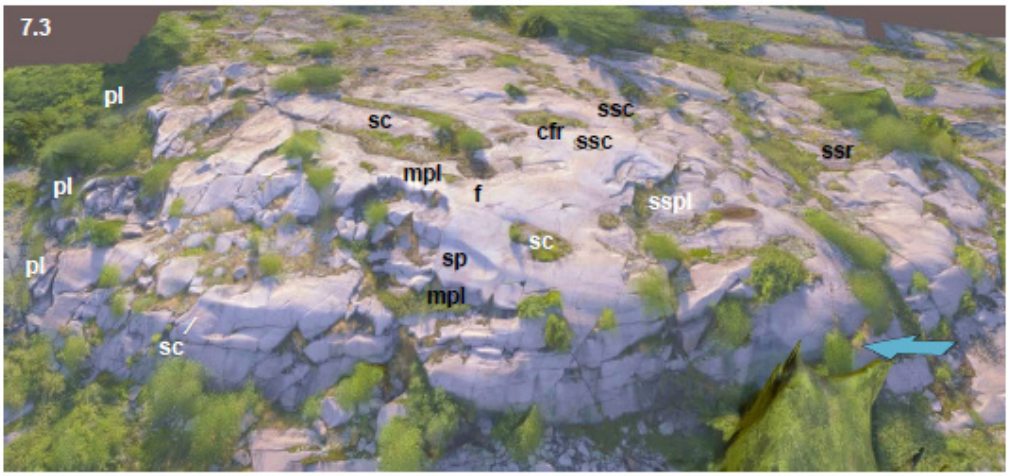

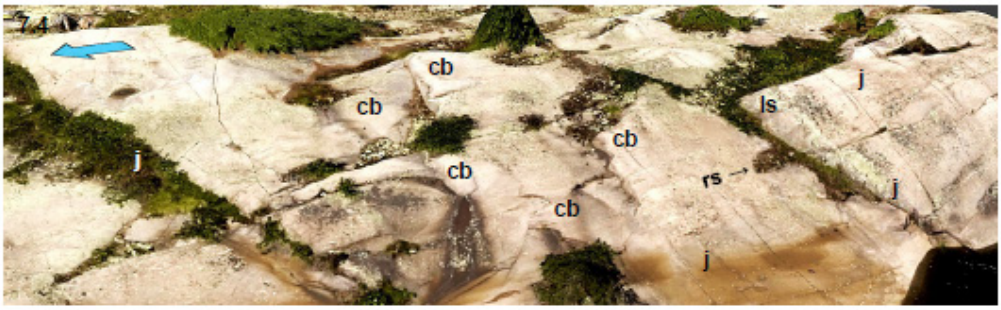

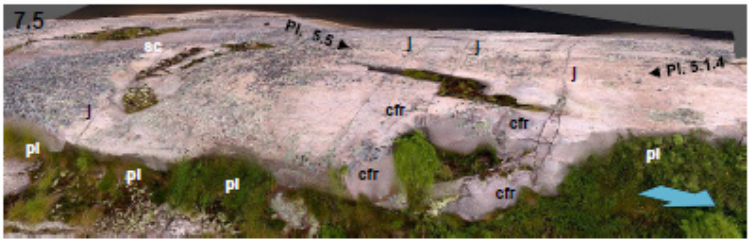

APPENDIX 8: Inlet East of Fox Island (site 15). 8.1, Aerial view of site 15 inlet looking South. Rock layers ((la) strike/dip in red) are parallel to the inlet. The down flow side of the inlet (west shore) is sculpted with stoss-side ramps (ssr), s-forms (see Plates 4.2 (►), 13.2) and rock drumlins (rd). The stoss-side ramps (ssr) are approximatively parallel to the bedding. The up-flow side of the inlet (east shore) is steep, sculpted with cavettos (ca, >1 m), plucked (see Pl. 13.2) and, exposes rock layers (la) and bedding joints (bj). The overall terrain has cuesta steps. **8.2** Aerial view of a rock drumlin ridge (rd) with a sculpted face (ss) on a stoss-side ramp (ssr) and a steep slope on lee side (Ls) which is sculpted with cavettos (ca, >1 m), plucked (pl) and exposes bedding joints (bj). Boulders occur in stoss-side crevasses (see Plate 8.3, located with label). White arrows show the trajectory of local flow from the inlet toward main flow up the ridge. Viewpoints Plates 13.1 and 13.3 are labeled (► & ◄). **8.3** Aerial view of ridge and inlet looking North. Stoss-side ramps (ssr) on down flow side (west shores) of inlet are almost parallel to rock layers (l, white dashed lines). Steep lee side (Ls) on up-flow side (east) of inlets. Photos courtesy of Guy Leduc.

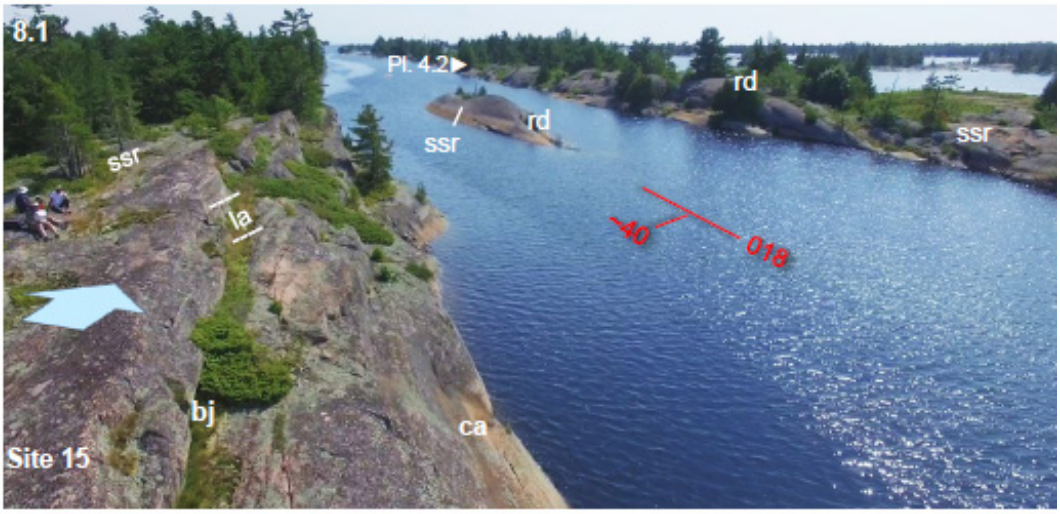

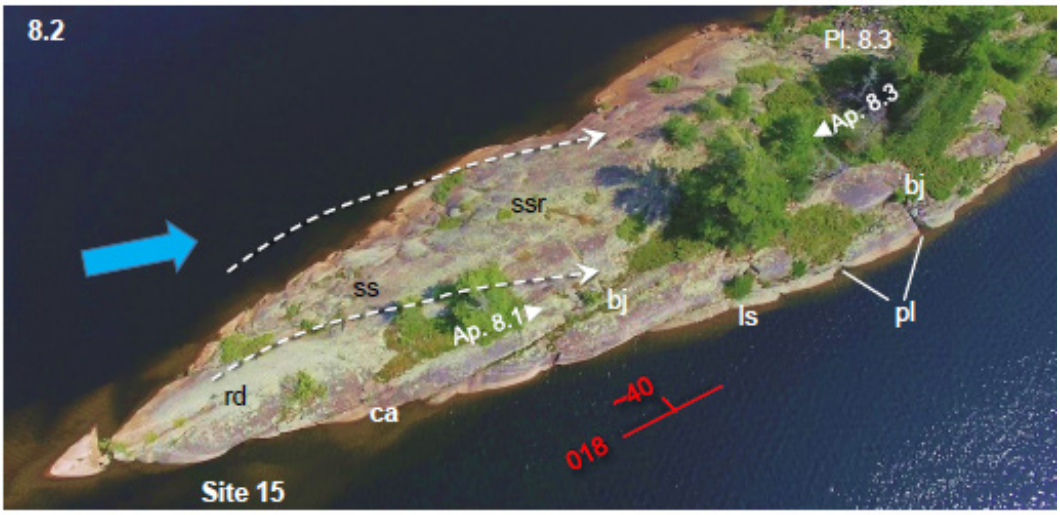

ACKNOWLEDGEMENTS

We appreciate the generous hospitality of Elizabeth and Cary Kokkonen who hosted our research team in July 2017 and August 2019 and 2022 at their home on Germain Island. They participated in research access by boat, in discussions and filming some of the included video records. We benefitted from dialogue with Bernard Hallet, Neil Iverson, Lorenz Sigurdson, and Matevz Dular**,** although we are responsible for any errors or omissions. We appreciate the review comments by Ross Knight. Funding is from Geological Survey of Canada, Groundwater Geoscience Program and Archetypal Aquifer project. We dedicate this report to our deceased colleague John Shaw who inspired us to seek answers from the sculpted rocks.

REFERENCES

Alley, R.B. Cuffey, K.M. Evenson, E.B. Strasser, J.C. Lawson D.E. and Larson, G.J. 1997. How Glaciers Entrain and Transport Basal Sediment and Physical Constraints, *Quaternary Science Reviews,* **16***:* l017-1038.

Alley, R.B., T.K., Dupont, B.R., Parizek, S., Anandakrishnan, D.E., Lawson, G.J., Larson, and Evenson, E.B. 2006. Outburst flooding and the initiation of ice-stream surges in response to climatic cooling: A hypothesis. *Geomorphology* 75, 76– 89.

Andrews, E. 1883. Glacial markings of unusual forms in the Laurentian hills. Bulletin of the Chicago Academy of Sciences, 1: 3-9.

Baker, V.R., 1973. Paleohydrology and sedimentology of Lake Missoula Flooding in Eastern Washington. Geological Society of America, Special Paper 144.

Baker, V.R., 1978, Paleohydraulics and hydrodynamics of Scabland floods, *in* Baker, V.R., and Nummedal, D., eds., The Channeled Scabland: Washington, D.C., National Aeronautics and Space Administration, p. 59–79.

Baker, V.R., 2009. The Channeled Scabland: A Retrospective *Annual Review of Earth and Planetary Sciences* **37**:393–411 doi:10.1146/annurev.earth.061008.134726

Barnes HL. 1956. Cavitation as a geological agent. American Journal of Science 254: 493–505.

Bourne N.K., and Field J.E. 1995. A high speed photographic study of cavitation damage. Journal of Applied Physics 78: 4423–4427.

Beaud, F., Flowers, G. E., and Venditti, J. G. 2016. Efficacy of bedrock erosion by subglacial water flow. *Earth Surface Dynamics,* **4**: 125–145. https://doi.org/doi:10.5194/esurf-4-125-2016

Bernard, C., 1971. Les marques sous glaciaires d'aspect plastique sur la roche en place (pforms). Observations sur la bordure du bouclier canadien et examen de la question (I). Revue Géographie de Montréal 25, 177–191.

Bjornson, H. 2009: Jökulhlaups in Iceland: sources, release and drainage. In Burr, D. M., Carling, P. A. & Baker, V. R. (eds.): Megaflooding on Earth and Mars, 50–64. Cambridge University Press, Cambridge.

Blasco, S.M. 2001. Geological history of Fathom Five National Marine Park over the past 15,000 years. In Ecology, culture and conservation of a protected area: Fathom Five National Marine Park, Canada. Edited by S. Parker and M. Munawar. Ecovision World Monograph Series 2001. Backhuys Publishers, Netherlands. pp. 45–62.

Brennand, T.A. and Shaw, J. 1994. Tunnel channels and associated landforms: their implication for ice sheet hydrology. *Canadian Journal of Earth Sciences,* **31:** 502–522.

Brennand, T.A., Russell, H.A.J. and Sharpe, D.R. 2006. Tunnel channel character and evolution in central southern Ontario; *in* Glaciers and Earth's changing environment; (ed.) P.G. Knight; Blackwell Publishing Limited, Oxford, United Kingdom, p. 37–39.

Brennand, T.A. and Sharpe, D.R. 1993. Ice-sheet dynamics and subglacial meltwater regime inferred from form and sedimentology of glaciofluvial systems: Victoria Island, District of Franklin, Northwest Territories. *Canadian Journal of Earth Sciences*, 30: 928-944.

Booth, D.B., 2004. Glaciofluvial infilling and scour of the Puget Sound Lowland, Washington during ice-sheet glaciation. Geology 22, 695–698.

Boulton, G.S., 1974. Processes and patterns of glacial erosion. In: Coates, D.R. (Ed.), Glacial Geomorphology. State University of New York, Binghamton, NY, pp. 41–87.

Bryant, E. A., and Young, R.W. 1996. Bedrock sculpturing by tsunami, south coast New South Wales, Australia. J. Geol. 104:565–582.

Carling, P.A., Herget, J., Lanz, J.A., Richardson, K. and Pacifici, A. 2009. Channel-scale erosional bedforms in bedrock and in loose granular material: character, processes and implications. In Mega-flooding on Earth and Mars, Edited by Burr, D., Carling, P. and Baker, V. Cambridge University Press, p. 13-32.

Carling P.A., Villanueva I, Herget J, Wright N, Borodavko P, Morvan H. 2010. Unsteady 1D and 2D hydraulic models with ice dam break for Quaternary megaflood, Altai Mountains, southern Siberia. Global and Planetary Change 70**:** 24-34.

Carling P.A., Perillo, M., Best, J., and M. H. Garcia, 2017. The bubble bursts for cavitation in natural rivers: laboratory experiments reveal minor role in bedrock erosion. Earth Surface Processes and Landforms, 42: 1308–1316.

Coleman, S.E., Fedele, J.J., &. Garcia, M. H. 2003. Closed-Conduit Bed-Form Initiation and Development *Journal of Hydraulic Engineering*,129 (12): 956- 965. doi: 10.1061/~ASCE!0733-9429~2003!129:12(956)
Corrigan D., Culshaw N.G., and Mortensen J.K. 1994. Pre-Grenvillian evolution and Grenvillian overprinting of the Parautochthonous Belt in Key Harbour area, Ontario: U-Pb constraints. Canadian Journal of Earth Sciences, **31**: 583–596.
Cowan, W.R., and Sharpe, D.R. 2007. Surficial geology of the Bruce Peninsula, southern Ontario, Ontario Geological Survey, Open file report 6211, 34p.
Dubinski. I. M. and Wohl, E, 2013. Relationships between block quarrying, bed shear stress, and stream power: A physical model of block quarrying of a jointed bedrock channel. Geomorphology, 180–181: 66–81.
Culshaw, D., Corrigan, J.W.F., Ketchum, P., Wallace and N. Wodicka, 1987 to 1990. Geological compilation by N.G. Culshaw, 1991 and 2004.
Culshaw, N.G., Corrigan, D., Ketchum, J.W.F., Wallace, P. and Wodicka, N. 2004. Precambrian geology, Key Harbour area; Ontario. Ontario Geological Survey, Preliminary Map P.3548, scale 1:50 000.
Dular, M., Bachert, B., Stoff, B., Sirok, B., 2004. Relationship between cavitation structures and cavitation damage. Wear 257, 1176–1184.
Dular, M., and Petkovšek, M. 2015. On the Mechanisms of Cavitation Erosion – Coupling High Speed Videos to Damage Patterns, Experimental Thermal and Fluid Science, doi: http://dx.doi.org/10.1016/ j.expthermflusci.2015.06.001
Dzulinski, S., Walton, E.K. 1965. Sedimentary Features of Flysch and Graywackes. Elsevier, Amsterdam 274 pp.
Elfstrom, A., 1987. Large boulders and catastrophic floods: a case study of the Baldakatj area, Swedish Lapland. Geograpfiska Annaler, 69: ser. A, 101-121.
Eyles, N., 2012. Rock drumlins and megaflutes of the Niagara Escarpment, Ontario, Canada: a hardbed landform assemblage cut by the Saginaw-Huron Ice Stream. Quat. Sci. Rev. 55, 34–49.
Falvey H.T. 1990. Cavitation in Chutes and Spillways, Engineering Monograph No. 42. USDI Bureau of Reclamation: Denver, CO.
Flowers, G.E., Björnsson, H., Pálsson, F. and Clarke, G.K.C. 2004: A coupled sheet-conduit mechanism for jökulhlaup propagation. Geophysical Research Letters, 31 doi:10.1029/2003GL019088
Gilbert, R., and Shaw, J., 1994. Inferred subglacial meltwater origin of lakes on the southern border of the Canadian Shield. Can. J. Earth Sci. 31, 1630–1637.
Gjessing, J., 1965. On 'plastic scouring' and 'subglacial erosion'. Norsk geografisk tidsskrift, **20**: 1-37.
Gray, J.M., 1981. P-forms from the isle of mull. Scottish J. Geol. 17: 39–47.
Hallet, B., 1981. Glacial abrasion and sliding: their dependence on the debris concentration in basal ice. Annals of Glaciology **2**: 23–28.
Hallet B. 1996. Glacial quarrying: a simple theoretical model. Annals of Glaciology 22: 1–8.
Hallet, B. 2011. Glacial erosion assessment, for OPG's Deep Geologic Repository for Low and Intermediate Level Waste NWMO DGR-TR-2011-18, 55p. January 2011.
Hjulström, F., 1935. Morphological activity of rivers as illustrated by the River Fyris. Bull. Geol. Inst. Univ. Uppsala 25 (221), 527.
Iverson NR. 1991a. Morphology of glacial striae: implications for abrasion of glacier beds and fault surfaces. Geological Society of America Bulletin 103: 1308–1316.
Iverson NR. 1991b. Potential effects of subglacial water-pressure fluctuations on quarrying. Journal of Glaciology 37: 27–36.
Kamb, B. Raymond, C. Harrison, W. Engelhardt, H. Echelmeyer, K. Humphrey, N. 1985. Glacier surge mechanism: 1982-1983 surge of Variegated Glacier, Alaska. *Science* 227: 469-479.
Kenn, M.J., Minton, P., 1968. Cavitation induced by vorticity at a smooth flat wall. Nature 217, 633-634
Koken, M., and G. Constantinescu, 2011. Flow and turbulence structure around a spur dike in a channel with a large scour hole, Water Resour. Res., 47, W12511, doi:10.1029/2011WR010710.
Kor, P.S.G., Shaw, J., and Sharpe, D.R. 1991. Erosion of bedrock by subglacial meltwater, Georgian Bay, Ontario: a regional view. Canadian Journal of Earth Sciences, 28, 623-642.
Kor, P.S.G., and Cowell, D.W. 1998. Evidence for catastrophic subglacial meltwater sheetflood events on the Bruce Peninsula. Canadian Journal of Earth Sciences, **35**(10): 1180–1202. doi:10.1139/cjes-35-10-1180.
Krabbendam, M., T. Bradwell, J.D. Everest, N. Eyles 2017. Joint-bounded crescentic scars formed by subglacial clast-bed contact forces: Implications for bedrock failure beneath glaciers. Geomorphology, 290 : 114–127.
Krabbendam, M., Bradwell T., Everest, J.D., and Eyles N. 2015. Joint-bounded crescentic scars formed by subglacial clast-bed contact forces: Implications for bedrock failure beneath glaciers. Geomorphology 290:114–127.
Krabbendam, M., Eyles, N., Putkinen, N., Bradwell, T., Arbeleaz-Moreno, L., 2016. Streamlined hard beds formed by palaeo-ice streams: a review. Sediment. Geol. 338: 24–50
Lelandais, T. Ravier, E. Pochat, S. Bourgeois, O. Clark, C. Mourgues, R. Strzerzynski, P. 2018. Modelled subglacial floods and tunnel valleys control the life cycle of transitory ice streams. *The Cryosphere* 12: 2759-72. s
Livingstone, S.J., Clark, C.D., and Tarasov, L. 2013. Modelling North American palaeo-subglacial lakes and their meltwater drainage pathways. Earth Planetary Science Letters, **375**: 13-33.

Lanzerstorfer D. and Hendrik C. Kuhlmann. 2012. Three-dimensional instability of the flow over a forward-facing step. Journal of Fluid Mechanics, 695: 390-404. Cambridge University Press 390 doi:10.1017/jfm.2012.28
Magmussen, Eyjo´lfur, Helgi Bjornsson, Helmut Rott, Matthew J. Roberts, Finnur Palsson, Sverrir Gudmondsson, Richard A. Bennett, Halldo´r Geirsson, Erik Sturkell. 2011. Localized uplift of Vatnajo¨kull, Iceland: subglacial water accumulation deduced from InSAR and GPS observations. Journal of Glaciology, 57: 203, 475-484.
Maizels, J. 1997. Jökoulhlaup deposits in proglacial areas. Quaternary Earth Science Reviews, 16: 793-819.
Munro-Stasiuk, M., Shaw, J., Sjogren, D., Brennand, T., Fisher, T., Sharpe, D., Kor, P., Beany, C., Rains, B., 2009. The morphology and sedimentology of landforms created by subglacial megafloods. In: Burr, D., Carling, P., Baker, V. (Eds.), Megaflooding on Earth and Mars. Cambridge University Press, pp. 78–103 106.
Munro-Stasiuk, M.J., Fisher, T.G., Nitzsche, C.R., 2005. The origin of western Lake Ontario grooves, Ohio: implications for the subglacial hydrology of the Great Lakes sector of the Laurentide Ice Sheet. Quat. Sci. Rev. 24, 2392–2409.
Nye, J.F., 1976. Water flow in glaciers: jökulhlaups, tunnels and veins. Journal of Glaciology, 17: 181-207.
Paik, J., Escauriaza, C., and Sotiropoulos, F., 2007. On the bimodal dynamics of the turbulent horseshoe vortex system in a wing-body junction. Phys. Fluids 19 (45107), 1–20.
Paik, J., Escauriaza, C., and Sotiropoulos, F., 2010. Coherent structure dynamics in turbulent flows past in-stream structures: some insights gained via numerical simulation. J. Hydraul. Eng. 136 doi: 1061/(ASCE)HY.1943-7900.000089.
Paola, C., and Borgman, L., 1991. Reconstructing random topography from preserved stratification: Sedimentology, **38**: 553–565.
Pugin, A.J.-M. Dietiker, B., Mulligan, R.P.M., Crow, H.L., Brewer, K., Cartwright, T., Hunter, J.A., Rainsford, D.R.B., Bajc, A.F., Sharpe, D.R., and Russell, H.A.J., 2018. High-resolution seismic-reflection profiles for groundwater studies in Simcoe County, southern Ontario; Geological Survey of Canada, Open File 8383 (*also* Ontario Geological Survey, Open File Report 6347), 1 .zip file. https://doi.org/10.4095/308388
Rea, B.R., Evans, D.J.A., Dixon, T.S., Whalley, W.B., 2000. Contemporaneous, localized, basal ice-flow variations for bedrock erosion and the origin of p-forms. Journal of Glaciology, **46**: 470-476.
Röthlisberger, H. and Iken A. 1981. Plucking as an effect of water-pressure variations at the glacier bed. Annals of Glaciology **2**: 57–62.
Röthlisberger, H., 1972. Water pressure in intra- and subglacial channels, Journal of Glaciology, **11**(62): 177–203.
Sharpe, D.R. and Russell, H.A.J. 2023. Sedimentary architecture and glacial hydrodynamic significance of the stratified Oak Ridges Moraine, southern Ontario, Canada. Boreas. https://doi.org/10.1111/bor.12612. ISSN 0300-9483.
Sharpe, D.R. and Shaw, J., 1989. Erosion of bedrock by subglacial meltwater, Cantley, Quebec. Geological Society of America Bulletin, **101**: 1011-1020.
Sharpe, D.R., Pugin, A.J.-M., and H.A.J. Russell, 2018. Geological framework of the Laurentian trough aquifer system, southern Ontario, *in* Special Issue entitled "Quaternary geology of southern Ontario and applications to hydrogeology". Canadian Journal of Earth Sciences, **55**: 677-708. https://doi.org/10.1139/cjes-2017-0113
Shaw, J. and Sharpe, D.R., 1987. Drumlin formation by subglacial meltwater erosion. Canadian Journal of Earth Sciences, v. 24, p. 2316-2322.
Shaw, J., Gilbert, R., 1990. Evidence for large-scale subglacial meltwater flood events in southern Ontario and northern New York State. Geology 18, 1169–1172.
Shaw, J., 1994b. Hairpin erosional marks, horseshoe vortices and subglacial erosion. Sediment. Geol. 91, 269–283.
Shaw, J., Pugin, A., Young, R., 2008. A meltwater origin for Antarctic Shelf bedforms with special attention to megalineations. Geomorphology 102, 364–375.
Shaw, J., Gilbert, R.G., Sharpe, D.R., Lesemann, J.-E., and Young, R.R. 2020: The origins of s-forms: Form similarity, process analogy, and links to high-energy, subglacial meltwater flows. *Earth-Science Reviews*, 200, https://doi.org/10.1016/j.earscirev.2019.102994.
Shoemaker, E.M. 1988. On the Formulation of Basal Debris Drag for the case of sparse debris Joumal of Glaciology, 34(118): 259-264 1988
Shoemaker, E.M. 1991: On the formation of large subglacial lakes. *Canadian Journal of Earth Sciences*, 28: 1975-1981.
Shoemaker, E.M., 1992. Water sheet outburst floods from the Laurentide ice sheet. Can. J. Earth Sci. 29, 1250–1264.
Shoemaker, E.M., 1999. Subglacial water-sheet floods, drumlins and ice-sheet lobes. Journal of Glaciology 45(150):201-213. DOI: 10.3189/s0022143000001702
Siegert, M.J., LeBrocq, A., Payne, A., 2007. Hydrological connections between Antarctic subglacial lakes and the flow of water beneath the East Antarctic Ice Sheet. *In*: Hambrey, M.J., Christoffersen, P., Glasser, N.F., Hubbard, B.P. (*Eds*.), Glacial Sedimentary Processes and Special Publication, vol. 39. Oxford, Blackwell Publishing, International Association of Sedimentologists, pp.3–10.
Stanley, G.M., 1934. Pleistocene potholes in the Cloche Mountains of Ontario. Papers, Michigan Academy of Science, Arts, and Letters 19, 401-416.
Sugden, D.E., and John, B.S. 1976. Glaciers and landscape: a geomorphological approach. London, Edward Arnold, 376.

Sugden D.E., Glasser N.F., Clapperton C.M. 1992. Evolution of large roches moutonnees. Geografiska Annaler 74A: 253–264.
Tinkler, K.J., Stenson R.E., 1992. Sculpted bedrock forms along the Niagara Peninsula, Ontario. Géographie physique et Quaternaire 46, 195-207.
Tinkler, K.J., and Parish, J., 1998, Recent adjustments to the long profile of Cooksville Creek, an urbanized bedrock channel in Mississauga, Ontario, in Tinkler, K.J., and Wohl, E.E., eds., Rivers Over Rock: Fluvial Processes in Bedrock Channels: American Geophysical Union Geophysical Monograph 107, p. 167–187, https://doi.org/10.1029/GM107p0167
Todd, B.J. and McNamara, G.D., 2018. Processing of seismic-reflection data from expedition 91800 of the RV *Laurentian*, Lake Huron and Georgian Bay, Ontario, Canada and Michigan, U.S.A.; Geological Survey of Canada, Open File 8428, 1 .zip file. https://doi.org/10.4095/308328
Whipple, K.X., Hancock, G.S., and Anderson, R.S., 2000. River incision into bedrock: Mechanics and relative efficacy of plucking, abrasion, and cavitation: Geological Society of America Bulletin, v. 112, p. 490–503, https:// doi .org /10 .1130 /0016 -7606 (2000)112<490: RIIBMA>2.0.CO;2.
Whipple, K.X., DiBiase, R.A., and Crosby, B.T., 2013. Bedrock rivers, *in* Shroder, J.F., ed., Treatise on Geomorphology: San Diego, Academic Press, p. 550–573, https://doi .org /10.1016/B978-0-12-374739-6.00254-2.
Wilkinson, C., Harbor, D.J., Helgans, E., and J.P. Kuehner, 2018. Plucking phenomena in non-uniform flow. Geosphere, 14(5): 217-2170.
Wilson, A., Hovius, N., Jens and Turowski, M., 2018. Upstream-facing convex surfaces: Bedrock bedforms produced by fluvial bedload abrasion Geomorphology 180-181: 187-204. https://doi.org/10.1016/j.geomorph.2012.10.010